VILNIUS UNIVERSITY
CENTER FOR PHYSICAL SCIENCES AND TECHNOLOGY

RYTIS KAZAKEVIČIUS

COMPLEX NONLINEAR SYSTEMS AFFECTED BY COLORED AND NON-GAUSSIAN EXTERNAL NOISE

Doctoral dissertation
Physical sciences, physics (02P)

Vilnius, 2017

The research was performed in 2013 - 2017 at Vilnius university.

Scientific supervisor:

dr. Julius Ruseckas (Vilnius University, physical sciences, physics – 02 P)

VILNIAUS UNIVERSITETAS
FIZINIŲ IR TECHNOLOGIJOS MOKSLŲ CENTRAS

RYTIS KAZAKEVIČIUS

SUDĖTINGOS NETIESINĖS SISTEMOS VEIKIAMOS SPALVOTO IR NE GAUSO IŠORINIO TRIUKŠMO

Daktaro disertacija
Fiziniai mokslai, fizika (02 P)

Vilnius, 2017

Disertacija rengta 2013 - 2017 Vilniaus universitete.

Mokslinis vadovas:

dr. Julius Ruseckas (Vilniaus universitetas, fiziniai mokslai, fizika – 02 P)

Contents

List of abbreviations

CTRW	Continuous time random walk
HDP	Heterogeneous diffusion precess
MSD	Mean squared displacement
ODE	Ordinary differential equation
PDF	Probability density function
PSD	Power spectral density
SDE	Stochastic differential equation

1 Introduction

Transport properties in complex systems are usually characterized by anomalous scaling, that is by a non-linear time dependency in the growth of the variance, $\sigma^2(t) \sim t^\mu$, where t is the elapsed time. This condition is known as an anomalous diffusion. In contrast to the anomalous diffusion, in a typical diffusion process the variance of the particle position (or mean squared displacement σ_x^2) is a linear function of time. Physically, the variance $\sigma^2(t)$ can be considered as the amount of space that the particle has "explored" in the system at given time t. Anomalous diffusion is classified by its power law exponent μ. If $\mu > 1$, the phenomenon is called super-diffusion. If $\mu < 1$, the particle undergoes subdiffusion.

Super-diffusion has been experimentally observed in a study of tracer particles in a two-dimensional rotating flow [1]. Theoretical models suggest that supper-diffusion can be caused by Lévy flights [2]. Analysis of the relaxation cascade of a photoexcited electron in graphene showed that the statistics of the entire cascade is described by Lévy flights with constant drift leading to anomalous diffusion [3]. Lévy flight is a generalization of the Brownian motion. The Brownian motion mimics the influence of the "bath" of surrounding molecules in terms of time-dependent stochastic force which is commonly assumed to be a white Gaussian noise. The Lévy α-stable distributions, characterized by the index of stability $0 < \alpha \leqslant 2$, constitute the most general class of stable processes. The Gaussian distribution is their special case, corresponding to $\alpha = 2$. Lévy flights resulting in a super-diffusion can be modeled by fractional Fokker-Planck equations [4] or Langevin equations with an additive Lévy stable noise. Langevin equations have been used to study the role of thermal and non-Gaussian noise on the dynamics of driven short overdamped [5] and long-overlap Josephson junctions [6]. The resonant activation and noise enhanced stability has been observed in a metastable system in the presence of Levy noise. Lévy motions can lead to anomalous diffusion in many physical systems: as an example we mention deterministic chaotic dynamics of Na adparticles on a Cu surface [7], anomalous diffusion of a gold nanocrystal, adsorbed on the basal plane of graphite [8].

Langevin equations with multiplicative Lévy stable noise have been used

for modeling inhomogeneous media [9] and for the description of the competition between two competing species in super-diffusive dynamical regimes. The multiplicative noise, in the presence of two different dynamical regimes (coexistence and exclusion) produces the appearance of anticorrelated oscillations and stochastic resonance phenomenon [10, 11]. The relation between Langevin equation with multiplicative Lévy stable noise and fractional Fokker-Planck equation has been introduced in [12]. The Langevin equation should be interpreted in Itô sense [13]. Unfortunately the relation between these two equations are not known in Stratonovich interpretation, therefore application of Lévy stable noise driven stochastic differential equations (SDEs) can be problematic. For equation driven by Gaussian noise we can always write the corresponding Fokker-Planck equation and vice versa. However, such statement is not always true for Langevin equation with Lévy stable noise. For example, particle diffusion on randomly folding heteropolymer can be described by space fractional Fokker-Planck equation [14], but for such equation counterpart Langevin equation has not been found [15] and may not exist [16].

There are some exceptional cases when stochastic differential equations with Lévy stable noise have generated a signal with statistical properties that mimics experiment data very well, like in a study of Lévy stable noise induced millennial climate changes from an ice-core record [17]. However, the choice of appropriate model for noisy system can be very difficult. In many experimental studies it is usually possible only to show that the systems exhibit Lévy law-tails: for example, distribution function of turbulent magnetized plasma emitters [18] and step-size distribution of photons in hot vapors of atoms [19] have Lévy tails. Financial data time series analysis show that other stochastic process can be indistinguishable from Lévy stable motion [20].

Another important subclass of anomalous diffusion processes constitute subdiffusion processes, characterized by the sublinear dependence with the power-law exponent in the range $0 < \mu < 1$. Subdiffusion processes have been reported in condensed matter systems [2], ecology [21], and biology [22]. Subdiffusion has been proposed as a measure of macromolecular crowding in the cytoplasm [23]. Sub-diffusion can be described with an additional assumption that diffusing particle become trapped for some times and the waiting time distribution is of a power law type. In this situation no finite mean jump time Δt

exists [2]. For example, assuming anomalously long waiting times $p(t) \sim 1/t^{1+m}$, $0 < m < 1$, one arrives at an anomalous, non-Markovian diffusion which is described by the fractional (in time) Fokker-Planck-Kolmogorov equation [24]. However, if it is unreasonable to assume existence of the trapping mechanism, alternative approach can be made by using models with multiplicative Lévy stable noise [25].

Anomalous diffusion does not uniquely indicate the processes occurring in the system, because there are different stochastic processes sharing the behavior of the MSD ($\sigma^2(t) \sim t$). The physical mechanisms leading to the deviations from the linear time dependence of the MSD can depend on the system or on the temporal and spatial ranges under consideration. For example, diffusion described by CTRW has been observed for sub-micron tracers in biological cells [26–28], structured coloidal systems [29] and for charge carrier motion in amorphous semiconductors [30, 31]. Fractional Brownian motion and fractional Langevin equations has been used to model the dynamics in membranes [32,33], motion of polymers in cells [34], tracer motion in complex liquids [35,36]. Diffusion of even smaller tracers in biological cells has been described by a spatially varying diffusion coefficient [37].

Recently, in Refs. [38–40] it was suggested that the anomalous diffusion can be a result of heterogeneous diffusion process (HDP), where the diffusion coefficient depends on the position. Spatially dependent diffusion can occur in heterogeneous systems. For example, heterogeneous medium with steep gradients of the diffusivity can be created in thermophoresis experiments using a local variation of the temperature [41,42]. Mesoscopic description of transport in heterogeneous porous media in terms of space dependent diffusion coefficients is used in hydrology [43, 44]. In turbulent media the Richardson diffusion has been described by heterogeneous diffusion processes [45]. Power-law dependence of the diffusion coefficient on the position has been proposed to model diffusion of a particle on random fractals [46, 47]. In bacterial and eukaryotic cells the local cytoplasmic diffusivity has been demonstrated to be heterogeneous [37,48]. Motion of a Brownian particle in an environment with a position dependent temperature has been investigated in Ref. [A2]. In random walk description the spatially varying diffusion coefficient can be included via position dependence of the waiting time for a jump event [49], the position dependence

occurs because in the heterogeneous medium the properties of a trap can reflect the medium structure. This is the case for diffusion on fractals and multifractals [12]. Inhomogeneous versions of continuous time random walk models for water permeation in porous ground layers were proposed in Ref. [50]. Heterogeneous diffusion process might be applicable to describe anomalous diffusion in such systems.

Theoretical models suggests that variety of systems affected by a colored noise instead of a white noise exhibit new interesting properties. For example: The correlations in colored noise are found to be able to enhance or suppress the growth rate of amplification above or below a critical detuning in the collective scattering of light from a laser with a colored noise in ultracold and collisionless atomic gas [51]. Investigation of the colored-noise effect on nonequilibrium phase transitions shows reentrant transitions from ordered into the disordered phase as the correlation time and the coupling strength increase [52]. The color and coupling induced disorders are pure colored-noise effects because of the absence of the white-noise limit. Some of the population growth models subjected to a white environmental noise changes the population-size dependence of the mean time to extinction from an exponential to a power-law with a large exponent [53]. The introduction of the colored Gaussian noise changes this exponent, reducing it at a fixed noise magnitude. For a long correlation time of the environmental noise the the mean time to extinction becomes independent of the population size for a strong enough noise [54].

Investigation of the effects caused by the presence of a colored noise in physical systems has some practical implications. Study of colored-noise-induced synchronization in chaotic systems indicates that the critical amplitude required for synchronization is generally smaller for the white noise as compared with the colored noise [55]. A practical implication is that, in situations where synchronization is undesirable, a simple control strategy is to place filters in the system so as to make the noise source as colored as possible. In the systems exhibiting the phenomenon of stochastic resonance an exponentially correlated noise ("red" noise) leads to a reduction of signal amplification and the peak of stochastic resonance moves to a larger noise intensity when the correlation time increases [56]. "Pink noise" or $1/f$ noise, as opposed to white noise also leads to a reduction of signal amplification, but resonance peak arises for lower noise

intensity, if special conditions are satisfied [57]. This is important for understanding weak signal transmission trough noisy environments.

Signals having the PSD at low frequencies f of the form $S(f) \sim 1/f^{\beta}$ with β close to 1 are commonly referred to as "pink noise" or "$1/f$ noise". Such signals are often found in physics and in many other fields [58–64]. Since the discovery of $1/f$ noise numerous models and theories have been proposed, for a recent review see [65]. Mostly $1/f$ noise is considered as a Gaussian process [66, 67], but sometimes the $1/f$ fluctuations are non-Gaussian [68, 69]. The Brownian motion as a source of $1/f$ noise was first proposed in the seminal paper by Marinari *et al.* [70], where it was suggested that $1/f$ noise can result from a random walk in a random environment. Starting from the model of $1/f$ noise as a Brownian motion of inter-pulse durations [71–73], nonlinear SDEs generating signals with $1/f$ spectrum have been derived in [74, 75]. A special case of this nonlinear SDE has been obtained using Kirman's agent model [76]. Such nonlinear SDEs have been used to describe signals in socio-economical systems [77, 78].

The general expression for the proposed class of Itô SDEs is

$$\mathrm{d}x = \sigma^2 \left(\eta - \frac{1}{2}\lambda \right) x^{2\eta-1}\mathrm{d}t + \sigma x^{\eta}\mathrm{d}W_t \,. \tag{1.1}$$

Here x is the signal, $\eta \neq 1$ is the exponent of the power-law multiplicative noise, λ defines the exponent of the power-law steady-state PDF of the signal, W_t is a standard Wiener process (the Brownian motion) and σ is a scaling constant determining the intensity of the noise. The Fokker-Planck equation corresponding to SDE (1.1) gives the power-law probability density function (PDF) of the signal intensity $P_0(x) \sim x^{-\lambda}$ with the exponent λ. The non-linear SDE (1.1) has the simplest form of the multiplicative noise term, $\sigma x^{\eta}\mathrm{d}W_t$. In papers [76, 79] the nonlinear SDE of type (1.1) has been obtained starting from a simple agent-based model describing the herding behavior.

Itô SDEs are typically used in economics [80] and biology [81]. On the other hand, Stratonovich SDEs are more suitable for real systems with correlated, non-white noise, for example, for noise-driven electrical circuits [82]. The Stratonovich SDE corresponding to Itô SDE (1.1) is [83]

$$\mathrm{d}x = \frac{1}{2}\sigma^2(\eta - \lambda)x^{2\eta-1}\mathrm{d}t + \sigma x^{\eta} \circ \mathrm{d}W_t \,. \tag{1.2}$$

Note, that the choice of Stratonovich or Itô convention depends not only on the correlation time of the noise but also on the delay in the feedback [84].

For $\lambda > 1$ the distribution $P_0(x)$ diverges as $x \to 0$, therefore the diffusion of the stochastic variable x should be restricted at least from the side of small values, or equation (1.1) should be modified. The simplest choice of the restriction is the reflective boundary conditions at $x = x_{\min}$ and $x = x_{\max}$. Another choice would be modification of equation (1.1) to get rapidly decreasing steady state PDF when the stochastic variable x acquires values outside of the interval $[x_{\min}, x_{\max}]$. For example, the steady state PDF

$$P_0(x) \sim \frac{1}{x^\lambda} \exp\left(-\frac{x_{\min}^m}{x^m} - \frac{x^m}{x_{\max}^m}\right) \tag{1.3}$$

with $m > 0$ has a power-law form when $x_{\min} \ll x \ll x_{\max}$ and exponential cutoffs when x is outside of the interval $[x_{\min}, x_{\max}]$. Such exponentially restricted diffusion is generated by the SDE

$$\mathrm{d}x = \sigma^2 \left[\eta - \frac{1}{2}\lambda + \frac{m}{2}\left(\frac{x_{\min}^m}{x^m} - \frac{x^m}{x_{\max}^m}\right)\right] x^{2\eta-1}\mathrm{d}t + \sigma x^\eta \mathrm{d}W_t \tag{1.4}$$

obtained from equation (1.1) by introducing the additional terms in the drift.

The PSD of the signals generated by the SDE (1.1) can be estimated using the (approximate) scaling properties of the signals, as it is done in [85]. Since the Wiener process has the scaling property $dW_{at} = a^{1/2} dW_t$, changing the variable x in equation (1.1) to the scaled variable $x_s = ax$ or introducing the scaled time $t_s = a^{2(\eta-1)}t$ one gets the same resulting equation. Thus change of the scale of the variable x and change of time scale are equivalent, leading to the following scaling property of the transition probability (the conditional probability that at time t the signal has value x' with the condition that at time $t = 0$ the signal had the value x):

$$aP(ax', t|ax, 0) = P(x', a^\nu t|x, 0)\,, \tag{1.5}$$

with the exponent ν being $\nu = 2(\eta - 1)$. As has been shown in [85], the power-law steady state PDF $P_0(x) \sim x^{-\lambda}$ and the scaling property of the transition

probability (1.5) lead to the power-law behavior of the PSD

$$S(f) \sim \frac{1}{f^{\beta}}\,, \qquad \beta = 1 + \frac{\lambda - 3}{2(\eta - 1)} \tag{1.6}$$

in a wide range of frequencies.

The presence of the restrictions of diffusion at $x = x_{\min}$ and $x = x_{\max}$ makes the scaling (1.5) not exact and this limits the power-law part of the PSD to a finite range of frequencies $f_{\min} \ll f \ll f_{\max}$. The frequency range where the PSD has $1/f^{\beta}$ behavior is estimated in [85] as

$$\begin{aligned} \sigma^2 x_{\min}^{2(\eta-1)} \ll 2\pi f \ll \sigma^2 x_{\max}^{2(\eta-1)}\,, \qquad \eta > 1\,, \\ \sigma^2 x_{\max}^{-2(1-\eta)} \ll 2\pi f \ll \sigma^2 x_{\min}^{-2(1-\eta)}\,, \qquad \eta < 1\,. \end{aligned} \tag{1.7}$$

This equation shows that the frequency range grows with increasing of the exponent η, the frequency range becomes zero when $\eta = 1$. By increasing the ratio $x_{\max}/x_{\min}$ one can get arbitrarily wide range of the frequencies where the PSD has $1/f^{\beta}$ behavior. Note, that pure $1/f^{\beta}$ PSD is physically impossible because the total power would be infinite. Therefore, we consider signals with PSD having $1/f^{\beta}$ behavior only in some wide intermediate region of frequencies, $f_{\min} \ll f \ll f_{\max}$, whereas for small frequencies $f \ll f_{\min}$ the PSD is bounded.

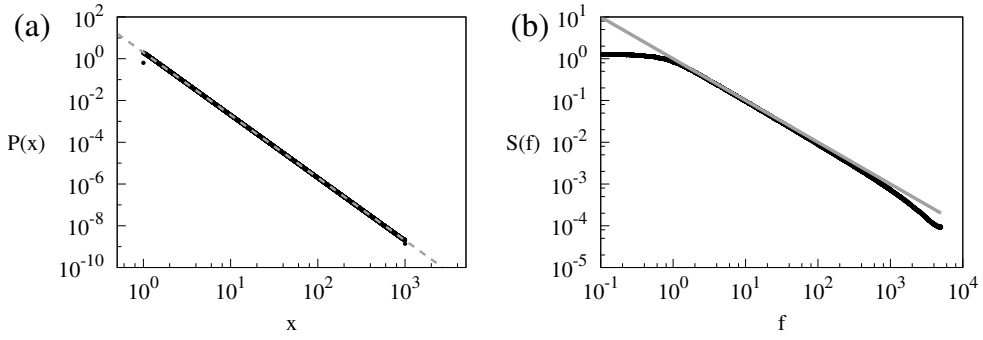

Figure 1: (a) The steady-state PDF of the signal generated by equation (1.1) with reflective boundaries at $x_{\min}$ and $x_{\max}$. The dashed line shows the power-law with the exponent -3. (b) The PSD of such a signal. The gray line shows the slope f^{-1}. Used parameters are $\eta = 2$, $\lambda = 3$, $x_{\min} = 1$, $x_{\max} = 1000$, and $\sigma = 1$.

For $\lambda = 3$ we get that $\beta = 1$ and SDE (1.1) gives signal exhibiting $1/f$ noise. Comparison of the numerically obtained steady state PDF and the PSD with analytical expressions for SDE (1.1) with $\eta = 2$ and $\lambda = 3$ is presented in figure 1.

We see a good agreement of the numerical results with analytical expressions. Methods of numerical solution are presented in the following section. A numerical solution of the equations confirms the presence of the frequency region for which the power spectral density has $1/f^{\beta}$ dependence. The $1/f$ interval in the PSD in figure 1 is approximately between $f_{\min} \approx 10^0$ and $f_{\max} \approx 10^3$ and is much narrower than the width of the region $1 \ll f \ll 10^6$ predicted by equation (1.7). The width of this region can be increased by increasing the ratio between the minimum and the maximum values of the stochastic variable x. In addition, the region in the power spectral density with the power-law behavior depends on the exponent η: if $\eta = 1$ then this width is zero; the width increases with increasing the difference $|\eta - 1|$ [86].

1.1 Numerical solution of SDEs

Euler-Maruyama and Milstein methods for SDEs

Let us write a general form of nonlinear SDE as:

$$\mathrm{d}x = f(x)\mathrm{d}t + g(x)\mathrm{d}W_t, \tag{1.8}$$

here $f(x)$ is a drift function and $g(x)$ is a diffusion function. The simplest method used to numerically solve SDE is based on a simple method used to numerically solve ODEs, Euler method [87]. Application of Euler method to SDEs is referred to as Euler-Maruyama approximation [88,89]. The iterative difference equation, when using this method, might take the following form:

$$x_{i+1} = x_i + f(x_i)\Delta t + g(x_i)\Delta W_t. \tag{1.9}$$

The iterative difference equation above has similar form, compared to the iterative difference equation obtained for ODE, with the only difference being W Wiener process. The Wiener process (one-dimensional Brownian motion) describes path (time evolution of coordinate) of the one-dimensional particle hit by some random force. Central limit theorem suggest that superposition of many independent random factors follows the Gaussian distribution, therefore it is expected that the changes of particles coordinate will also follow the Gaussian

distribution. The standard deviation of the distribution will depend on the size of time step, Δt, and increase as a square root of time step width. Thus we can write the difference equation, which is identical in distribution to (1.9), as follows [88, 89]:

$$x_{i+1} = x_i + f(x_i)\Delta t + g(x_i)\sqrt{\Delta t}\zeta_i, \tag{1.10}$$

where ζ_i is a Gaussian random variable with zero mean and unit variance. This difference equation is frequently referred to as Euler-Maruyama method, or Euler-Maruyama approximation for SDEs, [88, 89].

Another commonly used method is Milshtein method [88, 89]. Using this method iterative difference equation takes the following form,

$$x_{i+1} = x_i + f(x_i)\Delta t + g(x_i)\sqrt{\Delta t}\zeta_i + \frac{1}{2}g(x_i)\left(\left.\frac{\mathrm{d}g(x)}{\mathrm{d}x}\right|_{x=x_i}\right)\left(\zeta_i^2 - 1\right)\Delta t. \tag{1.11}$$

Using this method the error scales with Δt instead of $\sqrt{\Delta t}$ as in Euler-Maruyama method due the fourth term on the right hand side. Yet solving (1.1) using these two or higher-order methods would still require use of extremely small Δt which would increase computation times beyond the feasible.

Variable time step method

Note that in SDE (1.1) both drift, $f(x)$, and diffusion, $g(x)$, functions are power-law. Thus while solving (1.1) numerically using Euler-Maruyama or Milshtein methods it appears that time series of x at some point "explode". Although decreasing Δt appears to provide stability to numerical computations. But one cannot decrease Δt indefinitely as computation times grow unreasonably large.

Based on these observation it is rather natural to propose to scale Δt based on the value of x. Namely, if x is small, then its changes are small (the value changes slower), thus larger Δt values are able to provide sufficient precision. If x is large, then its changes become larger (the value changes faster), thus Δt should grow smaller. Thus in general case, building on the Euler method,

$$x_{i+1} = x_i + f(x_i)h(x_i) + g(x_i)\sqrt{h(x_i)}\zeta_i, \tag{1.12}$$

$$t_{i+1} = t_i + h(x_i). \tag{1.13}$$

From the previous experience of solving (1.1) [90–92], it appears that $h(x)$ should be chosen so that in the $x \to \infty$ limit it linearizes drift and diffusion terms:

$$f(x)h(x) \propto x^a, \;\; a \leq 1 \quad \text{and} \quad g(x)\sqrt{h(x)} \propto x^b, \;\; b \leq 1. \tag{1.14}$$

In case of (1.1) [90–92]:

$$h(x) = \kappa^2 x^{2-2\eta}, \tag{1.15}$$

where κ is a precision parameter which should be positive and at smaller than 1. Consequently difference equations solving (1.1) would take the following form:

$$x_{i+1} = x_i + \kappa^2 \left(\eta - \frac{\lambda}{2}\right) x_i + \kappa x_i \zeta_i, \tag{1.16}$$

$$t_{i+1} = t_i + \kappa^2 x^{2-2\eta}. \tag{1.17}$$

Note that for $\eta > 1$ in the limit of small x, $x \to 0$, $h(x)$ diverges to infinity. Thus, and as usually we need time series sampled at certain period T, it is natural to restrict $h(x)$ using $\min$ function: Another possible alternative is to use original $h(x)$ and interpolate to obtain the discretized time series. But this alternative is too tedious to implement, thus we stick with the simpler algorithm.

1.2 Main goal of the thesis

The objective of this dissertation is to study origins of $1/f$ noise and behavior of complex nonlinear systems exhibiting anomalous diffusion and affected by colored and non-Gaussian external noises.

1.3 Main tasks of the thesis

1. To study how $1/f$ fluctuations can arise from random walk in inhomogeneous media.

2. To analyze the affect of colored noise on the motion of a Brownian particle in an inhomogeneous environment.

3. To generalize nonlinear SDEs driven by Gaussian noise and generating signals with $1/f$ PSD by replacing the Gaussian noise with a more general Lévy stable noise.

4. To propose time-fractional Fokker-Planck describing the subdiffusion of particles in an inhomogeneous medium resulting due inhomogeneous distribution of traps in the media.

5. To examine the influence of external potentials on anomalous diffusion

6. To study anomalous diffusion in inhomogeneous media of Brownian particle experiencing Lévy flights.

1.4 Scientific novelty

1. We derived Nonlinear SDEs generating signals with $1/f$ spectrum in a wide range of frequencies together with power-law steady-state PDF from Langevin equations describing Brownian particle motion in heterogeneous media.

2. We showed that set of two nonlinearly coupled SDEs generates signals with power-law PSD in a wide range of frequencies together with the almost arbitrary steady-state PDF.

3. We studied the effect of colored noise on the motion of a Brownian particle in an inhomogeneous environment. Existence of colored noise leads to additional restriction of the diffusion seen as exponential cut-off of the distribution of particle positions and narrower range of frequencies where $1/f$ noise occurs.

4. We generalized nonlinear SDEs driven by Gaussian noise and generating signals with $1/f$ PSD by replacing the Gaussian noise with a more general Lévy stable noise.

5. We proposed time-fractional Fokker-Planck equation describing the subdiffusion of particles in an inhomogeneous medium resulting from inhomogeneous distribution of traps in the media. We analytically solved proposed Fokker-Planck equation and obtained analytic expression for PSD.

6. We studied the influence of external potentials on anomalous diffusion and obtained analytic expressions for the transition probability as well as for the first and the second moments. By using these expression we calculate the dependence of the mean MSD on time.

1.5 Statements of the thesis

1. Nonlinear SDEs generating signals with power-law PSD in a wide range of frequencies together with power-law steady-state PDF can be derived from Langevin equations describing Brownian particle motion in heterogeneous media.

2. Signals exhibiting power-law PSD in a wide range of frequencies together with the almost arbitrary steady-state PDF can be generated by using nonlinearly coupled stochastic differential equations.

3. Introduction of colored noise instead of white noise in to Langevin equations describing diffusion in heterogeneous media leads to: additional restriction of the diffusion seen as exponential cut-off of the distribution of particle positions and narrower range of frequencies where the spectrum has power law behavior.

4. A class of nonlinear SDEs with Lévy noise can give the power-law behavior of the PSD in any desirably wide range of frequencies and power-law steady PDF.

5. Time-subordinated nonlinear Langevin equations can generate signal exhibiting power-law PSD, $S(f) \sim f^{-\beta}$ with the power-law exponent β larger than 1 (or equal) contrary to linear time-subordinated Langevin equations.

6. Introduction of external force proportional to noise induced drift on to HDP changes diffusion coefficient but does not change value of anomalous diffusion exponent.

1.6 List of publications

The research covered in this dissertation was published in 8 papers. List, in chronological order, follows. Papers [A1-A7] were published in ISI indexed journals. [A8] paper was published in ISI indexed conference proceedings.

A1. **R. Kazakevicius**, J. Ruseckas, Lévy flights in inhomogeneous environments and $1/f$ noise, Physica A **411**, 95-103 (2014).

A2. **R. Kazakevicius**, J. Ruseckas, Power law statistics in the velocity fluctuations of Brownian particle in inhomogeneous media and driven by colored noise, J. Stat. Mech. **2015**, 02021 (2015).

A3. **R. Kazakevicius**, J. Ruseckas, Anomalous diffusion in nonhomogeneous media: Power spectral density of signals generated by time-subordinated nonlinear Langevin equations , Physica A **438**, 210-222 (2015).

A4. **R. Kazakevicius**, J. Ruseckas, Power-law statistics from nonlinear stochastic differential equations driven by Lévy stable noise, Chaos, Solitons & Fractals **81**, Part B, 432-442 (2015).

A5. J. Ruseckas, **R. Kazakevicius**, B. Kaulakys, 1/f noise from point process and time-subordinated Langevin equations, J. Stat. Mech. **2016** 054022 (2016).

A6. J. Ruseckas, **R. Kazakevicius**, B. Kaulakys, A Coupled nonlinear stochastic differential equations generating arbitrary distributed observable with 1/f noise, J. Stat. Mech. **2016**, 043209 (2016).

A7. **R. Kazakevicius**, J. Ruseckas, Influence of external potentials on heterogeneous diffusion processes, Phys. Rev. E **94**, 032109 (2016).

A8. **R. Kazakevicius**, J. Ruseckas, Influence of external potentials on heterogeneous diffusion processes, in *Noise and Fluctuations (ICNF), 2017 24th International Conference on* (Vilnius, Lithuania, 2017), 1–4.

1.7 Conference presentations

The research covered in this dissertation was presented in 15 conference presentations. List, in chronological order, follows. Of them 7 talks and 6 posters were presented by the author of this dissertation.

C1. R. Kazakevicius, J. Ruseckas, $1/f$ noise from nonlinear stochastic differential equations driven by Levy noise, in *DPG-frühjahrstagung*(Dresden, Germany, 2014) DY 10.8. // Talk given by R. Kazakevicius

C2. R. Kazakevicius and J. Ruseckas, Lévy flights in non-homogeneous media and $1/f$ noise, in *Open Readings 2014* (Vilnius, Lithuania, 2014), 196. // Poster by R. Kazakevicius

C3. J. Ruseckas, R. Kazakevicius, B. Kaulakys, Power-law statistics from nonlinear stochastic differential equations driven by Lévy stable noise, in *International Conference on Statistical Physics* (Rhodes, Greece, 2014), 143. // Talk given by J. Ruseckas

C4. R. Kazakevicius, J. Ruseckas, Lévy flights in non-homogeneous media and $1/f$ noise, in *Naujametė fizikos konferencija LT*Φ (Vilnius, Lithuania, 2015), 42. // Poster by R. Kazakevicius

C5. R. Kazakevicius, J. Ruseckas, Brauno judėjimas nehomogeninėje aplinkoje ir $1/f$ triukšmas, in *LMA penktoji jaunųjų mokslininkų konferencija, Fizinių ir technologijos mokslų tarpdalykiniai tyrimai* (Vilnius, Lietuva, 2015). // Talk given by R. Kazakevicius

C6. R. Kazakevicius, J. Ruseckas, Velocity fluctuations of Brownian particle in inhomogeneous media and driven by colored noise as a source of $1/f$ fluctuations, in *DPG-frühjahrstagung* (Dresden, Germany, 2015), DY 9.3. // Talk given by R. Kazakevicius

C7. R. Kazakevicius and J. Ruseckas, Fluctuations of Brownian particle in inhomogeneous media as a source of $1/f$ noise, in *Open Readings 2015* (Vilnius, Lithuania, 2015), 245. // Poster by R. Kazakevicius

C8. R. Kazakevicius, J. Ruseckas, Spalvotojo triukšmo įtaka Brauno judėjimui nehomogeninėje aplinkoje, Brownian motion in inhomogeneous media: influence of colored noise, in *41-oji Lietuvos nacionalinė fizikos konferencija: Programa ir pranešimų tezės* (Vilnius, Lietuva, 2015), 72. // Talk given by R. Kazakevicius

C9. R. Kazakevicius, J. Ruseckas, Laipsninė statistika ir anomalioji difuzija, Power-law statistics and anomalous diffusion, in *41-oji Lietuvos nacionalinė fizikos konferencija: Programa ir pranešimų tezės* (Vilnius, Lietuva, 2015), 356. // Poster by R. Kazakevicius

C10. R. Kazakevicius, J. Ruseckas, in *LMA šeštoji jaunųjų mokslininkų konferencija, Fizinių ir technologijos mokslų tarpdalykiniai tyrimai* (Vilnius, Lietuva, 2016). // Talk given by R. Kazakevicius

C11. R. Kazakevicius, J. Ruseckas, Anomalous diffusion and power law statistics, in *Open Readings 2015* (Vilnius, Lithuania, 2015), 291. // Poster by R. Kazakevicius

C12. R. Kazakevicius, J. Ruseckas, Sub-diffusion in nonhomogeneous media: Power spectral density of signals generated by time-subordinated nonlinear Langevin equations, in *Complex Transport with Lévy Walks: From Cold Atoms to Humans and Robots* (Bonn, Germany, 2016). // Poster by R. Kazakevicius

C13. R. KazakeviCius, B. Kaulakys, J. Ruseckas, Influence of external potentials on heterogeneous diffusion processes, in *Ergodicity Breaking and Anomalous Dynamics* (Coventry, England 2016).// Poster by B. Kaulakys

C14. R. Kazakevicius and J. Ruseckas, Diffusion in heterogeneous media *Open Readings 2017* (Vilnius, Lithuania, 2017), 41. // Talk given by R. Kazakevicius

C15. R. Kazakevicius, J. Ruseckas, Influence of external potentials on heterogeneous diffusion processes, in 24^{th} *International Conference on Noise and Fluctuations* (Coventry, England 2016), A5.5. // Talk given by R. Kazakevicius

Personal contribution of the author

The author of the dissertation has performed all of the numerical simulations as well as most of the analytical derivations presented in this dissertation.

1.8 Outline of the dissertation

The list of abbreviations used in this dissertation is given in the chapter previous to the introductory chapter.

In Chapter 2, we consider the motion of a Brownian particle in an inhomogeneous environment such that the motion can be described by the equation yielding $1/f$ spectrum in a broad range of frequencies together with power-law steady-state PDF. However in most systems steady-state PDF of is Gaussian. Thus we propose a system of two coupled nonlinear stochastic differential equations. The equations are derived from the scaling properties necessary for the achievement of $1/f^{\beta}$ noise. The proposed coupled stochastic differential equations allows us to obtain $1/f^{\beta}$ spectrum in a wide range of frequencies together with the almost arbitrary steady-state density of the signal. The original results were published in [A2, A6].

In Chapter 3, we have investigated the effect of colored noise on the motion of a Brownian particle in an inhomogeneous environment. Colored noise mimic the correlation of collisions between the Brownian particle and the surrounding molecules. The original results were published in [A2].

In Chapter 4, we generalize nonlinear SDEs driven by Gaussian noise and generating signals with $1/f$ power spectral density by replacing the Gaussian noise with a more general Lévy stable noise. The equations with the Gaussian noise arise as a special case when the index of stability $\alpha = 2$. We investigate numerically the frequency range where the spectrum has $1/f$ form and demonstrate that this frequency range depends on power-law exponent in steady state distribution as well as on the index of stability α. The original results were published in [A1, A4].

In Chapter 5, we study the PSD of signals generated by time-subordinated Langevin equations. In the homogeneous systems the power spectral density (PSD) of the signals generated by time-subordinated Langevin equations has power-law dependency $S(f) \sim f^{\alpha-1}$ on the frequency as $f \to 0$. We consider nonhomogeneous systems and show that in such systems the power spectral density can have power-law behavior with the exponent equal to or larger than 1 in a wide range of intermediate frequencies. The original results were published in [A3, A5].

In chapter 6, we consider HDP with the power-law dependence of the diffusion coefficient on the position and investigate the influence of external forces on the resulting anomalous diffusion. We obtain analytic expressions for the transition probability as well as for the first and the second moments. By using

these expression we calculate the dependence of the mean square displacement on time. Also we generalize proposed SDE driven by Gaussian noise by replacing the Gaussian noise with a more general Lévy stable noise. The original results were published in [A7].

In Refer to chapters, we gather up the main results presented in this dissertation.

2 Origins of nonlinear SDE generating 1/f noise

Many models have been proposed to explain the origin of $1/f$ noise; for a short overview of the models see introduction of [93]. In many condensed matter systems the $1/f$ spectrum is considered as a superposition Lorentzians with a wide range distribution of relaxation times [73, 94–97]. In this approach $1/f^{\beta}$ noise with the desirable slope β requires a certain distribution of parameters of the system [59, 73, 98–101]. However, it has been shown that only several well separated decay rates are sufficient to yield an approximately $1/f$ power spectrum [102]. The $1/f$ noise in the fluctuations of a mass was first seen in a sandpile model with threshold dissipation proposed in [103] and was analytically obtained in a one-dimensional directed model of sandpiles [104]. Yet another model of $1/f$ noise represents the signals as sequences of the renewal pulses or events with the power-law distribution of the inter-event time [105]. Recently, thermal finite-size fluctuations as mechanism for $1/f$ noise has been proposed [106]. Therefore internal mechanism leading to the emergence of the widely occurring 1/f noise still remains an open issue.

In some systems the $1/f$ fluctuations are non-Gaussian [68, 69]. Power-law distribution of signal intensity as well as power-law behavior of the PSD in a wide range of frequencies can be obtained using point processes where the time between the adjacent pulses experience relatively slow the Brownian-like motion [74, 75, 93]. Such nonlinear SDEs have been applied to describe signals in socio-economical systems [77, 78]. However the derivation of the equations has been quite abstract and physical interpretation of assumptions made in the derivation is not very clear. We present a physical models where such equation can be relevant. We expect that this derivation leads to a better understanding which systems can be described using equation (1.1).

In most cases $1/f$ noise is a Gaussian process [66, 67]. The drawback of the nonlinear SDEs (1.1) generating signals with $1/f^{\beta}$ PSD is the necessity of power-law steady-state probability density function (PDF) of the signal. It is impossible to obtain Gaussian PDF together with $1/f$ spectrum from such nonlinear SDEs. We dedicate Chapter 2.2 to remedy this drawback of nonlinear

SDEs as source of $1/f$ noise by considering not only one SDE, but a system of two coupled SDEs. We demonstrate that the proposed coupled stochastic differential equations allows us to obtain $1/f$ spectrum in a wide range of frequencies together with almost arbitrary steady-state PDF of the signal.

2.1 Nonlinear SDE resulting from motion in inhomogeneous medium

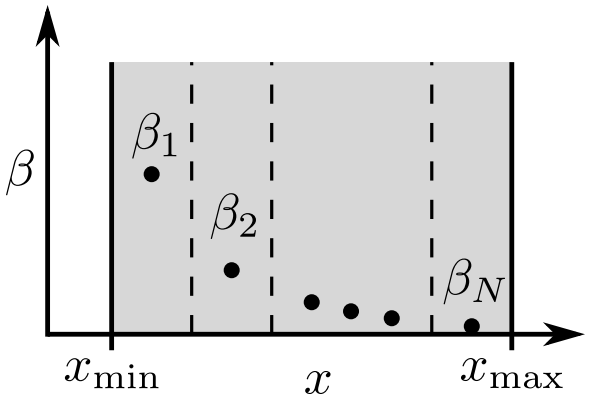

Figure 2: The schematic representation of an inhomogeneous medium. The non-equilibrium system is described as a large number N of regions at local equilibrium, each region having different inverse temperature β_i.

We will consider the Brownian motion of a small macroscopic particle in an inhomogeneous medium. We assume that this medium has reached local thermodynamical equilibrium but not the global one and the temperature can be considered as a function of coordinate. Schematically such a medium is shown in figure 2. Brownian motion of small macroscopic particles in a liquid or a gas results from unbalanced bombardments due to surrounding molecules. Usually the Brownian motion is described by a Langevin equation that includes the influence of the "bath" of surrounding molecules as a time-dependent stochastic force that is commonly assumed to be a white Gaussian noise. This assumption is valid when the correlation time of fluctuations is short, much shorter than the time scale of the macroscopic motion. The effect of large correlation time of fluctuations will be considered in Chapter 3. In the case of strong collisions between the particle and the surrounding environment the noise is non-Gaussian and we have so called Lévy flights [20]. Nonlinear SDEs Lévy noise and generating signals with $1/f$ spectrum we proposed in Chapter 4.

Langevin equations for one-dimensional motion of a Brownian particle are [107]

$$\frac{\mathrm{d}}{\mathrm{d}t}v(t) = -\gamma v(t) + \frac{1}{m}F(x) + \sqrt{\frac{2\gamma}{m}\frac{1}{\beta(x)}}\xi(t)\,, \tag{2.1}$$

$$\frac{\mathrm{d}}{\mathrm{d}t}x(t) = v(t) \tag{2.2}$$

Here x is the coordinate and v is the velocity of the Brownian particle, m is the mass of the particle, γ is the relaxation rate and $\xi(t)$ is the δ-correlated white noise. In general, equations similar to (2.1), (2.2) can be used to describe a variety of systems: noisy electronic circuits, laser light intensity fluctuations [107] and others. We assume that there is temperature gradient in the medium, therefore the inverse temperature $\beta(x)$ depends on coordinate x. In the case when $\beta(x) \equiv \beta = \mathrm{const}$, equations (2.1) and (2.2) describe Brownian motion in the medium with constant temperature $T = k_{\mathrm{B}}^{-1}/\beta$, where k_{B} is Boltzmann constant.

Performing adiabatic elimination of the velocity as in [108], we obtain the equation

$$\frac{\mathrm{d}}{\mathrm{d}t}x(t) = \frac{1}{\gamma m}F(x) + \frac{1}{2\gamma m}\frac{\beta'(x)}{\beta(x)^2} + \sqrt{\frac{2}{\gamma m}\frac{1}{\beta(x)}} \circ \xi(t)\,. \tag{2.3}$$

Here $\beta'(x) \equiv \mathrm{d}\beta(x)/\mathrm{d}x$. This SDE should be interpreted according to the Stratonovich convention. Note, that the second term in the right hand side of equation (2.3) arises due to position dependence of the stochastic force in equation (2.1) [108]. The Itô SDE corresponding to (2.3) is

$$\mathrm{d}x = \frac{1}{\gamma m}F(x)\mathrm{d}t + \sqrt{\frac{2}{\gamma m}\frac{1}{\beta(x)}}\mathrm{d}W_t\,. \tag{2.4}$$

For calculating stationary distribution of position x in high friction limit we will use a Fokker-Planck equation instead of SDE (2.3). The Fokker-Planck equation corresponding to (2.4) can be written as

$$\frac{\partial}{\partial t}P(x,t) = -\frac{1}{\gamma m}\frac{\partial}{\partial x}F(x)P(x,t) + \frac{1}{\gamma m}\frac{\partial^2}{\partial x^2}\frac{P(x,t)}{\beta(x)}\,. \tag{2.5}$$

By setting the time derivative to zero we obtain an analytical expression for

steady state distribution $P_0(x)$:

$$P_0(x) = C\beta(x) \exp\left(\int^x F(x')\beta(x')\mathrm{d}x'\right) . \tag{2.6}$$

Let us consider the situation when the dependence of the inverse temperature on the coordinate is described by a power law,

$$\beta(x) = bx^{-\theta} . \tag{2.7}$$

Here θ is a power law exponent and b is a constant. This is quite reasonable assumption; for example, if $\theta = 1$ equation (2.7) represents a case where we have steady state heat transfer due to temperature difference $T_2 - T_1$ between the beginning and the end of the system. We assume that there are reflective boundaries at $x_{\min}$ and $x_{\max}$ and the motion is limited to values of x between $x_{\min}$ and $x_{\max}$. When $\theta = 1$ then the temperatures should obey the relation $T_2/T_1 = x_{\max}/x_{\min}$ and the coefficient b is $b = (x_{\max} - x_{\min})/k_{\mathrm{B}}(T_2 - T_1)$. This case is presented in figure 2.

The external force affecting the particle $F(x)$ we express via the gradient of the potential $V(x)$:

$$F(x) = -\frac{\mathrm{d}}{\mathrm{d}x}V(x) . \tag{2.8}$$

We choose the subharmonic potential proportional to the temperature:

$$V(x) = \left(\frac{\lambda}{\theta} - 1\right) \frac{1}{\beta(x)} . \tag{2.9}$$

For convenience we write the coefficient of proportionality as $\lambda/\theta - 1$. As we will see in equation (2.12), the parameter λ gives the power law exponent in the steady state distribution of x. Taking into account equation (2.7) we see that the potential has the power law form with the same exponent θ. The expression for the external force then is

$$F(x) = \frac{\theta - \lambda}{b} x^{\theta - 1} . \tag{2.10}$$

Using inverse temperature (2.7) and force (2.10) the equation (2.3) for the

particle coordinate becomes

$$\frac{\mathrm{d}}{\mathrm{d}t}x(t) = \frac{1}{\gamma m b}\left(\frac{\theta}{2} - \lambda\right) x^{\theta-1} + x^{\frac{\theta}{2}}\sqrt{\frac{2}{\gamma m \mathrm{b}}} \circ \xi(t)\,. \tag{2.11}$$

By introducing new parameters $\sigma = \sqrt{2/bm\gamma}$, $\theta = 2\eta$ into equation (2.11) we obtain the Stratonovich SDE (1.2). By using equations (2.6), (2.7) and (2.10) we obtain distribution of particles in high friction limit

$$P_0(x) = \frac{\lambda - 1}{x_{\min}^{1-\lambda} - x_{\max}^{1-\lambda}} x^{-\lambda}\,. \tag{2.12}$$

Calculating distribution of particles we assumed that there are reflective boundaries at $x_{\min}$ and $x_{\max}$ and the motion is limited to values of x between $x_{\min}$ and $x_{\max}$. Equation (2.11) has the same form as Stratonovich SDE (1.2).

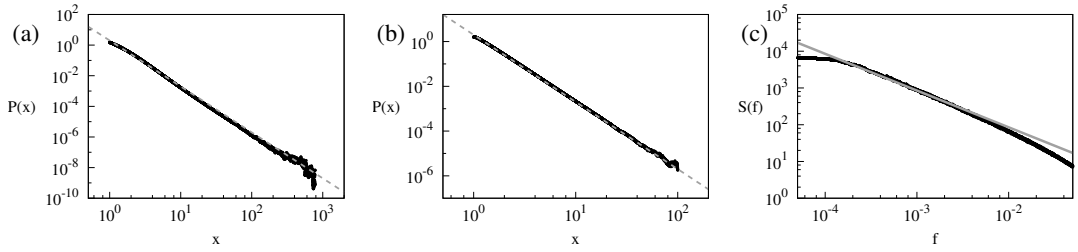

Figure 3: The steady-state PDF of the signal generated by the Langevin equations (2.15), (2.16) with reflective boundaries at $\tilde{x}_{\min}$ and $\tilde{x}_{\max}$ and the parameters: (a) $\theta = 1$, $\lambda = 3$, $\tilde{x}_{\min} = 1$, $\tilde{x}_{\max} = 1000$, (b) $\theta = 0$, $\lambda = 3$, $\tilde{x}_{\min} = 1$, $\tilde{x}_{\max} = 100$. The dashed line shows the power-law with the exponent -3. (c) The PSD of the signal corresponding to the parameters in (b) case. The gray line shows the slope f^{-1}.

To check the validity of the adiabatic elimination of the velocity, we solve the Langevin equations (2.1), (2.2) numerically. For numerical solution it is convenient to introduce dimensionless time $\tilde{t}$, position $\tilde{x}$ and velocity $\tilde{v}$. When the inverse temperature $\beta(x)$ and the force $F(x)$ are given by equations (2.7) and (2.10), we can use $\tilde{t} = \gamma t$ and

$$\tilde{x} = (\gamma^2 m b)^{\frac{1}{2-\theta}} x\,, \tag{2.13}$$

$$\tilde{v} = \gamma^{-1}(\gamma^2 m b)^{\frac{1}{2-\theta}} v\,. \tag{2.14}$$

The equations (2.1), (2.2) in the dimensionless variables have the form

$$\frac{\mathrm{d}}{\mathrm{d}\tilde{t}}\tilde{v} = -\tilde{v} + (\theta - \lambda)\tilde{x}^{\theta-1} + \sqrt{2\tilde{x}^{\theta}}\xi(\tilde{t})\,, \tag{2.15}$$

$$\frac{\mathrm{d}}{\mathrm{d}\tilde{t}}\tilde{x} = \tilde{v}\,. \tag{2.16}$$

The reflective boundaries at $x_{\min}$ and $x_{\max}$ become

$$\tilde{x}_{\min} = (\gamma^2 mb)^{\frac{1}{2-\theta}} x_{\min}\,, \tag{2.17}$$

$$\tilde{x}_{\max} = (\gamma^2 mb)^{\frac{1}{2-\theta}} x_{\max}\,. \tag{2.18}$$

The requirement of large friction γ, necessary for the adiabatic elimination of the velocity, leads to the requirement $\tilde{x}_{\min}, \tilde{x}_{\max} \gg 1$ when $\theta < 2$.

As an example we solve the Langevin equations (2.15), (2.16) with reflective boundaries at $\tilde{x}_{\min}$, $\tilde{x}_{\max}$ and the parameters $\lambda = 3$, $\theta = 1$ or $\theta = 0$. The value of the parameter $\theta = 0$ means that the temperature is constant. The steady state PDF of the particle position $P_0(\tilde{x})$ and the power spectral density $S(\tilde{f})$ are presented in figure 3. In figure 3a we see a good agreement with the distribution of particles in high friction limit (2.12). This confirms the validity of the adiabatic elimination of the velocity. Figure 3c confirms the presence of the frequency region with $1/f$ behavior of the power spectral density, the $1/f$ interval in the PSD is approximately between $\tilde{f}_{\min} \approx 10^{-4}$ and $\tilde{f}_{\max} \approx 10^{-2}$. The width of this interval can be increased by increasing the ratio $\tilde{x}_{\max}/\tilde{x}_{\min}$. The width of $1/f^{\beta}$ region in the PSD also increases with increasing of $|\theta/2 - 1|$.

Not only coordinate fluctuations yield power law PSD. The Langevin equation with postion dependent temperature (2.7) and external force (2.10) can also lead to the power law PSD of the absolute velocity fluctuations [A2].

2.2 Coupled SDEs generating Gaussian 1/f noise

In this section we obtain a pair of coupled nonlinear SDEs by considering the scaling properties required to get $1/f^{\beta}$ PSD. The method we use is similar to that in [85], however now we consider two stochastic variables and two equations. We assume that the first equation describes the fluctuations of the signal x_t, with the fluctuating rate of change y_t described by the second equation.

$$\mathrm{d}x_t = a(x_t)y_t^{2\eta}\mathrm{d}t + b(x_t)y^{\eta}\mathrm{d}W_t\,, \tag{2.19}$$

$$\mathrm{d}y_t = u(x_t)y_t^{2\eta+1}\mathrm{d}t + \sigma y_t^{\eta+1}\mathrm{d}W_t'\,. \tag{2.20}$$

We can obtain a pair of coupled nonlinear SDEs generating signals exhibiting $1/f$ noise by using the following considerations. The Wiener-Khintchine theorem relates the PSD $S(f)$ to the autocorrelation function $C(t)$. If the PSD has a power-law behavior $S(f) \sim f^{-\beta}$ in a wide range of frequencies $f_{\min} \ll f \ll f_{\max}$, then, when the influence of the limiting frequencies $f_{\min}$ and $f_{\max}$ is neglected, the PSD has a scaling property

$$S(af) \sim a^{-\beta}S(f) \tag{2.21}$$

for the frequencies in this range. We only consider signals with PSD having $1/f^{\beta}$ behavior only in some wide intermediate region of frequencies $f_{\min} \ll f \ll f_{\max}$. To avoid the divergence of the total power occuring for pure $1/f$ behavior at arbitrarily small frequencies we assume that the PSD is bounded for small frequencies $f \ll f_{\min}$ outside of this region. Compatibility with experimental data can be ensured by choosing sufficiently small limiting frequency $f_{\min}$.

One of the ways to obtain the required scaling property (2.21) is for the steady-state PDF to be a power-law function of the stochastic variable y,

$$P_0(x,y) \sim p(x)y^{-\lambda}\,, \tag{2.22}$$

and for the transition probability to have the scaling property [A6]

$$aP(x', ay, t|x, ay, 0) = P(x', y', a^{\nu}t|, x, y, 0)\,. \tag{2.23}$$

Here $\nu = 2\eta$ is the scaling exponent and λ is the power-law exponent of the steady-state PDF of the stochastic variable y. Equation (2.23) means that the change of the magnitude of the stochastic variable $y \to ay$ is equivalent to the change of time scale $t \to a^{\nu}t$.

In order to avoid the divergence of the steady-state PDF (2.22), the diffusion of stochastic variable y should be restricted at least from the side of small

values. In general, equation (2.22) can hold only in some region $y_{\min} \ll y \ll y_{\max}$. When the diffusion of stochastic variable y is restricted, equation (2.23) also cannot be exact. However, if the influence of the limiting values $y_{\min}$ and $y_{\max}$ can be neglected for the time t in some region $t_{\min} \ll t \ll t_{\max}$, we can expect for the scaling (2.21) to be approximately valid in this time region.

Thus the function $p(x)$ in (2.22) should be a solution of the differential equation

$$a(x)p(x) - \frac{1}{2}\frac{\mathrm{d}}{\mathrm{d}x}b^2(x)p(x) = 0\,. \tag{2.24}$$

This equation means that the steady-state PDF of the stochastic variable x is determined only by the coefficients $a(x)$ and $b(x)$ of the SDE (2.19). The y-component of the probability current J_y should vanish at the boundaries that are not parallel to y axis, if coefficient $u(x)$ is

$$u(x) = \sigma^2(\eta + 1 - \lambda/2)\,. \tag{2.25}$$

Therefore, required form for system of coupled SDEs generating $1/f^\beta$ noise is

$$\mathrm{d}x_t = a(x_t)y_t^{2\eta}\mathrm{d}t + b(x_t)y_t^{\eta}\mathrm{d}W_t\,, \tag{2.26}$$

$$\mathrm{d}y_t = \sigma^2\left(\eta + 1 - \frac{\lambda}{2}\right)y_t^{2\eta+1}\mathrm{d}t + \sigma y_t^{\eta+1}\mathrm{d}W_t'\,. \tag{2.27}$$

Note, that the second equation (2.27) has the form of non-linear SDEs proposed in [74, 75]. Equations similar to (2.26), (2.27) have been considered in [109]. It has been shown in Ref.: [A6] that the power-law exponent in the PSD of the signal generated by SDEs (2.26), (2.27) is related to the parameters η and λ as

$$\beta = 1 + \frac{\lambda - 1}{2\eta}\,. \tag{2.28}$$

To get a stationary process and avoid the divergence of steady-state PDF, equation (2.27) should be considered together with boundaries restricting the diffusion of stochastic variable y or be modified. The simplest choice restricting the range of diffusion of the stochastic variable y is the reflective boundaries at $y = y_{\min}$ and $y = y_{\max}$. Another possibility is the modification of equation (2.27) to get rapidly decreasing steady-state PDF when the stochastic variable y acquires values outside of the interval $[y_{\min}, y_{\max}]$. For example, the steady-state

PDF

$$P_0(x,y) \sim p(x) y^{-\lambda} \exp\left\{ -\left(\frac{y_{\min}}{y}\right)^m - \left(\frac{y}{y_{\max}}\right)^m \right\} \tag{2.29}$$

with $m > 0$ has a power-law dependence on y when $y_{\min} \ll y \ll y_{\max}$ and exponential cut-offs when y is outside of the interval $[y_{\min}, y_{\max}]$. This exponentially restricted steady-state PDF is a result of the SDE

$$\mathrm{d}y_t = \sigma^2 \left(\eta + 1 - \frac{\lambda}{2} + \frac{m}{2} \left(\frac{y_{\min}^m}{y_t^m} - \frac{y_t^m}{y_{\max}^m} \right) \right) y_t^{2\eta+1} \mathrm{d}t + \sigma y_t^{\eta+1} \mathrm{d}W_t' \tag{2.30}$$

obtained from equation (2.27) by introducing additional terms in the drift.

Limiting frequencies

The restriction of the diffusion of the stochastic variable y to the interval $y_{\min} \ll y \ll y_{\max}$ makes the scaling (2.23) only approximate. As a result, the power-law part of the PSD is limited to a finite range of frequencies $f_{\min} \ll f \ll f_{\max}$. Let us estimate the limiting frequencies $f_{\min}$ and $f_{\max}$. The limiting values $y = y_{\min}$ and $y = y_{\max}$ should also participate in the scaling and equation (2.23) for the transition probability corresponding to SDEs (2.26) and (2.27) becomes

$$aP(x', ay, t|x, ay, 0; ay_{\min}, ay_{\max}) = P(x', y', a^{2\eta}t|, x, y, 0; y_{\min}, y_{\max}) \,. \tag{2.31}$$

Here $y_{\min}$, $y_{\max}$ enter as parameters of the transition probability. Similarly, the steady-state PDF $P_0(x, y; y_{\min}, y_{\max})$ has the scaling property

$$aP_0(x, ay; ay_{\min}, ay_{\max}) = P_0(x, y; y_{\min}, y_{\max}) \,. \tag{2.32}$$

Autocorrelation function has scaling property [A6]

$$C(t, ay_{\min}, ay_{\max}) = C(a^{2\eta}t, y_{\min}, y_{\max}) \,. \tag{2.33}$$

From this scaling of the autocorrelation function it follows that time t should enter only in combinations with the limiting values $y_{\min}t^{1/2\eta}$ and $y_{\max}t^{1/2\eta}$. We can expect that the influence of the limiting values can be neglected and the scaling (2.23) be approximately valid when $y_{\min}t^{1/2\eta} \ll 1$ and $y_{\max}t^{1/2\eta} \gg 1$. In other words, we expect that the scaling (2.23) holds when time t is in the

interval $\sigma^{-2}y_{\max}^{-2\eta} \ll t \ll \sigma^{-2}y_{\min}^{-2\eta}$ when $\mu > 0$ and in the interval $\sigma^{-2}y_{\min}^{-2\eta} \ll t \ll \sigma^{-2}y_{\max}^{-2\eta}$ when $\eta < 0$. The frequency range where the PSD has $1/f^{\beta}$ behavior can be estimated as

$$\sigma^2 y_{\min}^{2\eta} \ll 2\pi f \ll \sigma^2 y_{\max}^{2\eta}\,, \qquad \eta > 0 \tag{2.34}$$

$$\sigma^2 y_{\max}^{2\eta} \ll 2\pi f \ll \sigma^2 y_{\min}^{2\eta}\,, \qquad \eta < 0 \tag{2.35}$$

We see that the width of the frequency range where the PSD has $1/f^{\beta}$ behavior grows with increase of the ratio $y_{\max}/y_{\min}$. For $\eta = 0$ the width of the frequency region (2.34) is zero and we do not have $1/f^{\beta}$ power spectral density.

2.3 Numerical approach

Since analytical solution of stochastic differential equations can be obtained only in particular cases, there is a need of numerical solution. Using Euler-Maruyama method with small time step Δt for numerical solution of SDEs (2.26) and (2.27), we get the discretized equations

$$x_{k+1} = x_k + a(x_k)y_k^{2\eta}\Delta t + b(x_k)y_k^{\eta}\sqrt{\Delta t}\varepsilon_k\,, \tag{2.36}$$

$$y_{k+1} = y_k + \sigma^2\left(\eta + 1 - \frac{\lambda}{2}\right)y_k^{2\eta+1}\Delta t + \sigma y_k^{\eta+1}\sqrt{\Delta t}\xi_k\,. \tag{2.37}$$

Here ε_k and ξ_k are independent random variables with the standard normal distribution. However, for numerical solution of nonlinear equations the solution schemes involving a fixed time step Δt can be inefficient. For example, in equations (2.26) and (2.27) with $\eta > 0$, large values of stochastic variable y lead to large coefficients and thus require a very small time step. The numerical solution scheme can by improved by using a variable time step that becomes small only when y becomes large. Such method of solution of a single nonlinear SDE has been proposed in [74]. The variable time step is equivalent to the introduction of the internal time τ that is different from the real, physical, time t [A5].

In order to make the solution more efficient we introduce an internal, operational, time τ by the equation

$$\mathrm{d}\tau_t = y_t^{2\eta}\mathrm{d}t\,. \tag{2.38}$$

We assume that the zero of the internal time τ coincides with the zero of the physical time t, thus the initial condition for the internal time is $\tau_{t=0} = 0$. Since $y_t > 0$, from equation (2.38) it follows that τ_t is a strictly increasing function of time t. Let us obtain the SDEs for the stochastic variables x and y in the internal time τ. To do this we proceed similarly as in Ref.: [A5] and consider the joint PDF $P_{x,y,\tau}(x, y, \tau; t)$ of the stochastic variables x, y and τ. The PDF $P(x, y; t)$ can be calculated using the equation

$$P_{x,y}(x, y, t) = \int P_{x,\tau}(x, y, \tau; t)\, \mathrm{d}\tau\,. \tag{2.39}$$

Equations (2.26), (2.27), and (2.38) lead to the Fokker-Planck equation for the PDF $P_{x,y,\tau}(x, y, \tau; t)$

$$\frac{\partial}{\partial t}P_{x,y,\tau} = -y^{2\eta}\frac{\partial}{\partial x}a(x)P_{x,y,\tau} - \sigma^2\left(\eta + 1 - \frac{\lambda}{2}\right)\frac{\partial}{\partial y}y^{2\eta+1}P_{x,y,\tau} - y^{2\eta}\frac{\partial}{\partial \tau}P_{x,y,\tau} + \frac{1}{2}y^{2\eta}\frac{\partial^2}{\partial x^2}b(x)^2P_{x,y,\tau} + \frac{1}{2}\sigma^2\frac{\partial^2}{\partial y^2}y^{2\eta+2}P_{x,y,\tau}. \tag{2.40}$$

Since the zero of the internal time τ coincides with the zero of the physical time t, the initial condition for equation (2.40) is $P_{x,y,\tau}(x, y, \tau; 0) = P(x, y; 0)\delta(\tau)$. Matching of the zeros of τ and t leads also to the boundary condition $P_{x,y,\tau}(x, y, 0; t) = 0$ for $t > 0$, because τ and t are strictly increasing.

Instead of x, y and τ we can consider x, y and t as stochastic variables. The physical time t is related to the operational time τ via equation (2.38), therefore, the joint PDF $P_{x,y,t}(x, y, t; \tau)$ of the stochastic variables x, y and t is related to the PDF $P_{x,y,\tau}(x, y, \tau; t)$ according to the equation

$$P_{x,y,t}(x, y, t; \tau) = y^{2\eta}P_{x,y,\tau}(x, y, \tau; t)\,. \tag{2.41}$$

Another way to get this relation is to notice that the third term on the right hand side of equation (2.40) contains the derivative $\frac{\partial}{\partial \tau}$ and thus should be equal to $-\frac{\partial}{\partial \tau}P_{x,y,t}$. Inserting (2.41) into equation (2.40) we get

$$\frac{\partial}{\partial \tau}P_{x,y,t} = -\frac{\partial}{\partial x}a(x)P_{x,y,t} - \sigma^2\left(\eta + 1 - \frac{\lambda}{2}\right)\frac{\partial}{\partial y}yP_{x,y,t} - \frac{\partial}{\partial t}\frac{1}{y^{2\eta}}P_{x,y,t} + \frac{1}{2}\frac{\partial^2}{\partial x^2}b(x)^2P_{x,y,t} + \frac{1}{2}\sigma^2\frac{\partial^2}{\partial y^2}y^2P_{x,y,t}\,. \tag{2.42}$$

The initial condition for equation (2.42) is $P_{x,y,t}(x,t;0) = P(x,y;0)\delta(t)$. In addition, there is a boundary condition $P_{x,y,t}(x,y,0;\tau) = 0$ for $\tau > 0$. The Fokker-Planck equation (2.42) can be obtained from the coupled SDEs

$$\mathrm{d}x_\tau = a(x_\tau)\mathrm{d}\tau + b(x_\tau)\mathrm{d}W_\tau\,, \tag{2.43}$$

$$\mathrm{d}y_\tau = \sigma^2\left(\eta + 1 - \frac{\lambda}{2}\right) y_\tau \mathrm{d}\tau + \sigma y_\tau \mathrm{d}W'_\tau\,, \tag{2.44}$$

$$\mathrm{d}t_\tau = \frac{1}{y_\tau^{2\eta}}\mathrm{d}\tau\,. \tag{2.45}$$

Discretizing the internal time τ with the step $\Delta\tau$ and using the Euler-Maruyama approximation for SDEs (2.43) and (2.44), we get

$$x_{k+1} = x_k + a(x_k)\Delta\tau + b(x_k)\sqrt{\Delta\tau}\varepsilon_k\,, \tag{2.46}$$

$$y_{k+1} = y_k + \sigma^2\left(\eta + 1 - \frac{\lambda}{2}\right) y_k\Delta\tau + \sigma y_k\sqrt{\Delta\tau}\xi_k\,, \tag{2.47}$$

$$t_{k+1} = t_k + \frac{\Delta\tau}{y_k^{2\eta}}\,. \tag{2.48}$$

Equations (2.46)–(2.48) provide the numerical method for solving coupled SDEs (2.26) and (2.27). One can interpret equations (2.46)–(2.48) as an Euler-Maruyama scheme with a variable time step $\Delta t_k = \Delta\tau/y_k^{2\eta}$ that adapts to the coefficients in the SDEs. As a consequence of the introduction of the internal time the increments of the real, physical, time t become random. To get the discretization of time with fixed steps the signal generated in such a way should be interpolated.

As an example, let us solve the equations

$$\mathrm{d}x_t = -\gamma y_t^{2\eta} x_t \mathrm{d}t + y_t^\eta \mathrm{d}W_t\,, \tag{2.49}$$

$$\mathrm{d}y_t = \sigma^2\left(\eta + 1 - \frac{\lambda}{2}\right) y_t^{2\eta+1}\mathrm{d}t + \sigma y_t^{\eta+1}\mathrm{d}W'_t\,. \tag{2.50}$$

For the stochastic variable y we assume reflective boundaries at $y = y_{\min}$ and $y = y_{\max}$. In this case the coefficients $a(x)$ and $b(x)$ in equation (2.26) are $a(x) = -\gamma x$ and $b(x) = 1$, leading to the Gaussian steady-state PDF of x,

$$p(x) = \sqrt{\frac{\gamma}{\pi}}\mathrm{e}^{-\gamma x^2}\,. \tag{2.51}$$

The quantity $y^{2\eta}$ in equation (2.49) represents a fluctuating relaxation rate.

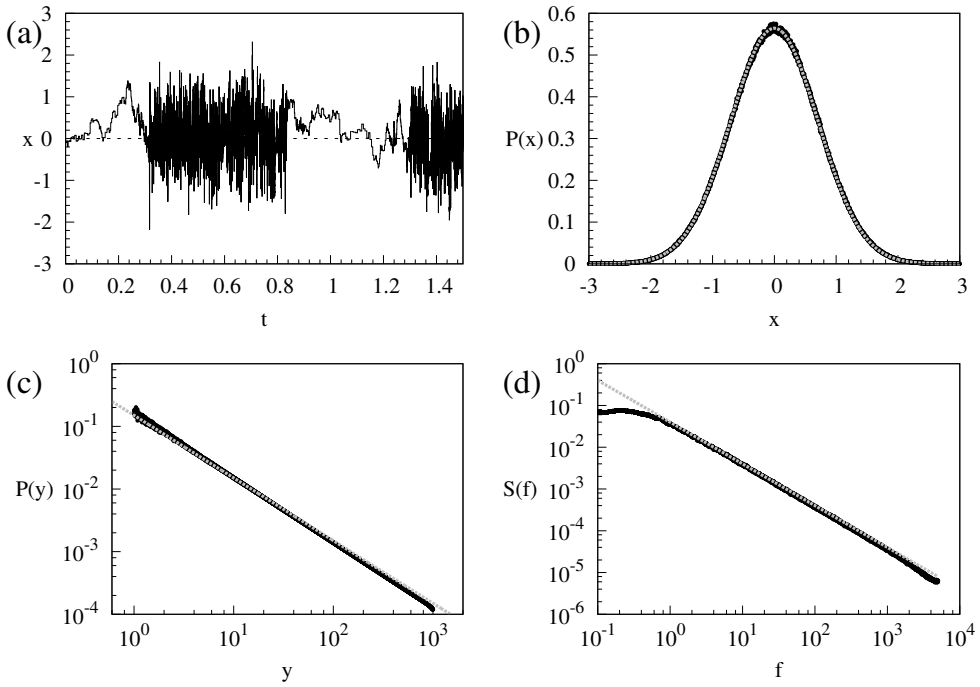

Figure 4: (a) Typical signal x generated by equations (2.49) and (2.50). Reflective boundaries at $y_{\min}$ and $y_{\max}$ have been used for equation (2.50). (b) The PDF of the signal intensity. The dashed (grey) line shows the Gaussian curve. (c) The PDF of the stochastic variable y. The dashed (grey) line shows the power-law with the exponent -1. (d) The PSD of the signal x. The dashed (grey) line shows the slope f^{-1}. Used parameters are $\eta = 1$, $\lambda = 1$, $y_{\min} = 1$, $y_{\max} = 1000$, $\gamma = 1$ and $\sigma = 1$.

Comparison of the numerically obtained steady state PDF and the PSD with analytical expressions for the system of SDEs (2.49) and (2.50) with $\eta = 1$ and $\lambda = 1$ is presented in figure 4. Typical signal x_t generated by equations (2.49) and (2.50) is shown in figure 4(a). As one can see, the signal exhibits a structure consisting of the periods of slow and fast fluctuations. The fast fluctuations correspond to the peaks or bursts of the stochastic variable y. Note, that due to large difference between slowest and fastest fluctuation rates the signal in the periods of fast fluctuations in figure 4(a) visually resembles white noise. However, the actual signal changes according to SDE (2.49), the periods of fast fluctuations are similar to the periods of slow fluctuations compressed in time. Analysis of nonlinear SDEs similar to (2.50), performed in [93], reveals that the sizes of the bursts are approximately proportional to the squared durations of the bursts. The distributions of burst and inter-burst durations have power-law parts, with the numerically estimated power-law exponent of the PDF of the inter-burst durations approximately equal to $-3/2$. Intermittent behavior, similar to the behavior shown in figure 4(a), can be connected with $1/f$ noise. For example, it is known that intermittent behavior in iterative maps at the edge of chaos can lead to $1/f$ noise [110]. In figures 4(b) and 4(c) we see a good agreement of the numerically calculated steady-state PDFs of the stochastic variables x and y with the analytical expressions. The PSD of the signal x_t is shown in figure 4(d). Numerical solution of the equations confirms the presence of the frequency region for which the power spectral density has $1/f^{\beta}$ dependence with $\beta = 1$.

2.4 Coupled Langevin equations as a model of particle jumps in potential barrier with fluctuating height

Coupled Langevin equations have been used to describe many physical phenomena. For example, hot-carrier transport in semiconductors has been modeled by linearly coupled Langevin equations [111]; nonlinear coupled Langevin equations have been used to study pressure time series [112]. One nonlinear SDE with fluctuating parameter can be interpreted as a pair of coupled SDEs [113]. Equations with time varying parameter being a Gaussian colored

noise (Ornstein-Uhlenbeck process) have been used to model wind farm power production output dependence on wind velocity [114] and atmospheric turbulence in radio signal detection [115]. Here we study nonlinear SDEs where the fluctuating parameter enters both diffusion and drift coefficients as a power-law function.

To illustrate the situation that can be described by the proposed SDEs (2.26) and (2.27), let us consider the case with $\eta = -\frac{1}{2}$. Equations (2.26) and (2.27) then become

$$\mathrm{d}x_t = a(x_t)\frac{1}{y_t}\mathrm{d}t + b(x_t)\frac{1}{\sqrt{y_t}}\mathrm{d}W_t\,, \tag{2.52}$$

$$\mathrm{d}y_t = \frac{1}{2}\sigma^2(1-\lambda)\mathrm{d}t + \sigma\sqrt{y_t}\mathrm{d}W'_t\,. \tag{2.53}$$

The quantity y^{-1} in equation (2.52) has the meaning of the rate of change, whereas y has the meaning of time interval. According to equation (2.28), the PSD of the signal x_t has power-law behavior for a wide range of frequencies with the power-law exponent

$$\beta = 2 - \lambda\,. \tag{2.54}$$

We get $1/f$ noise when $\lambda = 1$. Assuming that the coefficients $a(x)$ and $b(x)$ are sufficiently small, we can take $\Delta\tau = 1$ in the numerical solution scheme (2.46)–(2.48), leading to the discrete equations

$$x_{k+1} = x_k + a(x_k) + b(x_k)\varepsilon_k\,, \tag{2.55}$$

$$y_{k+1} = y_k\left(1 + \frac{1}{2}\sigma^2(1-\lambda) + \sigma\xi_k\right)\,, \tag{2.56}$$

$$t_{k+1} = t_k + y_k\,. \tag{2.57}$$

In particular, when $\lambda = 1$ and the signal x has $1/f$ spectrum, equation (2.56) becomes $y_{k+1} = y_k(1 + \sigma\xi_k)$. We can interpret equations (2.55)–(2.57) as follows: equations (2.56) and (2.57) describe a process consisting of discrete events occurring at time moments t_k. The inter-event duration is random and equal to the stochastic variable y_k. This inter-event duration slowly changes with time in such a way, that the duration of the next time interval is equal to the duration of the previous interval multiplied by some random factor close to 1. The signal x_k

changes only during the occurrence of the events at time moments t_k and this change is described by equation (2.55).

Equation (2.53) results in the steady-state PDF $P_0(y_t)$ of the stochastic variable y_t having a power-law form with the exponent $-\lambda$. The PDF $P_k(y_k)$ of a sequence of y_k values generated according to equation (2.56) differs from $P_0(y_t)$. When y_k changes slowly with the index k, the PDF $P_k(y_k)$ should satisfy the equation $P_0(y_k) \approx \frac{y_k}{\langle y_k \rangle} P_k(y_k)$, because going back from discrete equations to the continuous time one should assume that each value y_k last for the duration also equal y_k. Consequently, the PDF $P_k(y_k)$ is also a power-law with the exponent $-\lambda'$, $\lambda' = \lambda + 1$. Thus, if λ is close to 1 then λ' is close to 2.

There are many processes in the nature with the power-law inter-event time distribution. For example, many human-related activities show power-law decaying inter-event time distribution with exponents usually varying between 1 and 2 [116–119]. Power-law distribution of inter-event times has been observed in neuron-firing sequences [120] and in the timings of earthquakes [121, 122]. In addition, power-law decaying inter-event time distribution is often accompanied by the power-law decaying autocorrelation function [123].

Let us further assume that the events are due to jumps over the potential barrier of the height v. In many physical systems the escape rate exponentially depends on the barrier height, therefore we take $y = \mathrm{e}^v$. Changing the variables in equations (2.52) and (2.53) we get the SDEs

$$\mathrm{d}x_t = a(x_t)\mathrm{e}^{-v_t}\mathrm{d}t + b(x_t)\mathrm{e}^{-v_t/2}\mathrm{d}W_t\,, \tag{2.58}$$

$$\mathrm{d}v_t = -\frac{1}{2}\sigma^2\lambda\mathrm{e}^{-v_t}\mathrm{d}t + \sigma\mathrm{e}^{-v_t/2}\mathrm{d}W'_t\,. \tag{2.59}$$

Similar to equations (2.55)–(2.57), numerical solution scheme with the variable time step $\Delta t_k = \mathrm{e}^{v_k}$ yields discrete equations

$$x_{k+1} = x_k + a(x_k) + b(x_k)\varepsilon_k\,, \tag{2.60}$$

$$v_{k+1} = v_k - \frac{1}{2}\sigma^2\lambda + \sigma\xi_k\,, \tag{2.61}$$

$$t_{k+1} = t_k + \mathrm{e}^{v_k}\,. \tag{2.62}$$

From equation (2.61) we see that the potential v performs a simple random walk with a constant drift. When the potential has the value v_k, the time interval that

one needs to wait till the next event is e^{v_k}. Both signal x and the potential v change during the jump at time moment t_k. One can also consider the case where the time interval between events is random, with the average equal to e^{v_k}. We can expect that the randomness of the time interval should not change the PSD of the signal x_t at low frequencies.

2.5 Summary

The nonlinear SDE (1.1) generating signals with $1/f$ spectrum in a wide range of frequencies has been used so far to describe socio-economical systems [77, 78]. The derivation of the equations has been quite abstract and physical interpretation of assumptions made in the derivation is not very clear. In this chapter we propose a physical model where such equations can be relevant. This model is described by Stratonovich (1.2) instead of Itô (1.1) SDE and provides insights which physical systems can be described by such nonlinear SDEs.

We have shown that nonlinear SDEs generating power-law distributed processes with $1/f^{\beta}$ spectrum can result from diffusive particle motion in inhomogeneous medium. The SDE (2.11) for particle coordinate are simplified versions of Langevin equations (2.1), (2.2) for one-dimensional motion of a Brownian particle. We neglected viscosity dependence on temperature and inertia of particle. In general, equations similar to these can be used to describe a variety of systems: noisy electronic circuits, laser light intensity fluctuations [107] and others. We assumed that the inverse temperature $\beta(x)$ depends on coordinate x and this dependence is of a power law form. Such a description is valid for a medium that has reached local thermodynamical equilibrium but not the global one, and the temperature can be considered as a function of coordinate. The power law dependence of the inverse temperature $\beta(x)$ on the stochastic variable x can be caused by non-homogeneity of a bath. This non-homogeneity can arise from a complex scale free structure of the bath as is in the case of porous media [124] or from the bath not being in an equilibrium.

In high friction limit, if the particle is affected by a subharmonic potential proportional to the local temperature, the motion of the particle can be described by the equation similar to equation (1.2). For example, we can consider a Brownian particle affected by a linear potential $V(x)$ and moving in

the medium where steady state heat transfer is present due to the difference of temperatures at the ends of the medium. From the properties of equation (1.2), presented in Chapter 2, it follows that the spectrum of the fluctuations of the particle position $x(t)$ in such a system can have a frequency region where the spectrum has a power-law behavior. The width of this frequency region increases with the increase of the length of the medium in which the particle moves. Equation (1.2) can also describe the fluctuations of the local average of the absolute value of the velocity, if temperature fluctuations are slow and the superstatistical approach can be used. We obtain $1/f$ noise in the fluctuations of the absolute value of the velocity when the velocity distribution has a power-law part $P(v) \sim v^{-3}$ and temperature distribution is flat, $f(\beta) = \text{const}$.

Additionally, we have proposed a pair of coupled nonlinear SDEs (2.26) and (2.27) that generate the signal x_t having the power-law PSD $S(f) \sim f^{-\beta}$ in arbitrarily wide range of frequencies. The exponent β is given by equation (2.28). In contrast to a single nonlinear SDE generating $f^{-\beta}$ noise, the signal x_t generated by the proposed pair of SDEs can have almost arbitrary steady-state PDF. The steady-state PDF of the signal x_t is determined only by the coefficients $a(x)$ and $b(x)$ of the first SDE (2.26). One can interpret the first equation (2.26) as describing the fluctuations of the signal, with the fluctuating rate of change, described by the second equation (2.27). Thus, the proposed SDEs exhibit a separation between the magnitude of the fluctuations of the signal x_t and the rate of fluctuations. We expect that the proposed equations will be useful for the description of $1/f$ noise in various physical and social systems. In addition, the equations can be used to numerical generation of $1/f$ noise with the desired steady-state PDF of the signal.

3 Influence of noise color

One of the characteristics of the noise is the power spectral density (PSD). The white noise has a frequency-independent PSD, whereas the PSD of a colored noise depends on the frequency, the characteristic behavior of the PSD is referred to as a "color" of the noise. There are various applications where the noise in the physical system under investigation has a non-trivial spatio-temporal structure and where it is not realistic to model it is as a white noise process. For example, for a Brownian particle the driving noise is actually colored, i.e. it has a characteristic non-zero correlation time τ on a short time-scale of the order of tens of nanoseconds [125]. Noise color arises due entrainment of fluid around diffusing particle. The particle accelerates the entrained fluid and this acceleration depends on the past motion of the particle and introduce an inertial memory effect [126].

The influence of the colored noise on the dynamics of a Brownian particle immersed in a fluid where a temperature gradient is present can lead to interesting phenomena. The particle can exhibit a directed motion in response to the temperature gradient. Furthermore, study of stationary particle distribution shows that particles can accumulate towards the colder (positive thermophoresis) or the hotter (negative thermophoresis) regions depending on their physical parameters and, in particular, on the dependence of their mobility on the temperature [127]. The velocity of this motion can vary both in magnitude and sign, as observed in experiments [128]. However, in this case, no external force is actually acting on the particles [129]. Theoretical models suggest [127] the presence of a colored noise, as opposed to a white noise, is crucial for the emergence of such thermophoretic effects. Analysis of the steady-state dynamics of an overdamped classical particle in asymmetric multidimensional potential driven by the noise with an arbitrary correlation function has shown that the correlated noise breaks detailed balance, thereby exploiting the spatial asymmetries in potential to produce local drifts and rotations [130]. These interesting findings motivated us to investigate the motion of a Brownian particle in an inhomogeneous environment and subjected to a colored noise, as opposed to a white noise.

3.1 Adiabatic approximation for system affected by colored noise

A system subjected to the colored noise is described by the Langevin equation with a time-dependent stochastic force that includes the influence of the "bath" of surrounding molecules:

$$\frac{\mathrm{d}x}{\mathrm{d}t} = f(x) + g(x)\varepsilon(t)\,. \tag{3.1}$$

It is a well known result that if we approximate white noise by a smooth, colored process, then at the limit as the correlation time of the approximation tends to zero, the smoothed stochastic integral converges to the Stratonovich stochastic integral [131]. We assume that the stochastic force in equation (3.1) is a Gaussian noise having correlation time comparable with time scale of the macroscopic motion and that $\varepsilon(t)$ is Markovian process. In such a case the noise ε satisfies Ornstein-Uhlenbeck process with exponential correlation function [132]. Thus we describe the system perturbed by a colored noise as two-dimensional Markovian flow:

$$\frac{\mathrm{d}x}{\mathrm{d}t} = f(x) + g(x)\varepsilon\,, \tag{3.2}$$

$$\frac{\mathrm{d}\varepsilon}{\mathrm{d}t} = -\frac{1}{\tau}\varepsilon + \frac{\sqrt{2D}}{\tau}\xi(t)\,. \tag{3.3}$$

Here $\xi(t)$ is the white noise, $\langle \xi(t)\xi(s)\rangle = \delta(t-s)$, the parameter τ is the correlation time of the colored noise and D is the noise intensity. The autocorrelation function of the colored noise is

$$\langle \varepsilon(t)\varepsilon(s)\rangle = \frac{D}{\tau}\exp\left(-\frac{|t-s|}{\tau}\right)\,. \tag{3.4}$$

It is possible to write two dimensional Fokker-Planck equation for equations (3.2), (3.3) and obtain two dimensional $P(x,\varepsilon)$ density as its solution. However, usually it is enough to know the distribution $P(x)$ of the signal x, which can be formally obtained by averaging $P(x,\varepsilon)$ over the noise ε. It is problematic even get approximate analytical solutions for $P(x,\epsilon)$ [133]. More convenient way is to get $P(x)$ from an approximate Fokker-Planck equation just for one variable. Such equation can be obtained by using the unified colored noise

approximation [134], which is a form of adiabatic approximation. To make this approximation we eliminate the variable ε and get the equation

$$\frac{\mathrm{d}^2x}{\mathrm{d}t^2} = \frac{g'(x)}{g(x)}\left(\frac{\mathrm{d}x}{\mathrm{d}t}\right)^2 - \left(\frac{1}{\tau} - f'(x) + f(x)\frac{g'(x)}{g(x)}\right)\frac{\mathrm{d}x}{\mathrm{d}t} + \frac{1}{\tau}f(x) + \frac{\sqrt{2D}}{\tau}g(x)\xi(t)\,. \quad (3.5)$$

We assume that the variable x changes slowly and drop small terms containing $\mathrm{d}^2x/\mathrm{d}t^2$ and $(\mathrm{d}x/\mathrm{d}t)^2$, obtaining the approximate equation

$$\frac{\mathrm{d}x}{\mathrm{d}t} = \frac{f(x)}{1-\tau\left(f'(x) - f(x)\frac{g'(x)}{g(x)}\right)} + \frac{\sqrt{2D}g(x)}{1-\tau\left(f'(x) - f(x)\frac{g'(x)}{g(x)}\right)}\xi(t)\,. \quad (3.6)$$

This equation should be interpreted in the Stratonovich sense. In more general case, when we cannot neglect inertia and drop the second derivative d^2x/dt^2, the question whether the equation obtained using adiabatic approximation should be interpreted in Itô or Stratonovich sense still remains an open question, so called Itô-Stratonovich problem [135]. However, at least for specific systems in white noise limit, it can be determined which interpretation is correct. For example, it has been shown for a simplified model of the preferential concentration of inertial particles in a turbulent velocity field [136], that the equation obtained using adiabatic elimination in white noise limit became the Stratonovich equation [137]. The Stratonovich interpretation should be used if the correlation time of the noise is much larger than the relaxation rate of the system. In an opposite case the equation should be interpreted in Itô sense. If relaxation rates are of the similar magnitude as the correlation time, we get an equation with noise induced drift that is different from Stratonovich drift.

The Fokker-Planck equation corresponding to the Stratonovich equation $\mathrm{d}x/\mathrm{d}t = f_\mathrm{c}(x) + g_\mathrm{c}(x)\xi(t)$ is [83]

$$\frac{\partial}{\partial t}P(x,t) = -\frac{\partial}{\partial x}f_c(x)P(x,t) + \frac{1}{2}\frac{\partial}{\partial x}g_c(x)\frac{\partial}{\partial x}g_c(x)P(x,t)\,. \quad (3.7)$$

The applicability of equations (3.6) and (3.7) has limitation due to neglect of higher order derivatives in equation (3.5). These equations describe the dynamics correctly [134] for times t obeying

$$t \gg \frac{\tau}{1-\tau\left(f'(x) - f(x)\frac{g'(x)}{g(x)}\right)} \quad (3.8)$$

and in the space regions obeying

$$\frac{\sqrt{2D\tau}g(x)}{1-\tau\left(f'(x)-f(x)\frac{g'(x)}{g(x)}\right)}\left|\frac{f'(x)}{f(x)}\right| \ll 1\,. \tag{3.9}$$

3.2 Influence of colored noise on the SDE generating signals with $1/f$ spectrum

If the nonlinear SDE generating signals with $1/f$ spectrum is a result of a Brownian motion in an inhomogeneous medium then the finite correlation time of the "bath" can become important. Instead of white noise we add colored noise $\varepsilon(t)$ to the Stratonovich equation (1.2) obtaining the equations

$$\frac{\mathrm{d}x}{\mathrm{d}t} = \frac{1}{2}\sigma^2(\eta-\lambda)x^{2\eta-1} + \sigma x^\eta \varepsilon(t)\,, \tag{3.10}$$

$$\frac{\mathrm{d}\varepsilon}{\mathrm{d}t} = -\frac{1}{\tau}\varepsilon + \frac{1}{\tau}\xi(t)\,. \tag{3.11}$$

After unified colored noise approximation (3.6) we get

$$\frac{\mathrm{d}x}{\mathrm{d}t} = \frac{\frac{1}{2}\sigma^2(\eta-\lambda)x^{2\eta-1}}{1-\frac{1}{2}\tau\sigma^2(\eta-1)(\eta-\lambda)x^{2(\eta-1)}} + \frac{\sigma x^\eta}{1-\frac{1}{2}\tau\sigma^2(\eta-1)(\eta-\lambda)x^{2(\eta-1)}}\xi(t)\,. \tag{3.12}$$

If τ is large then equation (3.12) has a simpler form

$$\frac{\mathrm{d}x}{\mathrm{d}t} = -\frac{x}{\tau(\eta-1)} + \frac{2x^{2-\eta}}{\tau\sigma(\eta-1)(\lambda-\eta)}\xi(t)\,. \tag{3.13}$$

Equation (3.12) should be interpreted in the Stratonovich sense. Converting to Itô interpretation [83] we have

$$\mathrm{d}x = \frac{1}{2}\frac{\sigma^2 x^{2\eta-1}}{\gamma(x)}\left[\eta-\lambda+\frac{2-\eta}{\gamma(x)}+\frac{2(\eta-1)}{\gamma(x)^2}\right]\mathrm{d}t + \frac{\sigma x^\eta}{\gamma(x)}\mathrm{d}W_t\,, \tag{3.14}$$

where

$$\gamma(x) \equiv 1-\frac{1}{2}\tau\sigma^2(\eta-1)(\eta-\lambda)x^{2(\eta-1)} \tag{3.15}$$

According to equation (3.9), approximation (3.12) is valid when

$$\frac{\sqrt{\tau}\sigma|2\eta-1|x^{\eta-1}}{1-\frac{1}{2}\tau\sigma^2(\eta-1)(\eta-\lambda)x^{2(\eta-1)}} \ll 1 \tag{3.16}$$

Steady state PDF corresponding to equation (3.12) is

$$P_0(x) \sim x^{-\lambda}\left(1-\frac{1}{2}\tau\sigma^2(\eta-1)(\eta-\lambda)x^{2(\eta-1)}\right)\exp\left[-\frac{1}{4}\tau\sigma^2(\eta-\lambda)^2x^{2(\eta-1)}\right] \quad (3.17)$$

We see that the colored noise introduces an exponential cut-off in the steady state PDF $P_0(x)$ and naturally limits the range of diffusion of the stochastic variable x. The exponential cut-off is at large values of x when $\eta > 1$ and at small values of x when $\eta < 1$.

Comparing equation (3.12) with (1.2) we see that the influence of the finite correlation time τ of the noise can be neglected when

$$\frac{1}{2}\tau\sigma^2|\eta-1||\eta-\lambda|x^{2(\eta-1)} \ll 1\,. \quad (3.18)$$

Let us consider the case $\eta > 1$. Then according to equation (3.18), the influence of the finite correlation time τ of the noise can be neglected when $x \ll x_\tau$, where

$$x_\tau \equiv \left[\frac{2}{\tau\sigma^2(\eta-1)|\eta-\lambda|}\right]^{\frac{1}{2(\eta-1)}} \quad (3.19)$$

If the diffusion is restricted to the region $x_{\min} < x < x_{\max}$ then the spectrum has a power-law part in the frequency range given by (1.7). If $x_\tau > x_{\max}$ we expect no change in the power-law part of the spectrum. If $x_\tau < x_{\max}$ then, replacing the maximum value of x by x_τ we get that the replacement of the white noise by the colored noise leaves the power-law part of the spectrum in the frequency range

$$\sigma^2 x_{\min}^{2(\eta-1)} \ll 2\pi f \ll \frac{2}{\tau(\eta-1)|\eta-\lambda|}\,. \quad (3.20)$$

If $\eta < 1$ then the influence of the finite correlation time τ of the noise can be neglected when $x \gg x_\tau$, where x_τ is given by (3.19). When the diffusion is restricted to the region $x_{\min} < x < x_{\max}$, we expect no change in the power-law part of the spectrum when $x_\tau < x_{\min}$. If $x_\tau > x_{\min}$ then replacing the minimum value of x by x_τ in equation (1.7) we can estimate that the power-law part of the spectrum should be in the frequency range

$$\sigma^2 x_{\max}^{-2(1-\eta)} \ll 2\pi f \ll \frac{2}{\tau(1-\eta)|\eta-\lambda|}\,. \quad (3.21)$$

Thus the introduction of the colored noise into equation (1.2) can narrow the

range of frequencies where the PSD behaves as $1/f^{\beta}$ by decreasing the upper limiting frequency.

3.3 Numerical solution

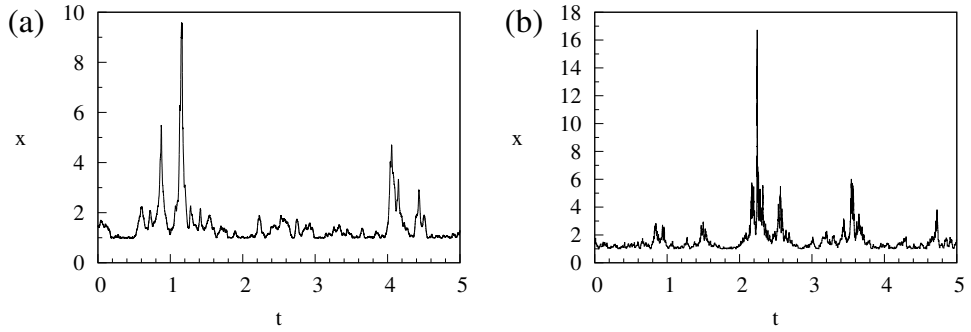

Figure 5: (a) Typical signal generated by equations (3.10), (3.11) with $\tau = 0.01$. (b) Typical signal generated by equation (1.2) corresponding to $\tau = 0$ (white noise). We used reflective boundaries at $x_{\min} = 1$ and $x_{\max} = 1000$. Other parameters of equations are $\eta = 2$, $\lambda = 3$, and $\sigma = 1$.

To check the validity of the approximations we performed numerical solution of equations (3.10), (3.11). For numerical solution we used the variable time step method presented in Chapter 1.1

As an example, we solve equations (3.10), (3.11) with the parameters $\eta = 2$, $\lambda = 3$, $\sigma = 1$ and reflective boundaries at $x_{\min} = 1$, $x_{\max} = 1000$. The generated signal is shown in figure 5. We see that the finite correlation time τ of the noise leads to a smoother signal compared to the equation with $\tau = 0$. The steady state PDF $P_0(x)$ and the power spectral density $S(f)$ for two different values of τ are presented in figure 6. From figure 6a we see that the unified colored noise approximation correctly predicts the exponential cut-off in the steady state PDF at large values of x, although the actual position of the cut-off slightly differs from the cut-off predicted by equation (3.17). As figure 6b shows, the presence of the finite correlation time τ makes the power-law part in the spectrum narrower. The upper limiting frequency of the power-law region grows with decreasing of τ, as is qualitatively predicted by equation (3.20). The steady state PDF and the PSD of the generated signal corresponding to much smaller value of the correlation time τ are shown in figure 6b,d. For this value of τ the exponential cut-off due to finite correlation time is larger than the upper

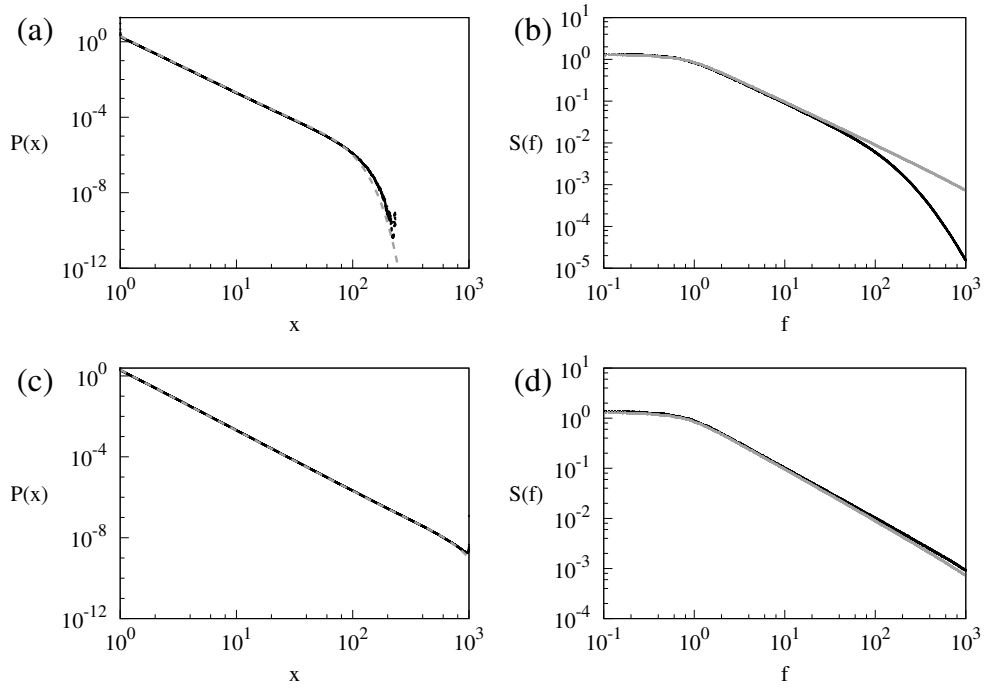

Figure 6: (a,c) The steady-state PDF of the signal generated by equations (3.10) and (3.11) with reflective boundaries at $x_{\min}$ and $x_{\max}$. The dashed line shows analytical approximation (3.17). (b,d) The PSD of such a signal. The gray line shows the PSD of the signal generated by equation (1.2). The correlation time is (a,b) $\tau = 10^{-3}$, (c,d) $\tau = 10^{-5}$. Other parameters are $\eta = 2$, $\lambda = 3$, $x_{\min} = 1$, $x_{\max} = 1000$, and $\sigma = 1$.

boundary $x_{\max}$, thus we see almost no differences from the case of uncorrelated noise, $\tau = 0$.

3.4 Summary

The correlation of collisions between the Brownian particle and the surrounding molecules can lead to the situation where the finite correlation time becomes important, thus we have investigated the effect of colored noise in our model. Using the unified colored noise approximation we get that the finite correlation time leads to the additional restriction of the diffusion. Existence of colored noise leads to an exponential cut-off of the PDF of particle positions either from large values when $\eta > 1$, or from small values when $\eta < 1$. Such a restriction of the diffusion is a result of the multiplicative colored noise in equation (3.10). Narrower power law part in the PDF of the particle positions results in the narrower range of frequencies where the spectrum has $1/f^{\beta}$ behavior. When $\eta > 1$, the end of the power-law part of the spectrum at large frequencies is inversely proportional to the correlation time τ of the noise. However, for sufficiently small correlation time, when the restriction of the diffusion due to colored noise is larger than the upper boundary $x_{\max}$ of the medium, the effects of the colored noise are negligible (see figure 6) and the properties of the signal do not differ significantly from the white noise case.

4 Generalization of nonlinear SDE generating 1/f noise

The Lévy α-stable distributions, characterized by the index of stability $0 < \alpha \leqslant 2$, constitute the most general class of stable processes. The Gaussian distribution is their special case, corresponding to $\alpha = 2$. If $\alpha < 2$, the Lévy stable distributions have power-law tails $\sim 1/x^{1+\alpha}$. There are many systems exhibiting Lévy α-stable distributions: distribution function of turbulent magnetized plasma emitters [18] and step-size distribution of photons in hot vapors of atoms [19] have Lévy tails; theoretical models suggest that velocity distribution of particles in fractal turbulence is Lévy stable distribution [138] or at least has Lévy tails [139]. If system behavior depends only on large noise fluctuations, such noise intensity distributions can be approximated by Lévy stable distribution, leading to Lévy flights. Lévy flights can be found in many physical systems: as an example we can point out anomalous diffusion of Na adatoms on solid Cu surface [7], anomalous diffusion of a gold nanocrystal, adsorbed on the basal plane of graphite [8] and anomalous diffusion in optical lattices [140]. Lévy flights can be modeled by the fractional Fokker-Planck equations [4] or Langevin equations with Lévy stable noise.

The purpose of this chapter is to generalize nonlinear SDEs driven by the Gaussian noise and generating signals with $1/f$ PSD by replacing the Gaussian noise with a more general Lévy stable noise. The previously proposed SDEs then arise as a special case when $\alpha = 2$. We can expect that this generalization may be useful for describing $1/f$ fluctuations in the systems subjected to Lévy stable noise.

4.1 SDEs driven by Lévy noise

Nonlinear stochastic differential equations (SDEs) with additive Lévy stable noise have been explored quite extensively for the past 15 years [141–143]. Such stochastic differential equations lead to the fractional Fokker-Planck equations with constant diffusion coefficient. Models with multiplicative Lévy stable noise have been used for modeling inhomogeneous media [9], ecological population density with fluctuating volume of resources [144]. The relation be-

tween the Langevin equation with multiplicative Lévy stable noise and fractional Fokker-Planck equation has been introduced in Ref. [12], where Langevin equation is interpreted in Itô sense [13]. The relation between these two equations is not known in Stratonovich interpretation. Fractional Fokker-Planck equation models have been applied to model enzyme diffusion on polymer chain [145] and some cases of anomalous diffusion [25]. However, application of SDEs driven by Lévy stable noise can be problematic. We can always write Fokker-Planck equation corresponding to Langevin equation driven by the Gaussian noise and vice versa, but such statement is not always true for the Langevin equation with Lévy stable noise. For example, particle (enzyme) dispersion on rapidly folding random heteropolymer can be described by space fractional Fokker-Planck equation [14], but for such equation counterpart Langevin equation has not been found [15] and might not even exit [16].

We consider the Langevin equation with Lévy stable noise of the form [4, 146, 147]

$$\frac{dx}{dt} = a(x) + b(x)\xi(t)\,. \tag{4.1}$$

SDE (4.1) should be interpreted into Itô sense. Here $a(x)$ describes the deterministic drift term and $b(x)$ describes the amplitude of the noise. The stochastic force $\xi(t)$ is uncorrelated white noise, $\langle \xi(t)\xi(t')\rangle = \delta(t-t')$ and is characterized by Lévy α-stable distribution. For simplicity we only use symmetric stable distributions, for this reason we take the characteristic function of $\xi(t)$ as

$$\langle \exp(ik\xi)\rangle = \exp(-\sigma^{\alpha}|k|^{\alpha})\,, \tag{4.2}$$

where σ is the scale parameter and α is the index of stability. The Lévy α-stable distributions arise form generalized central limit theorem and constitute the most general class of stable processes. These distributions are characterized by the index of stability $0 < \alpha \leqslant 2$. The Gaussian distribution corresponds to a special case when $\alpha = 2$, whereas the Lévy stable distributions have power-law tails $\sim 1/x^{1+\alpha}$ for $\alpha < 2$. There are many systems exhibiting such power law-tails: for example, distribution function of turbulent magnetized plasma emitters [18] and step-size distribution of photons in hot vapors of atoms [19] have Lévy tails; theoretical models impose that velocity distribution of particles in fractal turbulence is Lévy stable distribution [138] or at least has Lévy tails [139]. If properties of a system system subjected to noise depend mainly only on

large noise fluctuations, such noise intensity distributions can by approximated by Lévy stable distribution, leading to Lévy flights. Eq. (4.1) can also be written in the form

$$dx = a(x)dt + b(x)dL_t^\alpha \,, \tag{4.3}$$

where dL_t^α stands for the increments of Lévy α-stable motion L_t^α [20, 148]. It is easier to calculate the steady state PDF of the signal x by using the space fractional Fokker-Planck equation instead of stochastic differential equation (4.1). The fractional Fokker-Planck equation corresponding to Eq. (4.1) is [12, 149]

$$\frac{\partial}{\partial t}P(x,t) = -\frac{\partial}{\partial x}a(x)P(x,t) + \sigma^\alpha \frac{\partial^\alpha}{\partial |x|^\alpha} b(x)^\alpha P(x,t)\,. \tag{4.4}$$

The operator $\partial^\alpha/\partial|x|^\alpha$ is the Riesz-Weyl fractional derivative. The Riesz-Weyl fractional derivative acting on the function $f(x)$ is defined by its Fourier transform [150],

$$\mathcal{F}\left[\frac{\partial^\alpha}{\partial|x|^\alpha} f(x)\right] = -|k|^\alpha \tilde{f}(k)\,. \tag{4.5}$$

The SDE (4.1) having multiplicative noise with the power-law dependence of the noise amplitude $b(x)$ on the signal size and generating signals with the power law steady state PDF

$$P_0(x) \sim x^{-\lambda}\,, \tag{4.6}$$

has recently been proposed in Ref. [A1]. The proposed equation has the form

$$dx = \sigma^\alpha \gamma x^{\alpha(\eta-1)+1}dt + x^\eta dL_t^\alpha \,, \tag{4.7}$$

where the coefficient γ is given by the equation

$$\gamma = \frac{\sin\left[\pi\left(\frac{\alpha}{2} - \alpha\eta + \lambda\right)\right]}{\sin[\pi(\alpha(\eta-1)-\lambda)]} \frac{\Gamma(\alpha\eta - \lambda + 1)}{\Gamma(\alpha(\eta-1)-\lambda+2)}\,. \tag{4.8}$$

The special case of Eq. (4.7) for free particle ($a(x) = 0$) with Lévy stable noise having $\alpha < 2$ has been derived from coupled continuous time random walk (CTRW) models [25], when jumping rate ν of CTRW process depends on signal intensity as $\nu(x) = x^{\alpha\eta}$, $x > 0$. It has been obtained in Ref. [A4] that the power law exponent λ of the steady state PDF should take the values from the interval

$$\alpha(\eta-1) + 1 < \lambda < \alpha\eta + 1\,. \tag{4.9}$$

In fact, this condition assures that the values of the parameters in equation (4.8) are outside of the poles.

If $\lambda > 1$ then the steady state PDF $P_0(x)$ diverges as $x \to 0$. The requirement of the stationarity of the process leads to the necessity to restrict the diffusion in some finite interval of values. Thus the SDE (4.7) should be considered together with the appropriate restrictions of the diffusion. The simplest choice of restriction is provided by the reflective boundaries at $x = x_{\min}$ and $x = x_{\max}$. Nevertheless, other forms of restrictions are possible by introducing additional terms in the drift term of Eq. (4.7).

Eq. (4.7) is a generalization of the nonlinear SDE with Gaussian noise proposed in [74, 75]. As a particular case, when $\alpha = 2$ then the expression (4.8) for the coefficient γ simplifies to $(2\eta - \lambda)$ and from Eq. (4.7) we get previously proposed SDE with the Gaussian noise [74, 75]

$$dx = \sigma^2(2\eta - \lambda)x^{2\eta-1}dt + x^\eta dL_t^2\,. \tag{4.10}$$

According to the definition (4.2), the scale parameter σ differs from the standard deviation of the Gaussian noise. Another simple case is when $\alpha = 1$. For $\alpha = 1$ Eq. (4.7) becomes

$$dx = \sigma\cot[\pi(\lambda - \eta)]x^\eta dt + x^\eta dL_t^1\,. \tag{4.11}$$

Recently it was suggested that the non-homogeneity arising from the bath not being in an equilibrium can be described by the dependence of the diffusion coefficient on the particle coordinate x [A2]. For example, if $\eta = 1/2$, Eq. (4.10) describes the diffusion of a Brownian particle in a medium where steady state heat transfer is present due to the difference of temperatures at the ends of the medium. The appropriate choice of γ (Eq. (4.8)) preserves original scaling properties of the signal as Lévy stable noise is introduced instead of Gaussian noise. Therefore, Eq. (4.7) should apply to Brownian motion in non-homogeneous media in presence of anomalous scaling.

4.2 Estimation of the power spectral density

The power law exponent of the PSD can be estimated by using the approximate scaling properties of the signals, as it is done in the Appendix A of Ref. [151] and in Ref. [85]. The PSD can be obtained from the autocorrelation function $C(t)$ by using Wiener-Khintchine theorem. The autocorrelation function can be calculated using the steady state PDF $P_0(x)$ and the transition probability $P(x', t|x, 0)$ [83]:

$$C(t) = \int dx \int dx'\, xx' P_0(x) P(x', t|x, 0)\,. \tag{4.12}$$

The transition probability (the conditional probability that at time t the signal has value x' with the condition that at time $t = 0$ the signal had the value x) can be obtained from the solution of the fractional Fokker-Planck equation (4.4) with the initial condition $P(x', t = 0|x, 0) = \delta(x' - x)$.

The Lévy α-stable motion has the increments dL_t^α with the scaling property $dL_{at}^\alpha = a^{1/\alpha} dL_t^\alpha$ [148]. By introducing the scaled time $t_s = a^{\alpha(\eta-1)}t$ or changing the variable x in Eq. (4.7) to the scaled variable $x_s = ax$ we get the same resulting equation. Thus change of the time scale and change of the scale of the variable x are equivalent, leading to the scaling property of the transition probability

$$aP(ax', t|ax, 0) = P(x', a^\mu t|x, 0)\,. \tag{4.13}$$

The exponent μ is

$$\mu = \alpha(\eta - 1)\,. \tag{4.14}$$

In Ref. [85] it has been shown that the steady state PDF $P_0(x) \sim x^{-\lambda}$ and the scaling property of the transition probability (6.3) lead to the power law form of the PSD $S(f) \sim f^{-\beta}$ in a wide range of frequencies. The power law exponent in the PSD of the signal generated by SDE (4.7) is

$$\beta = 1 + \frac{\lambda - 3}{\alpha(\eta - 1)}\,. \tag{4.15}$$

This equation is valid when the resulting β has values in the interval $0 < \beta < 2$. Eq. (4.15) is a generalization of the expression for the power law exponent in the PSD with $\alpha = 2$ obtained in Ref. [75]. From Eq. (4.15) it follows that we get

$1/f$ PSD when $\lambda = 3$.

Due to restrictions of diffusion at $x = x_{\min}$ and $x = x_{\max}$ the scaling (4.13) is not exact. This limits the power law part of the PSD to a finite range of frequencies $f_{\min} \ll f \ll f_{\max}$. Note, that pure $1/f^{\beta}$ PSD is physically impossible because the total power would be infinite. Therefore we consider signals with PSD having $1/f^{\beta}$ behaviour only in some wide intermediate region of frequencies, $f_{\min} \ll f \ll f_{\max}$, whereas for small frequencies $f \ll f_{\min}$ the PSD is bounded. We can estimate the limiting frequencies similarly as in Ref. [85]. Taking into consideration the reflective boundaries $x_{\min}$ and $x_{\max}$ the autocorrelation function has the scaling property [85]

$$C(t; ax_{\min}, ax_{\max}) = a^2 C(a^{\mu}t, x_{\min}, x_{\max})\,. \tag{4.16}$$

From this equation it follows that time t in the autocorrelation function should enter only in combinations with the limiting values, $x_{\min}t^{1/\mu}$ and $x_{\max}t^{1/\mu}$. One can expect that the influence of the limiting values is negligible when the first combination is small and the second large. This limits the time t to the interval $\sigma^{-\alpha}x_{\max}^{\alpha(1-\eta)} \ll t \ll \sigma^{-\alpha}x_{\min}^{\alpha(1-\eta)}$. Then the frequency range where the PSD has $1/f^{\beta}$ behaviour can be estimated as

$$\sigma^{\alpha}x_{\min}^{\alpha(\eta-1)} \ll 2\pi f \ll \sigma^{\alpha}x_{\max}^{\alpha(\eta-1)}\,. \tag{4.17}$$

Eq. (4.17) shows that the frequency range grows with increasing of the difference of the exponent η from 1. The frequency range becomes zero when $\eta = 1$. One can get arbitrarily wide range of the frequencies where the PSD has $1/f^{\beta}$ behaviour by increasing the ratio $x_{\max}/x_{\min}$. Unfortunately, the numerical calculation shows that the estimation of the frequency range given by Eq. (4.17) is too wide.

4.3 Method of numerical solution

It was rigorously proven by numerical simulations and algorithm convergence analysis that Euler's scheme can be used for stochastic differential equations with Lévy α stable process [148, 152] and even for more complicated case when both time and space derivatives are fractional in the corresponding

Fokker-Planck equation [153]. Therefore, we transform differential equations to difference equation by using Euler's approximation scheme. The difference equation

$$x_{k+1} = x_k + \sigma^\alpha \gamma x_k^{\alpha(\eta-1)+1} h_k + x_k^\eta h_k^{1/\alpha} \xi_k^\alpha \,, \tag{4.18}$$

corresponding to Eq. (4.7). We interpret the stochastic integral in Itô sense, because the relation between the Langevin equation Eq. (4.1) and the Fokker-Planck equation is known only in Itô interpretation. However an attempt to use Stratonovich interpretation also has been made [13]. Here $h_k = t_{k+1} - t_k$ is the discrete time step and ξ_k^α is a random variable having α-stable Lévy distribution with the characteristic function (4.2). The Eq. (4.18) could be solved numerically with the constant step $h_k = \mathrm{const}$. When $\eta > 1$ the coefficients in the equation become large at large values of x, thus a very small time step is needed. It is more efficient to use a variable time step, as has been done solving SDE with Gaussian noise in Ref. [74]. We choose the time step in such a way that the change of the variable x_k in one step is proportional to the value of the variable x. If we consider the variable step of integration such as

$$h_k = \frac{\kappa^\alpha}{\sigma^\alpha} x_k^{-\alpha(\eta-1)} \,, \tag{4.19}$$

Eq. (4.18) simplifies to

$$x_{k+1} = x_k + \kappa^\alpha \gamma x_k + \frac{\kappa}{\sigma} x_k \xi_k^\alpha \,. \tag{4.20}$$

Here $\kappa \ll 1$ must be a small parameter. We get very similar numerical results by using the Milstein approximation.

We introduce the reflective boundaries at $x = x_{\min}$ and $x = x_{\max}$ using the projection method [154, 155]. The projection method is realized as follows, if the variable x_{k+1} acquires the value outside of the interval $[x_{\min}, x_{\max}]$ then the value of the nearest reflective boundary is assigned to x_{k+1}.

When $\lambda = 3$, we get that $\beta = 1$ and SDEs (4.7), (4.10), (4.11) should give a signal exhibiting $1/f$ fluctuations. As an example, we will solve numerically the SDE (4.7) with the index of stability of Lévy stable noise $\alpha = 1.5$ and the exponent of the steady state PDF $\lambda = 3$. In addition, we include the reflective boundaries at $x = x_{\min}$ and $x = x_{\max}$. The numerical results are presented in Fig. 7. We use a variable step integration sampled on constant time step

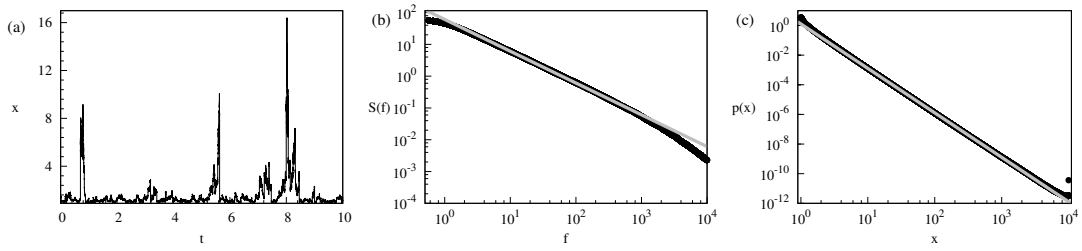

Figure 7: (a) Signal generated by SDE with Lévy stable noise (4.11) with reflective boundaries at $x = x_{\min}$ and $x = x_{\max}$. (b) Steady state PDF $P_0(x)$ of the signal. The gray line shows the slope x^{-3}. (c) Power spectral density $S(f)$ of the signal. The gray line shows the slope $1/f$. Parameters used are $\alpha = 1$, $\lambda = 3$, $\eta = 1.8$, $x_{\min} = 1$, $x_{\max} = 10^4$, $\sigma = 1$.

equal to 10^{-5}. The generated signal is shown in Fig. 7a. In the signal we can see large peaks or bursts corresponding to the large deviations of the variable x. Comparison of the steady state PDF $P_0(x)$ with the analytical power law estimation $\sim x^{-3}$ is shown in Fig. 7b. The steady state PDF deviates from the power law prediction near reflecting boundaries. Such increase of the steady state PDF near boundaries is typical for equations with Lévy stable noise having $\alpha < 2$ [143] and is similar to the behaviour of the analytical expression obtained in Ref. [143] for the simplest stochastic differential equation Lévy stable noise having constant noise amplitude and zero drift.

Comparison of the PSD $S(f)$ with the analytical estimation $S(f) \sim 1/f$ is shown in Fig. 7c. This comparison confirms the presence of the frequency region for which the PSD has $1/f$ dependence. The width of this region increases as increase the ratio between the minimum and the maximum values of the stochastic variable x. Furthermore, the region in the PSD with the power law behaviour depends on α and the exponent η: the width increases with increasing the difference $\eta - 1$ and increasing α; when $\eta = 1$ then this width is zero. Such behaviour is quantitatively predicted by Eq. (4.17). However, Eq. (4.17) predicts too wide frequency range. The numerical estimation of the dependence of the $1/f^{\beta}$ PSD frequency range on the parameters of the SDEs4.8 In Ref. [A4].

4.4 Summary

We have proposed nonlinear SDEs with Lévy stable noise and generating signals exhibiting $1/f$ noise in any desirably wide range of frequency. Proposed SDEs (4.7) and (5.69) are a generalization of nonlinear SDEs driven by Gaussian

noise and generating signals with $1/f$ PSD. The generalized equations can be obtained by replacing the Gaussian noise with the Lévy stable noise and changing the drift term to preserve statistical properties of the generated signal. We have investigated two cases: in the first case the stochastic variable can acquire only positive values (SDE (4.7)), in the second case the stochastic variable can also be negative (SDEs (5.69)). In contrast to the SDEs with the Gaussian noise, the constant in the drift term, given by Eqs. (4.8) is different in those two cases and becomes the same only for $\alpha = 2$.

The analytical estimation (4.17) of the frequency range where the spectrum has $1/f^{\beta}$ behaviour does not coincide with the numerical calculations. In this chapter we numerically investigated how this frequency range depends on the parameters of the SDE. We show that, in contrast to Eq. (4.17), the width of this frequency range depends not only on the exponent of the multiplicative noise η but also on the power law exponent of the steady state distribution λ.

Nonlinear SDEs with Lévy noise similar to Eq. (4.10) have been used to investigate the wide-spectrum energy harvesting out of colored fluctuations in monostable piezoelectric transducers [156]. The system has been modeled as a linear oscillator disturbed by $1/f^{\beta}$ noise. It has been shown that for noisy linear oscillator the efficiency of the noise energy conversion process depends only on the correlation time and the bandwidth of the noise and not on the noise amplitude [157]. We expect that knowledge of the size of $1/f$ noise frequency range bandwidth can be useful for various applications for such noisy electronic circuits.

5 PSD of signals generated by time-subordinated nonlinear Langevin equations

Continuous time random walks (CTRWs) with on-site waiting-time distributions falling slowly as $t^{-\alpha-1}$ and lacking the first moment predicts a subdiffusive behavior and is a powerful tool to describe systems which display subdiffusion [2, 30]. Starting from the generalized master equation or from the CTRW the fractional Fokker-Planck equation can be rigorously derived [158, 159]. Fractional Fokker-Planck equation provides a useful approach for the description of transport dynamics in complex systems which are governed by anomalous diffusion [2] and nonexponential relaxation patterns [160]. It has been used to model dynamics of protein systems and for reactions occurring in disordered media [2, 161–167]. Description equivalent to a fractional Fokker-Planck equation consist of a Markovian dynamics governed by an ordinary Langevin equation but proceeding in an auxiliary, operational time instead of the physical time [168]. This Markovian process is subordinated to the process defining the physical time; the subordinator introduces memory effects [4]. Other approaches for the theoretical description of the subdiffusion use the generalized Langevin equation [169–171], fractional Brownian motion [172], or the Langevin equation with multiplicative noise [9].

In the homogeneous systems the power spectral density (PSD) of the signals generated by time-subordinated Langevin equations has power-law dependency $S(f) \sim f^{\alpha-1}$ on the frequency as $f \to 0$. [173]. Since $0 < \alpha < 1$, the power-law exponent $1 - \alpha$ is smaller than 1. The purpose of this chapter is to consider the PSD in nonhomogeneous systems exhibiting anomalous diffusion. We demonstrate, that in such systems the PSD can have power-law behavior with the exponent equal to or larger than 1 in a wide range of intermediate frequencies.

5.1 Time-fractional Fokker-Planck equation for non-homogeneous media

In this section derive the time-fractional Fokker-Planck equation describing diffusion of a particle in nonhomogeneous media. Usually the description of the anomalous diffusion is given by the CTRW theory assuming heavy-tailed waiting-time distributions between successive jumps of the diffusing particle. Here we use the method of the derivation that is similar to that outlined in Refs. [153, 168]. We start with the Markovian process described by the Itô stochastic differential equation (SDE)

$$\mathrm{d}x(\tau) = a(x(\tau))\mathrm{d}\tau + b(x(\tau))\mathrm{d}W(\tau)\,. \tag{5.1}$$

Here $W(\tau)$ is the standard Brownian motion (Wiener process). The drift coefficient $a(x)$ and the diffusion coefficient $b(x)$ explicitly depend on the particle position x. This dependence on the position reflects the nonhomogeneity of a medium. Following Ref. [168] we interpret the time τ in Eq. (5.1) as an internal, operational time. Equation (5.1) we consider together with an additional equation that relates the operational time τ to the physical time t. The difference between physical time t and the operational time τ occurs due to trapping of the diffusing particle. For the trapping processes that have distribution of the trapping times with power law tails, the physical time $t = T(\tau)$ is given by the the strictly increasing α-stable Lévy motion defined by the Laplace transform

$$\langle \mathrm{e}^{-kT(\tau)} \rangle = \mathrm{e}^{-\tau k^{\alpha}}\,. \tag{5.2}$$

Here the parameter α takes the values from the interval $0 < \alpha < 1$. Thus the physical time t obeys the SDE

$$\mathrm{d}t(\tau) = \mathrm{d}L^{\alpha}(\tau)\,, \tag{5.3}$$

where $\mathrm{d}L^{\alpha}(\tau)$ stands for the increments of the strictly increasing α-stable Lévy motion $L^{\alpha}(\tau)$. For such physical time t the operational time τ is related to the physical time t via the inverse α-stable subordinator [174, 175]

$$S(t) = \inf\{\tau : T(\tau) > t\}\,. \tag{5.4}$$

The processes $x(\tau)$ and $S(t)$ are assumed to be independent. Equations (5.1) and (5.3) define the subordinated process $y(t)$ obtained by a random change of time

$$y(t) = x(S(t))\,. \tag{5.5}$$

The process $y(t)$ describes the diffusion of a particle in a medium with traps.

We will derive the equation for the probability density function (PDF) of y. For the derivation we use the method of Laplace transform. The PDF $P_x(x,\tau)$ of the stochastic variable x as a function of the operational time τ obeys the Fokker-Planck equation corresponding to the Itô SDE (5.1)

$$\frac{\partial}{\partial\tau}P_x(x,\tau) = L_{\mathrm{FP}}(x)P_x(x,\tau)\,, \tag{5.6}$$

where $L_{\mathrm{FP}}(x)$ is the time-independent Fokker-Planck operator [83]

$$L_{\mathrm{FP}}(x) = -\frac{\partial}{\partial x}a(x) + \frac{1}{2}\frac{\partial^2}{\partial x^2}b^2(x)\,. \tag{5.7}$$

The Laplace transform of Eq. (5.6) is

$$k\tilde{P}_x(x,k) - P_x(x,0) = L_{\mathrm{FP}}(x)\tilde{P}_x(x,k)\,. \tag{5.8}$$

Since the processes $x(\tau)$ and $S(t)$ are independent, the PDF of the random process $x(S(t))$ is given by

$$P(x,t) = \int P_x(x,\tau)P_S(\tau,t)\,\mathrm{d}\tau\,. \tag{5.9}$$

Here $P_S(\tau,t)$ is the PDF of the inverse α-stable subordinator $S(t)$. From Eq. (5.9) it follows that the Laplace transform $\tilde{P}(x,k)$ of the PDF $P(x,t)$ is related to the Laplace transform $\tilde{P}_S(\tau,k)$ of the inverse subordinator $S(t)$:

$$\tilde{P}(x,k) = \int P_x(x,\tau)\tilde{P}_S(\tau,k)\,\mathrm{d}\tau\,. \tag{5.10}$$

The Laplace transform $\tilde{P}_S(\tau,k)$ of the inverse subordinator $S(t)$ we obtain as follows: from the definition of the inverse subordinator (5.4) we have $\Pr(S(t) < \tau) = \Pr(T(\tau) \geqslant t)$, therefore

$$P_S(\tau,t) = -\frac{\partial}{\partial\tau}\int_0^t P_T(t',\tau)\,\mathrm{d}t'\,. \tag{5.11}$$

Here $P_T(t,\tau)$ is the PDF of the strictly increasing α-stable Lévy motion $T(\tau)$. The PDF $P_T(t,\tau)$ fulfills the scaling relation

$$P_T(t,\tau) = \frac{1}{\tau^{\frac{1}{\alpha}}} P_T\left(\frac{t}{\tau^{\frac{1}{\alpha}}}, 1\right) , \tag{5.12}$$

since the strictly increasing α-stable Lévy motion is $1/\alpha$ self-similar [20]. Combining Eqs. (5.11) and (5.12) we obtain

$$P_S(\tau,t) = \frac{t}{\alpha\tau} P_T(t,\tau) . \tag{5.13}$$

Consequently, the Laplace transform of $P_S(\tau,t)$ is equal to

$$\tilde{P}_S(\tau,k) = k^{\alpha-1}\mathrm{e}^{-\tau k^\alpha} . \tag{5.14}$$

Here we used Eq. (5.2) for the Laplace transform of $P_T(t,\tau)$.

Using Eqs. (5.10) and (5.14) we get

$$\tilde{P}(x,k) = k^{\alpha-1}\tilde{P}_x(x,k^\alpha) . \tag{5.15}$$

Acting with the operator $L_{\mathrm{FP}}(x)$ on Eq. (5.15) we have

$$\tilde{P}(x,k) = k^{-1}P_x(x,0) + k^{-\alpha}L_{\mathrm{FP}}(x)\tilde{P}(x,k) . \tag{5.16}$$

The inverse Laplace transform of this equation yields

$$P(x,t) = P_x(x,0) + \frac{1}{\Gamma(\alpha)}\int_0^t \mathrm{d}t' \, (t-t')^{\alpha-1} L_{\mathrm{FP}}(x) P(x,t') . \tag{5.17}$$

Introducing the fractional Riemann–Liouville operator [150]

$${}_0D_t^{-\alpha} f(t) \equiv \frac{1}{\Gamma(\alpha)}\int_0^t \frac{f(t')}{(t-t')^{1-\alpha}}\mathrm{d}t' , \qquad 0<\alpha<1 \tag{5.18}$$

we can write Eq. (5.17) as

$$P(x,t) = P_x(x,0) + {}_0D_t^{-\alpha} L_{\mathrm{FP}}(x) P(x,t) \tag{5.19}$$

By differentiating this equation with respect to time we get the time-fractional

Fokker-Planck equation

$$\frac{\partial}{\partial t}P(x,t) = {}_0D_t^{1-\alpha}\left(-\frac{\partial}{\partial x}[a(x)P] + \frac{1}{2}\frac{\partial^2}{\partial x^2}[b^2(x)P]\right), \tag{5.20}$$

where

$${}_0D_t^{1-\alpha}f(t) \equiv \frac{1}{\Gamma(\alpha)}\frac{\partial}{\partial t}\int_0^t \frac{f(t')}{(t-t')^{1-\alpha}}\mathrm{d}t', \qquad 0<\alpha<1 \tag{5.21}$$

The operator ${}_0D_t^{1-\alpha}$ is expressed via the convolution with a slowly decaying kernel, which is typical for memory effects in complex systems [176]. Equation (5.20) is the equation describing the subdiffusion of particles in an inhomogeneous medium. This equation generalizes the previously obtained time-fractional Fokker-Planck equation with the position-independent diffusion coefficient.

5.2 Position-dependent trapping time

The properties of a trap in a nonhomogeneous medium can reflect the structure of the medium. In the description of the transport in such a medium the waiting time should explicitly depend on the position [49]. Instead of Eq. (5.3) we assume that the physical time t is related to the operational time τ via the SDE

$$dt(\tau) = g(x)\mathrm{d}L^\alpha(\tau)\,. \tag{5.22}$$

Here the function $g(x)$ is the intensity of random time and models the position of structures responsible for either trapping or accelerating the particle. Large values of $g(x)$ corresponds to trapping of the particle, whereas small $g(x)$ leads to the acceleration of diffusion. Similar equation has been used in Ref. [49].

Equations (5.1) and (5.22) together define the subordinated process. However, now the processes $x(\tau)$ and $t(\tau)$ are not independent and the previously presented derivation of the Fokker-Planck equation is not applicable. Nevertheless, we can show that also with position dependent trapping time the resulting equation has the form of Eq. (5.20). To do this let us consider the joint PDF $P_{x,t}(x,t;\tau)$ of the stochastic variables x and t. The Fokker-Planck equation describing the evolution of the joint PDF $P_{x,t}(x,t;\tau)$ with the operational time τ has the form

$$\frac{\partial}{\partial \tau}P_{x,t}(x,t;\tau) = L_{\mathrm{FP}}(x)P_{x,t} - {}_0D_t^\alpha g(x)^\alpha P_{x,t}\,. \tag{5.23}$$

The fractional derivative in the last term of the Fokker-Planck equation (5.23) appears as a consequence of the increments of Lévy α-stable motion in Eq. (5.22) [12, 149]. The zero of the physical time t coincides with the zero of the operational time τ, therefore, the initial condition for Eq. (5.23) is $P_{x,t}(x,t;0) = P_x(x,0)\delta(t)$. In addition, since t is strictly increasing, we have a boundary condition $P_{x,t}(x,0;\tau) = 0$ when $\tau > 0$. The fractional Riemann–Liouville operator ${}_0D_t^\alpha$ in Eq. (5.23) we can write as ${}_0D_t^\alpha = \frac{\partial}{\partial t}{}_0D_t^{\alpha-1}$.

Now let us consider x and τ as stochastic variables instead of x and t. Since the stochastic variable t is related to the operational time τ via Eq. (5.22), the joint PDF $P_{x,\tau}(x,\tau;t)$ of the stochastic variables x and τ is related to the PDF $P_{x,t}(x,t;\tau)$ according to the equation

$$P_{x,\tau}(x,\tau;t) = {}_0D_t^{\alpha-1} g(x)^\alpha P_{x,t}(x,t;\tau)\,. \tag{5.24}$$

This equation can be obtained by noting that the last term in Eq. (5.23) contains derivative $\frac{\partial}{\partial t}$ and thus should be equal to $-\frac{\partial}{\partial t}P_{x,\tau}$. From Eq. (5.24) if follows that

$$P_{x,t} = {}_0D_t^{1-\alpha}\frac{1}{g(x)^\alpha}P_{x,\tau}\,. \tag{5.25}$$

Using Eqs. (5.23) and (5.25) we obtain

$$\frac{\partial}{\partial t}P_{x,\tau}(x,\tau;t) = {}_0D_t^{1-\alpha}L_{\mathrm{FP}}(x)\frac{1}{g(x)^\alpha}P_{x,\tau} - \frac{\partial}{\partial\tau}{}_0D_t^{1-\alpha}\frac{1}{g(x)^\alpha}P_{x,\tau} \tag{5.26}$$

The PDF $P_{x,\tau}$ has the initial condition $P_{x,\tau}(x,\tau;0) = P_x(x,0)\delta(\tau)$ and the boundary condition $P_{x,\tau}(x,0;t) = 0$. The PDF of the subordinated random process $x(t)$ is $P(x,t) = \int P_{x,\tau}(x,\tau;t)\,d\tau$. Integrating both sides of Eq. (5.26) we get

$$\frac{\partial}{\partial t}P(x,t) = {}_0D_t^{1-\alpha}L'_{\mathrm{FP}}(x)P\,, \tag{5.27}$$

where the new Fokker-Planck operator is

$$L'_{\mathrm{FP}}(x) = -\frac{\partial}{\partial x}a'(x) + \frac{1}{2}b'(x)^2\,. \tag{5.28}$$

Here the new drift and the diffusion coefficient are

$$a'(x) = \frac{a(x)}{g(x)^\alpha}\,, \qquad b'(x) = \frac{b(x)}{g(x)^{\frac{\alpha}{2}}}\,. \tag{5.29}$$

Thus position-dependent trapping leads to position-dependent coefficients in the time-fractional Fokker-Planck equation, even if the initial SDE (5.1) has constant coefficients.

5.3 Power spectral density and time-fractional Fokker-Planck equation

In this section we derive a general expression for the PSD of the fluctuations of the diffusing particle in nonhomogeneous medium. The evolution of the PDF of particle position x is described by the time-fractional Fokker-Planck equation (5.20). For calculation of the spectrum we use the eigenfunction expansion of the Fokker-Planck operator L_{FP}. Method of eigenfunctions for solving of time-dependent fractional Fokker-Planck equation has been used in Ref. [177]. Spectrum of fluctuations when the diffusion coefficient is constant has been obtained in Ref. [173]. Similar derivation of the spectrum for nonlinear SDE has been performed in [86].

The eigenfunctions of the Fokker-Planck operator $L_{\mathrm{FP}}(x)$ are the solutions of the equation

$$L_{\mathrm{FP}}(x)P_\rho(x) = -\rho P_\rho(x)\,. \tag{5.30}$$

are the corresponding eigenvalues. The eigenfunctions obey the orthonormality relation [107]

$$\int \mathrm{e}^{\Phi(x)} P_\rho(x) P_{\rho'}(x)\mathrm{d}x = \delta_{\rho,\rho'}\,, \tag{5.31}$$

where

$$\Phi(x) = -\ln P_0(x) \tag{5.32}$$

is the potential associated with the operator $L_{\mathrm{FP}}(x)$. Here $P_0(x)$ is the steady-state solution of Eq. (5.20).

We can write the time-dependent solution of the fractional Fokker-Planck equation (5.20) corresponding to a single eigenfunction as

$$P(x,t) = P_\rho(x) f_\rho(t)\,. \tag{5.33}$$

Inserting into Eq. (5.20) we get that the function $f(t)$ obeys the equation

$$\frac{\mathrm{d}}{\mathrm{d}t} f_\rho(t) = -\rho_0 D_t^{1-\alpha} f_\rho(t) \tag{5.34}$$

with the initial condition $f(0) = 1$. The Laplace transform of this equation yields

$$k\tilde{f}_\rho(k) = 1 - \rho k^{1-\alpha}\tilde{f}_\rho(k)\,. \tag{5.35}$$

The solution of Eq. (5.35) is

$$\tilde{f}_\rho(k) = \frac{1}{k + \rho k^{1-\alpha}}\,. \tag{5.36}$$

The inverse Laplace transform is given in terms of the monotonically decreasing Mittag-Leffler function [177]

$$f_\rho(t) = E_\alpha(-\rho t^\alpha)\,. \tag{5.37}$$

The Mittag-Leffler function has a series expansion

$$E_\alpha(z) \equiv E_{\alpha,1}(z) = \sum_{n=0}^{\infty} \frac{z^n}{\Gamma(\alpha n + 1)}\,. \tag{5.38}$$

The autocorrelation function can be calculated from the transition probability $P(x,t|x_0,0)$ (the conditional probability that at time t the stochastic variable has value x with the condition that at time $t = 0$ it had the value x_0):

$$C(t) = \int \mathrm{d}x \int \mathrm{d}x_0\, x_0 x P_0(x_0) P(x,t|x_0,0) - \left[\int \mathrm{d}x\, x P_0(x)\right]^2 \tag{5.39}$$

The transition probability is the solution of the Fokker-Planck equation (5.20) with the initial condition $P(x,0|x_0,0) = \delta(x - x_0)$. Expansion of the transition probability density in a series of the eigenfunctions has the form

$$P(x,t|x_0,0) = \sum_\rho P_\rho(x) e^{\Phi(x_0)} P_\rho(x_0) E_\alpha(-\rho t^\alpha)\,, \tag{5.40}$$

where we used Eqs. (5.33) and (5.37). Inserting Eq. (5.40) into Eq. (5.39) we

get the expression for the autocorrelation function

$$C(t) = \sum_{\rho>0} X_\rho^2 E_\alpha(-\rho t^\alpha)\,. \tag{5.41}$$

Here

$$X_\rho = \int x P_\rho(x)\,\mathrm{d}x \tag{5.42}$$

is the first moment of the stochastic variable x evaluated with the ρ-th eigenfunction $P_\rho(x)$. Such an expression for the autocorrelation function has been obtained in Ref. [173].

According to Wiener-Khintchine relations, the power spectral density is related to the autocorrelation function:

$$S(f) = 4\int_0^\infty C(t)\cos(\omega t)\,\mathrm{d}t\,, \tag{5.43}$$

where $\omega = 2\pi f$. Using Eq. (5.41) we obtain

$$S(f) = 4\sum_{\rho>0} X_\rho^2 \int_0^\infty E_\alpha(-\rho t^\alpha)\cos(\omega t)\,\mathrm{d}t \tag{5.44}$$

The integral can be calculated by noting that the Laplace transform of $E_\alpha(-\rho t^\alpha)$ is given by Eq. (5.36). We obtain the desired expression for the PSD

$$S(f) = 4\frac{\sin\left(\frac{\pi}{2}\alpha\right)}{\omega^{1-\alpha}}\sum_\rho \frac{\rho}{\rho^2+\omega^{2\alpha}+2\rho\omega^\alpha\cos\left(\frac{\pi}{2}\alpha\right)} X_\rho^2\,. \tag{5.45}$$

Eq. (5.45) becomes the usual expression for the PSD when $\alpha \to 1$. Similar expression for the spectrum has been obtained in Ref. [173].

For small frequencies $\omega \ll \rho_1^{1/\alpha}$ we can neglect the frequency when it appears together with the eigenvalues ρ. Here ρ_1 is the smallest eigenvalue larger than zero. Thus for small frequencies Eq. (5.45) approximately is

$$S(f) \approx 4\frac{\sin\left(\frac{\pi}{2}\alpha\right)}{\omega^{1-\alpha}}\sum_\rho \frac{X_\rho^2}{\rho}\,. \tag{5.46}$$

We obtain that for small frequencies the PSD has a power-law dependency on the frequency $S(f) \sim f^{-(1-\alpha)}$. However, the power-law exponent is always smaller than 1, since $0 < \alpha < 1$. It is not possible to get pure $1/f$ spectrum

this way. In the next section we show that it is possible to get larger power-law exponents in the PSD in a wide range of intermediate frequencies when the diffusion coefficient is not constant and depends on x.

5.4 Time-fractional Fokker-Planck equation with power-law coefficients

In this section we consider a particular case of the time-fractional Fokker-Planck equation (5.20). We assume that the diffusion coefficient has a power-law dependence on the particle position x and Eq. (5.20) takes the form

$$\frac{\partial}{\partial t}P(x,t) = \sigma^2{}_0D_t^{1-\alpha}\left\{\left(\frac{\lambda}{2}-\eta\right)\frac{\partial}{\partial x}\left[x^{2\eta-1}P(x,t)\right] + \frac{1}{2}\frac{\partial^2}{\partial x^2}\left[x^{2\eta}P(x,t)\right]\right\}. \tag{5.47}$$

Here η is the power-law exponent of the multiplicative noise in Eq. (6.7) and ν defines the behavior of the steady-state PDF $P_0(x)$. The power-law form of the diffusion coefficient is natural for systems exhibiting self-similarity, for example disordered materials, and has been used to describe diffusion on fractals [46, 178], turbulent two-particle diffusion, transport of fast electrons in a hot plasma [179]. Equation (5.47) is a generalization of the Fokker-Planck equation resulting form nonlinear SDEs proposed in Ref. [74, 75]. Such nonlinear SDEs generate signals having $1/f$ spectrum in a wide range of frequencies and have been used to describe signals in socio-economical systems and Brownian motion in inhomogeneous media (2.1).

The steady-state PDF $P_0(x)$ obtained from Eq. (5.47) has a power-law form

$$P_0(x) \sim x^{-\lambda}. \tag{5.48}$$

For $\lambda > 1$ the PDF $P_0(x)$ diverges as $x \to 0$, thus the diffusion should be restricted at least from the side of small values. This can be done by introducing an additional potential that becomes large only when x acquires values outside of the interval $[x_{\min}, x_{\max}]$ into the drift term of Eq. (5.47). The simplest choice is the reflective boundaries at $x = x_{\min}$ and $x = x_{\max}$.

In Ref. [86] an approximate expression for the first moment X_ρ has been obtained for the Fokker-Planck operator appearing in Eq. (5.47) assuming reflective boundaries at $x_{\min} = 1$ and $x_{\max} = \xi$, $\xi \gg 1$. According to the results of

Ref. [86]

$$X_\lambda \sim \frac{c_\rho}{|1-\eta|}\frac{1}{\nu^{\beta_1}}\,, \tag{5.49}$$

where

$$c_\rho = \sqrt{\frac{|1-\eta|}{z_{\max}}\frac{\lambda-1}{1-\xi^{1-\lambda}}\pi\nu}\,, \qquad \nu = \frac{\sqrt{2\rho}}{|\eta-1|}\,, \qquad \beta_1 = 1+\frac{\lambda-3}{2(\eta-1)}\,. \tag{5.50}$$

The parameters $z_{\min}$ and $z_{\max}$ depend on the boundaries $x_{\min}$ and $x_{\max}$. When $\nu z_{\max} \gg 1$, replacing summation by integration in Eq. (5.45) we obtain the expression for the PSD

$$S(f) \approx 4\frac{\sin\left(\frac{\pi}{2}\alpha\right)}{\omega^{1-\alpha}}\int \frac{\rho}{\rho^2+\omega^{2\alpha}+2\rho\omega^\alpha\cos\left(\frac{\pi}{2}\alpha\right)}X_\rho^2 D(\rho)\,\mathrm{d}\rho \tag{5.51}$$

The density of eigenvalues $D(\rho)$ has been estimated as [86]

$$D(\rho) \sim \frac{1}{\sqrt{\rho}}\,. \tag{5.52}$$

Using Eqs. (5.49) and (5.52) we get

$$S(f) \sim 4\frac{\sin\left(\frac{\pi}{2}\alpha\right)}{\omega^{1+\alpha(\beta_1-1)}}\int_{\frac{z_{\max}^{-2}}{\omega^\alpha}}^{\frac{z_{\min}^{-2}}{\omega^\alpha}} \frac{1}{u^{\beta_1-1}}\frac{1}{\left(u^2+1+2u\cos\left(\frac{\pi}{2}\alpha\right)\right)}\mathrm{d}u \tag{5.53}$$

Here the upper range of integration is limited because X_λ becomes small when $\nu z_{\min} \gg 1$ [86]. When $z_{\max}^{-2} \ll \omega^\alpha \ll z_{\min}^{-2}$ and $0 < \beta_1 < 2$ then we can approximate the lower limit of integration by 0 and the upper limit by ∞. In this case the PSD depends on the frequency as $S(f) \sim f^{-1-\alpha(\beta_1-1)}$. When $\beta_1 > 2$ then the largest contribution is from the lower limit of the integration. Thus, when $z_{\max}^{-2} \ll \omega^\alpha \ll z_{\min}^{-2}$ then the leading term in the expansion of the approximate expression for the PSD in the power series of ω is

$$S(f) \sim \begin{cases} \frac{1}{\omega^{1+\alpha(\beta_1-1)}}\,, & 0<\beta_1<2\,, \\ \frac{1}{\omega^{1+\alpha}}\,, & \beta_1>2\,. \end{cases} \tag{5.54}$$

This expressions for PSD can also be written as

$$S(f) \sim \begin{cases} \frac{1}{\omega^{\beta}}\,, & 1-\alpha < \beta < 1+\alpha\,, \\ \frac{1}{\omega^{1+\alpha}}\,, & \beta > 1+\alpha\,. \end{cases} \tag{5.55}$$

Here

$$\beta = 1 + \alpha(\beta_1 - 1) = 1 + \frac{\alpha(\lambda-3)}{2(\eta-1)} \tag{5.56}$$

is the power-law exponent of the PSD. Equation (5.56) generalizes the expression for the power-law exponent obtained for nonlinear SDEs (1.1). When $\lambda = 3$ then from Eq. (5.56) follows that we obtain $1/f$ spectrum.

5.5 Power spectral density from scaling properties

Power-law exponent (5.56) in the PSD can be obtained from the scaling properties of Eq. (5.47), similarly as it has been done for the nonlinear SDEs [85]. Changing the variable x to the scaled variable $x_s = ax$ in Eq. (5.47) yields

$$\frac{\partial}{\partial t}P(x_s,t) = \frac{\sigma^2}{a^{2(\eta-1)}}{}_0D_t^{1-\alpha}\left\{\left(\frac{\lambda}{2}-\eta\right)\frac{\partial}{\partial x_s}\left[x_s^{2\eta-1}P(x_s,t)\right] + \frac{1}{2}\frac{\partial^2}{\partial x_s^2}\left[x_s^{2\eta}P(x_s,t)\right]\right\}. \tag{5.57}$$

The Riemann–Liouville fractional derivative has the following scaling property: ${}_0D_t^{1-\alpha}f(ct) = c^{1-\alpha}{}_0D_{ct}^{1-\alpha}f(ct)$. Thus, changing the time t to the scaled time $t_s = a^{\nu}t$ we get

$$a^{\nu}\frac{\partial}{\partial t_s}P(x,t_s) = \sigma^2{}_0a^{\nu(1-\alpha)}D_{t_s}^{1-\alpha}\left\{\left(\frac{\lambda}{2}-\eta\right)\frac{\partial}{\partial x}\left[x^{2\eta-1}P(x,t_s)\right] + \frac{1}{2}\frac{\partial^2}{\partial x^2}\left[x^{2\eta}P(x,t_s)\right]\right\}. \tag{5.58}$$

The change of the variable x to the scaled variable ax or the change of the time t to the scaled time $a^{\nu}t$ produce the same fractional Fokker-Planck equation if

$$\nu = \frac{2(\eta-1)}{\alpha}\,. \tag{5.59}$$

It follows, that the transition probability $P(x,t|x_0,0)$ has the following scaling property:

$$aP(ax,t|ax_0,0) = P(x,a^{\nu}t|x_0,0)\,. \tag{5.60}$$

As has been shown in Ref. [85], the power-law steady state PDF $P_0(x) \sim x^{-\nu}$ and the scaling property of the transition probability (5.60) lead to the power-law form PSD $S(f) \sim f^{-\beta}$ in a wide range of frequencies. The power-law exponent β is given by

$$\beta = 1 + (\lambda - 3)/\nu \,. \tag{5.61}$$

Using Eq. (5.59) we obtain the same expression for β as in Eq. (5.56).

The presence of restrictions at $x = x_{\min}$ and $x = x_{\max}$ makes the scaling (5.60) not exact. This limits the power-law part of the PSD to a finite range of frequencies $f_{\min} \ll f \ll f_{\max}$. Similarly as in Ref. [85], we estimate the limiting frequencies as

$$\begin{aligned} \sigma^{\frac{2}{\alpha}} x_{\min}^{\frac{2}{\alpha}(\eta-1)} &\ll 2\pi f \ll \sigma^{\frac{2}{\alpha}} x_{\max}^{\frac{2}{\alpha}(\eta-1)} \,, \qquad \eta > 1 \,, \\ \sigma^{\frac{2}{\alpha}} x_{\max}^{-\frac{2}{\alpha}(1-\eta)} &\ll 2\pi f \ll \sigma^{\frac{2}{\alpha}} x_{\min}^{-\frac{2}{\alpha}(1-\eta)} \,, \qquad \eta < 1 \,. \end{aligned} \tag{5.62}$$

This equation shows that the frequency range grows with decrease of α. By increasing the ratio $x_{\max}/x_{\min}$ one can get an arbitrarily wide range of the frequencies where the PSD has $1/f^{\beta}$ behavior.

5.6 Numerical approximation of sample paths

Since analytical solution of time-fractional Fokker-Planck equation can be obtained only in separate cases, there is a need of numerical solution. Numerical solution of time-fractional Fokker-Planck equation is complicated [180]. It is easier to numerically solve Langevin equations (5.1), (5.3) instead. The desired properties of the solution of the Fokker-Planck equation then can be calculated by averaging over many sample paths obtained by solving the Langevin equations. The numerical method of solution of the Langevin equations with constant drift coefficient is outlined in [153, 181]. We can use the same method also when the drift coefficient is position-dependent.

Choosing the time step $\Delta\tau$ of the operational time τ the inverse subordinator $S(t)$ is approximated as [182]

$$S_{\Delta\tau}(t) = [\min\{n \in \mathbb{N} : T(n\Delta\tau) > t\} - 1]\Delta\tau \,. \tag{5.63}$$

Such approximation satisfies [183]

$$\sup_{0\leqslant t\leqslant T}[S_{\Delta\tau}(t)-S(t)]\leqslant\Delta\tau\,. \tag{5.64}$$

The values $T(n\Delta\tau)$ are generated by summing up the independent and stationary increments of the Lévy process:

$$T(n\Delta\tau)=T([n-1]\Delta\tau)+\Delta\tau^{1/\alpha}\xi_n\,. \tag{5.65}$$

Here ξ_n are independent totally skewed positive α-stable random variables with the distribution specified by the Laplace transform $\langle e^{-k\xi}\rangle=e^{-k^\alpha}$. Such variables can be generated using the formula [184]

$$\xi=\frac{\sin\left[\alpha\left(U+\frac{\pi}{2}\right)\right]}{\cos(U)^{\frac{1}{\alpha}}}\left(\frac{\cos\left[U-\alpha\left(U+\frac{\pi}{2}\right)\right]}{W}\right)^{\frac{1-\alpha}{\alpha}}\,. \tag{5.66}$$

Here U is uniformly distributed on $\left(-\frac{\pi}{2},\frac{\pi}{2}\right)$ and W has an exponential distribution with mean 1. Note, that in Ref. [153] incorrect formula for generating totally skewed positive α-stable random variables has been used. The definition of the Lévy α-stable distribution using the Laplace transform (5.2) differs from the more common definition using the Fourier transform. This has been corrected in Ref. [181].

The SDE (5.1) in the operational time τ can be numerically solved using the Euler-Maruyama scheme with the time step $\Delta\tau$. For each value of the stochastic variable x_k we assign the physical time t_k generated by the process $T(\tau)$ using Eq. (5.65). Thus the numerical method of solution of Langevin equations (5.1), (5.3) is given by the following equations:

$$x_{k+1} = x_k+a(x_k)\Delta\tau+b(x_k)\sqrt{\Delta\tau}\varepsilon_k\,, \tag{5.67}$$

$$t_{k+1} = t_k+\Delta\tau^{\frac{1}{\alpha}}\xi_k\,. \tag{5.68}$$

Here ε_k are i.i.d. random variables having standard normal distribution.

For numerical solution of nonlinear equations, such as those resulting in Eq. (5.47), the fixed time step $\Delta\tau$ can be inefficient. For example, in Eq. (5.47) with $\eta>1$ large values of stochastic variable x lead to large coefficients and thus require a very small time step. A more efficient way of solution is to use

a variable time step that adapts to the coefficients in the equation. Similar method has been used in Refs. [74, 75] for solving nonlinear SDEs. Such a variable time step is equivalent to changing of the operational time τ to the position-dependent operational time τ'. If we choose the intensity of random time in Eq. (5.22) as $g(x) = b(x)^{-\frac{2}{\alpha}}$ then, according to Eq. (5.29) instead of initial Langevin equations (5.1), (5.3) we get the new Langevin equations

$$\mathrm{d}x(\tau') = \frac{a(x(\tau'))}{b(x(\tau'))^2}\mathrm{d}\tau' + \mathrm{d}W(\tau')\,, \tag{5.69}$$

$$\mathrm{d}t(\tau') = b(x(\tau'))^{-\frac{2}{\alpha}}\mathrm{d}L^\alpha(\tau')\,. \tag{5.70}$$

Discretizing the operational time τ' with the time step $\Delta\tau'$ and using the Euler-Maruyama approximation for Eq. (5.69) instead of Eqs. (5.67), (5.68) we have

$$x_{k+1} = x_k + \frac{a(x_k)}{b(x_k)^2}\Delta\tau' + \sqrt{\Delta\tau'}\varepsilon_k\,, \tag{5.71}$$

$$t_{k+1} = t_k + \left(\frac{\Delta\tau'}{b(x_k)^2}\right)^{\frac{1}{\alpha}}\xi_k\,. \tag{5.72}$$

Comparison with Eqs. (5.67), (5.68) shows that Eqs. (5.71), (5.72) can be obtained by replacing the time step $\Delta\tau$ in Eqs. (5.67), (5.68) by

$$\Delta\tau \to \frac{\Delta\tau'}{b(x_k)^2}\,. \tag{5.73}$$

As an example, we solve the Langevin equations

$$\mathrm{d}x = \left(\eta - \frac{\lambda}{2}\right)x^{2\eta-1}\mathrm{d}\tau + x^\eta \mathrm{d}W(\tau)\,, \tag{5.74}$$

$$\mathrm{d}t = \mathrm{d}L^\alpha(\tau) \tag{5.75}$$

resulting in the time-fractional Fokker-Planck equation (5.47). For restriction of the diffusion region we use the reflective boundaries at $x = x_{\min}$ and $x_{\max}$. More effective numerical solution scheme is obtained changing the operational time τ to the time τ' defined by the equation

$$\mathrm{d}t(\tau') = x(\tau')^{-\frac{2}{\alpha}(\eta-1)}\mathrm{d}L^\alpha(\tau')\,. \tag{5.76}$$

This change is equivalent to the introduction of the variable time step $\Delta\tau_k = \Delta\tau' x_k^{-2(\eta-1)}$. Discretizing the operational time τ' with the step $\Delta\tau'$ from Eqs. (5.74)–

(5.76) we get the following numerical approximation:

$$x_{k+1} = x_k + \left(\eta - \frac{\lambda}{2}\right) x_k \Delta\tau' + x_k \sqrt{\Delta\tau'}\varepsilon_k \,, \tag{5.77}$$

$$t_{k+1} = t_k + \left(\frac{\Delta\tau'}{x_k^{2(\eta-1)}}\right)^{\frac{1}{\alpha}} \xi_k \,. \tag{5.78}$$

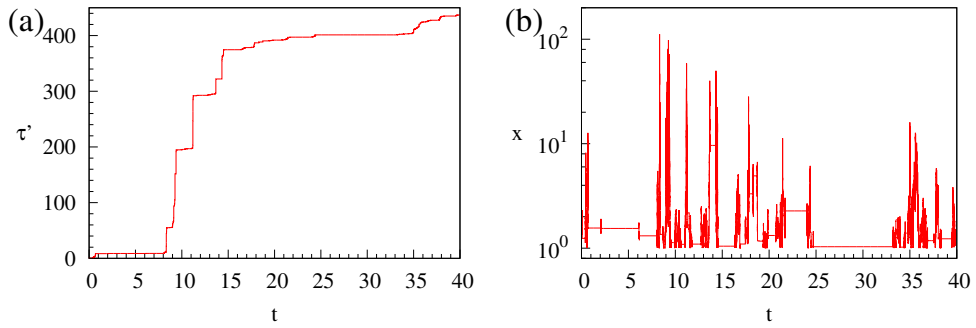

Figure 8: Sample path obtained from Langevin equations (5.74), (5.75) using numerical solution scheme given by Eqs. (5.77), (5.78). (a) Dependence of the operational time τ', defined by Eq. (5.76), on the physical time t. (b). Dependence of the stochastic variable x on the physical time t. The parameters are $\alpha = 0.7$, $\eta = 2$, $\nu = 3$. Reflective boundaries are placed at $x_{\min} = 1$ and $x_{\max} = 1000$.

Sample path obtained using Eqs. (5.77), (5.78) with the parameters $\eta = 2$ and $\nu = 3$ is shown in Fig. 8. The change of the operational time τ' with the physical time t is shown in Fig. 8(a) and the dependence of the stochastic variable x on the physical time t is shown in Fig. 8(b). Due to nonlinear coefficients in Eq. (5.74) the sample path in Fig. 8(b) exhibits peaks or bursts, corresponding to the large deviations of the variable x. The intervals with x being constant indicate the heavy-tailed trapping times. Comparing Fig. 8(a) with Fig. 8(b) we see that the operational time τ' increases faster when x acquires larger values, in accordance to Eq. (5.76).

5.7 Power spectral density

Since the equations exhibit a slow (power-law instead of a usual exponential) relaxation [177], calculation of the PSD using sample paths is very slow. More efficient way is to find the eigenvalues and eigenfunctions of the Fokker-Planck operator (5.7) and calculate the PSD using the rapidly converging series

in Eq. (5.45). This is the approach for calculating the PSD used in Ref. [173] for the case of constant diffusion coefficient.

As an example let us calculate the PSD of the diffusion described by the time-fractional Fokker-Planck equation (5.47) with $\eta \neq 1$ and the reflective boundaries at $x_{\min} = 1$ and $x_{\max} = \xi$. The equation (5.30) for the eigenfunctions of the Fokker-Planck operator that enters Eq. (5.47) is

$$-\left(\eta - \frac{\lambda}{2}\right)\frac{\partial}{\partial x}x^{2\eta-1}P_\rho(x) + \frac{1}{2}\frac{\partial^2}{\partial x^2}x^{2\eta}P_\rho(x) = -\rho P_\rho(x)\,. \tag{5.79}$$

The reflective boundaries lead to the conditions $S_\rho(1) = 0$ and $S_\rho(\xi) = 0$, where

$$S_\rho(x) = \left(\eta - \frac{\lambda}{2}\right)x^{2\eta-1}P_\rho(x) - \frac{1}{2}\frac{\partial}{\partial x}x^{2\eta}P_\rho(x) \tag{5.80}$$

is the probability current related to the eigenfunction $P_\rho(x)$. The steady state solution of Eq. (5.47) is

$$P_0(x) = \frac{\lambda - 1}{1 - \xi^{1-\lambda}}x^{-\lambda}\,. \tag{5.81}$$

It is more convenient to transform Eq. (5.79) into the Schrödinger equation [107]. To do this we first make the diffusion coefficient constant by changing the variable x to

$$z = \frac{x^{1-\eta}}{|\eta - 1|}\,. \tag{5.82}$$

Eq. (5.79) then becomes

$$\frac{\lambda'}{2}\frac{\partial}{\partial z}\frac{1}{z}P'_\rho(z) + \frac{1}{2}\frac{\partial^2}{\partial z^2}P'_\rho(z) = -\rho P'_\rho(z) \tag{5.83}$$

with the reflective boundaries at $z_{\min}$ and $z_{\max}$, where

$$z_{\min} = \begin{cases} \frac{1}{\eta-1}\frac{1}{\xi^{\eta-1}}\,, & \eta > 1\,, \\ \frac{1}{1-\eta}\,, & \eta < 1\,, \end{cases} \qquad z_{\max} = \begin{cases} \frac{1}{\eta-1}\,, & \eta > 1\,, \\ \frac{1}{1-\eta}\xi^{1-\eta}\,, & \eta < 1\,. \end{cases} \tag{5.84}$$

Here

$$\lambda' = \frac{\eta - \lambda}{\eta - 1}\,. \tag{5.85}$$

Eq. (5.83) can be transformed into the Schrödinger equation [107]

$$-\frac{1}{2}\frac{\mathrm{d}^2}{\mathrm{d}z^2}\psi_\rho(z) + V(z)\psi_\rho(z) = \rho\psi_\rho(z) \tag{5.86}$$

with the potential

$$V(z) = \frac{1}{8z^2}\lambda'(2+\lambda')\,. \tag{5.87}$$

Here $\psi_\rho(z) = P'_\rho(z)/\sqrt{P'_0(z)}$. The condition of zero probability current at the reflective boundaries $z = z_{\min}$ and $z = z_{\max}$ become

$$\left(\frac{\mathrm{d}}{\mathrm{d}z} + \frac{\lambda'}{2}\frac{1}{z}\right)\psi_\rho(z)\bigg|_{z=z_{\min},z_{\max}} = 0\,. \tag{5.88}$$

The solution of Eq. (5.86) corresponding to the eigenvalue $\rho = 0$ is

$$\psi_0(z) = \sqrt{\frac{\lambda'-1}{z_{\min}^{1-\lambda'} - z_{\max}^{1-\lambda'}}}\, z^{-\frac{\lambda'}{2}}\,. \tag{5.89}$$

Eq. (5.86) can be solved using standard finite-difference or finite-element methods. Having the eigenfunction $\psi_\rho(z)$ the first moment of the stochastic variable x can be calculated using the equation

$$X_\lambda = \int_{z_{\min}}^{z_{\max}} \psi_0(z)|\eta-1|^{\frac{1}{1-\eta}} z^{\frac{1}{1-\eta}}\psi_\rho(z)\,\mathrm{d}z\,. \tag{5.90}$$

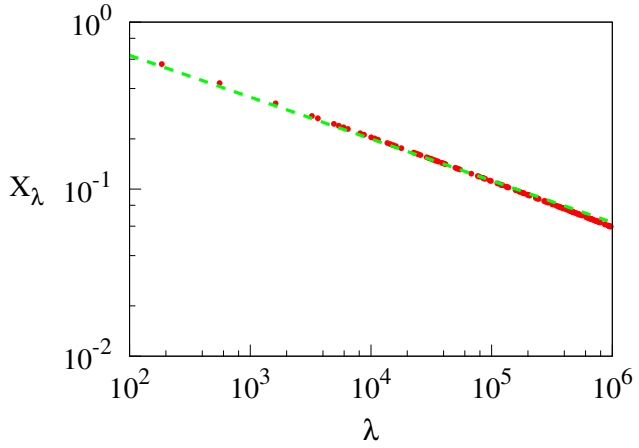

Figure 9: Dependence of numerically obtained first moments of the variable x on the eigenvalues λ for the lowest eigenvalues (dots). Eigenvalues and eigenfunctions are obtained numerically solving Eq. (5.86). The dashed line shows the slope $\lambda^{-0.25}$, predicted by Eq. (5.49). The parameters used are $\eta = \frac{5}{2}$, $\lambda = 3$, $x_{\min} = 1$ and $x_{\max} = 1000$.

Let us take the following values of the parameters in Eq. (5.47): $\eta = \frac{5}{2}$, $\lambda = 3$. The dependence of the numerically calculated first moment X_ρ on the eigenvalue ρ for lowest eigenvalues is shown in Fig. 9. We see a good agreement with the analytical prediction (5.49) of power-law dependence on ρ. For larger eigenvalues ρ than those shown in Fig. 9 the power-law dependence does not hold and X_ρ decrease faster.

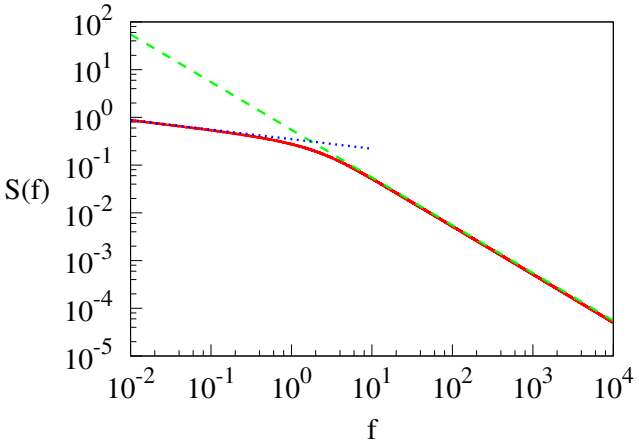

Figure 10: Power spectral density for the diffusion process defined by Eq. (5.47) with the parameter $\alpha = 0.8$. The solid line shows the result of numerical calculation using Eq. (5.45). The dashed line in right hand side shows the slope $1/f$, whereas the dotted line in left hand side shows the slope $f^{-0.2}$. Other parameters are the same as in Fig. 9.

The PSD calculated using Eq. (5.45) is presented in Fig. 10. Eigenvalues ρ and the first moments X_ρ shown in Fig. (9) have been used. We see a good agreement with the predicted power-law dependency of the PSD on the frequency for frequencies $f > f_{\min} \approx 1$. The power-law exponent coincides with Eq. (5.56). For smaller frequencies $f < 1$ the PSD exhibits the power-law behavior (5.46) with the exponent $1 - \alpha$.

5.8 Summary

In summary, we proposed Eq. (5.20) describing the subdiffusion of particles in an inhomogeneous medium that generalizes the previously obtained time-fractional Fokker-Planck equation with the position-independent diffusion coefficient. Fokker-Planck equation with the position-independent diffusion coefficient has been used to model various phenomena such as ion channel gating [185] and the translocation dynamics of a polymer chain threaded through

a nanopore [186]. Properties of such equations has been studied extensively. We analyzed a more general case when both drift and diffusion coefficients are position-dependent. We hope that the present model can serve as a basis to study trapping induced subdiffusion in complex inhomogeneous media.

We derived the analytical expression of power spectral density of signals described by the one-dimensional time fractional Fokker–Planck equation in a more general case when diffusion coefficient depends on the position. The general expression for the PSD (5.45) we applied to a particular case (5.47) when the drift and diffusion coefficients have power-law dependence on the position. The resulting PSD has a power-law form $S(f) \sim f^{-\beta}$ in a wide range of frequencies, with the power-law exponent β given by Eq. (5.56). This approximate results is confirmed by the numerical simulation (see Fig. 10). Thus, according to Eq. (5.56), time-fractional Fokker-Planck equation with power-law coefficients yields the PSD with the power-law exponent equal to or larger than 1 in a wide range of intermediate frequencies. In contrast, if the diffusion coefficient do not depend on position, the PSD for small frequencies has a power-law dependency on the frequency in the form of $f^{-(1-\alpha)}$.

Since an analytical solution of time-fractional Fokker-Planck equation can be obtained only in separate cases, there is a need of numerical solution. For the numerical solution of the nonlinear equations, such as those resulting in Eq. (5.47), we propose to use a variable time step that adapts to the coefficients in the equation. Such a variable time step is equivalent to changing of the operational time τ to the position-dependent operational time τ'.

6 Anomalous diffusion

In many systems we can observe processes exhibiting nonlinear dependence of the mean-square displacement (MSD) on time [2]. A family of such processes described by deviations from the linear time dependence of the MSD, typical for a classical Brownian motion, is called anomalous diffusion. Anomalous diffusion is characterized by the dependence of MSD on time in the form of a power-law $\langle \Delta x \rangle \sim t^{\theta}$. If θ varies between 1 and 2 we have so called super-diffusion. Super-diffusion has been experimentally observed in a study of tracer particles in a two-dimensional rotating flow [1]. If $\theta < 1$, we have another subclass of anomalous diffusion processes called the sub-diffusion. Theoretical models suggest that sub-diffusion can occur in polymer translocation through a nanopore [186].

6.1 HDP

Recently [38] it has been suggested that both cases of anomalous diffusion can be a result of a heterogeneous diffusion process (HDP), where the diffusion coefficient depends on the position. For example, heterogeneous diffusion processes has been used model subdiffusion in the study of thermal Markovian diffusion of tracer particles in a 2D medium with spatially varying diffusivity [40], mimicking recently measured, heterogeneous maps of the apparent diffusion coefficient in biological cells [187].

Here we consider HDPs with the power-law dependence of the diffusion coefficient on the particle position and analytically investigate the influence of external potentials on the resulting anomalous diffusion. The influence of the external forces on HDPs has not been methodically analyzed. We assume that introduction of the external potentials leads to drift terms in the from of power-law function of position. Such a drift terms appears in Langevin equation describing overdamped fluctuations of the position of a particle in nonhomogeneous medium [108]. As we demonstrate, the external force having a specific value of the power-law exponent does not restrict the region of diffusion. Such an external force does not change the scaling exponent θ, only the anomalous diffusion coefficient depends on the force. Other values of the power-law expo-

nent in the deterministic force can cause the exponential cut-off in the probability density function (PDF) of the particle positions leading to the restriction of the time interval when the anomalous diffusion occurs.

6.2 Influence of External Potentials on HDP

HDPs with the nonlinear dependence of the diffusion coefficient on the position is described by the Langevin equation

$$dx = \sigma|x|^{\eta} \circ dW_t \,. \tag{6.1}$$

Here x is the signal, η is the exponent of the power-law of multiplicative noise, parameter σ gives the intensity of the noise and W_t is a standard Wiener process. Eq. (6.1) is interpreted in Stratonovich sense. For mathematical convenience, we will use the Itô convention:

$$dx = \frac{1}{2}\sigma^2\eta|x|^{2(\eta-1)}xdt + \sigma|x|^{\eta}dW_t \,. \tag{6.2}$$

First member of right hand side of Eq. (6.2) represents noise-induced drift. It has been shown that Eq. (6.1) leads to a nonlinear time dependence of the MSD [38]

$$\langle (x - \langle x \rangle)^2 \rangle \sim (\sigma^2 t)^{\frac{1}{1-\eta}} \,. \tag{6.3}$$

The HDP (6.1) displays weak non-ergodicity, that is the scaling of time and ensemble averages is different. Specifically, in Ref. [38] it has been shown that the average over the trajectories

$$\left\langle \overline{\delta^2(\Delta)} \right\rangle = \frac{1}{N}\sum_{i=1}^{N} \overline{\delta_i^2(\Delta)} \tag{6.4}$$

of the the time-averaged MSD

$$\overline{\delta^2(\Delta)} = \frac{1}{T-\Delta}\int_0^{T-\Delta} [x(t+\Delta) - x(t)]^2 dt \tag{6.5}$$

scales as

$$\left\langle \overline{\delta^2(\Delta)} \right\rangle \sim \frac{\Delta}{T^{\frac{\eta}{\eta-1}}} \,. \tag{6.6}$$

Thus time-averaged MSD depends on the time difference Δ linearly, in contrast

to the power-law behavior of MSD in Eq. (6.3).

Another interesting property of HDPs is the behavior of the distribution of the time-averaged MSD $\overline{\delta^2}$ of individual realizations. When $\eta < 0$, the distribution of $\overline{\delta^2}$ decays to zero at $\overline{\delta^2} = 0$ [40]. This behavior of the distribution in HDPs is different than the behavior in CTRWs, where there is a finite fraction of immobile particles resulting in the finite value of the distribution at $\overline{\delta^2} = 0$. This difference allows to distinguish between different origins of anomalous diffusion.

We will generalize the HDP by introducing an external force via the equation

$$dx = \sigma^2 \left(\eta - \frac{\lambda}{2} \right) x^{2\eta - 1} dt + \sigma x^{\eta} dW_t \,. \tag{6.7}$$

We chose to introduce external force in such a way that HDP take the form of Eq. (1.1). Parameter λ describes influence of external potential on HDP. λ also defines the exponent of the steady-state PDF of the signal in interval $[x_{\min}, x_{\max}]$, $P_0(x) \sim x^{-\lambda}$. Here $x_{\min}$, $x_{\max}$ are reflective boundaries at positive small and large x values, respectively.

Transformation of the variable x to a new variable $y = x^{1-\eta}$ (assuming that $\eta \neq 1$) leads to the stochastic differential equation (SDE)

$$dy = -\frac{1}{2} \sigma'^2 \lambda' \frac{1}{y} dt + \sigma' dW_t \,, \tag{6.8}$$

where

$$\lambda' = \frac{\eta - \lambda}{\eta - 1} \,, \qquad \sigma' = |\eta - 1| \sigma \,. \tag{6.9}$$

Equation (6.8) has the form of a Bessel process. The known analytic form of the solution of the Fokker-Planck equation

$$\frac{\partial}{\partial t} P_y = \frac{1}{2} \sigma'^2 \lambda' \frac{\partial}{\partial y} y^{-1} P_y + \frac{1}{2} \sigma'^2 \frac{\partial^2}{\partial y^2} P_y \tag{6.10}$$

corresponding to SDE (6.8) is

$$P(y, t | y_0, 0) = \frac{y^{\frac{1-\lambda'}{2}} y_0^{\frac{1+\lambda'}{2}}}{\sigma'^2 t} \exp\left(-\frac{y^2 + y_0^2}{2\sigma'^2 t} \right) I_{-\frac{\lambda'+1}{2}} \left(\frac{y y_0}{\sigma'^2 t} \right) \,. \tag{6.11}$$

Here $I_n(z)$ is the modified Bessel function of the first kind. This PDF satisfies the initial condition $P(y, t = 0 | y_0, 0) = \delta(y - y_0)$. The PDF (6.11) can be normalized

if $\lambda' < 1$.

Transforming back to x we obtain the time-dependent PDF

$$P(x,t|x_0,0) = \frac{x^{\frac{1-2\eta-\lambda}{2}} x_0^{\frac{1-2\eta+\lambda}{2}}}{|\eta-1|\sigma^2 t} \exp\left(-\frac{x^{2(1-\eta)}+x_0^{2(1-\eta)}}{2(\eta-1)^2\sigma^2 t}\right) \times I_{\frac{\lambda+1-2\eta}{2(\eta-1)}}\left(\frac{x^{(1-\eta)}x_0^{(1-\eta)}}{(\eta-1)^2\sigma^2 t}\right) . \tag{6.12}$$

This PDF satisfies the initial condition $P(x, t = 0|x_0, 0) = \delta(x - x_0)$. Using the PDF (6.12) the time-dependent average of a power of x can be calculated:

$$\begin{aligned}\langle x^a\rangle_{x_0} =& \int_0^\infty x^a P(x,t|x_0,0)dx \\ =& \frac{\Gamma\left(\frac{\lambda-1-a}{2(\eta-1)}\right)}{\Gamma\left(\frac{\lambda-1}{2(\eta-1)}\right)} \left(2(\eta-1)^2\sigma^2 t\right)^{\frac{a}{2(1-\eta)}} \\ & \times {}_1F_1\left(\frac{a}{2(\eta-1)}; \frac{\lambda-1}{2(\eta-1)}; -\frac{x_0^{2(1-\eta)}}{2(\eta-1)^2\sigma^2 t}\right)\end{aligned} \tag{6.13}$$

Here ${}_1F_1(a; b; z)$ is the Kummer confluent hypergeometric function. For large time the hypergeometric function is approximately equal to 1, thus

$$\langle x^a\rangle_{x_0} \approx \frac{\Gamma\left(\frac{\lambda-1-a}{2(\eta-1)}\right)}{\Gamma\left(\frac{\lambda-1}{2(\eta-1)}\right)} \left(2(\eta-1)^2\sigma^2 t\right)^{\frac{a}{2(1-\eta)}} . \tag{6.14}$$

From Eq. (6.14) we can see that the average of the square of x depends on time as $\langle x^2\rangle_{x_0} \sim t^{1/(1-\eta)}$ for large time t, that is when

$$\frac{x_0^{2(1-\eta)}}{2(\eta-1)^2\sigma^2 t} \ll 1 . \tag{6.15}$$

The average of the x depends on time as $t^{1/2(1-\eta)}$. Therefore the MSD $\langle(x - \langle x\rangle)^2\rangle = \langle x^2\rangle - \langle x\rangle^2$ has the same dependence on time

$$\langle(x - \langle x\rangle)^2\rangle \sim t^{1/(1-\eta)} \tag{6.16}$$

as the original HDP equation (6.1).

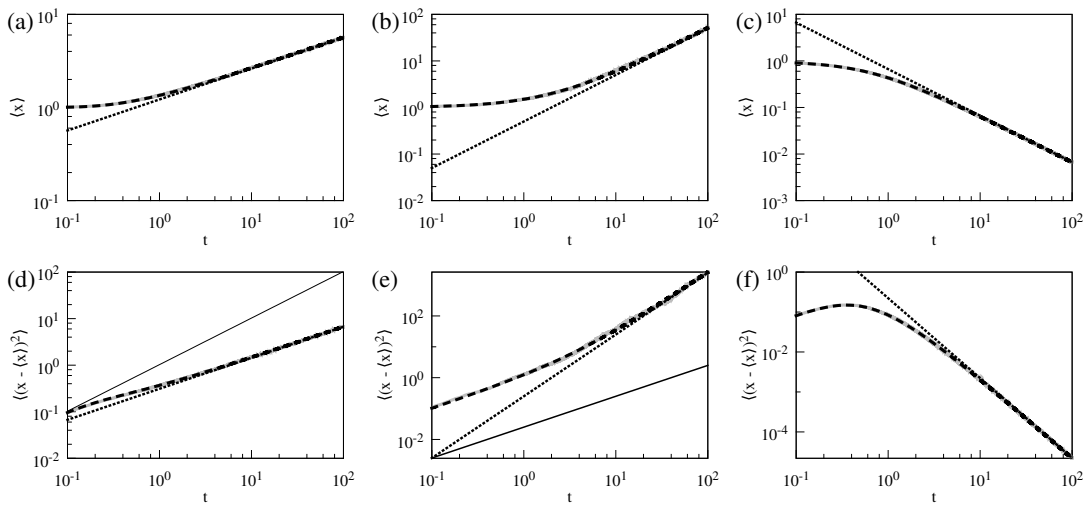

Figure 11: Dependence of the mean (a,b,c) and variance (d,e,f) on time for various values of the parameters η and λ when the position of the diffusing particle changes according to Eq. (6.7). Solid gray lines show numerical result, dashed black lines are calculated using Eq. (6.13), black dotted lines show the power-law dependence on time $\sim t^{1/[2(1-\eta)]}$ for (a,b,c) and $\sim t^{1/(1-\eta)}$ for (d,e,f). The solid black line in (e,d) shows mean squared displacement (MSD) linear dependence on time. In (d) we see subdiffusion and supper diffusion in (e). The parameters are $\sigma = 1$ and $\eta = -\frac{1}{2}$, $\lambda = -1$ for (a,d); $\eta = \frac{1}{2}$, $\lambda = 0$ for (b,c); $\eta = \frac{3}{2}$, $\lambda = 5$ for (c,f). The initial position is $x_0 = 1$.

6.3 Exponential restriction of diffusion

Here we introduce an external deterministic force that is no longer proportional to the noise induced drift, but has a power-law dependence on x with the power-law exponent different than $2\eta - 1$. In particular, the external force can linearly dependence on x,

$$dx = \left(\mu x + \sigma^2 \left(\eta - \frac{\lambda}{2}\right) x^{2\eta-1}\right) dt + \sigma x^{\eta} dW_t \,. \tag{6.17}$$

Analytical expression of time-dependent PDF for SDE (6.17) can also be obtained by performing the same steps as in previous section.

$$
\begin{aligned}
P(x,t|x_0,0) &= \frac{2|\eta-1|x_{\rm m}^{2(\eta-1)}}{1-e^{-2\mu(\eta-1)t}} x^{\frac{1-\lambda-2\eta}{2}} x_0^{\frac{1+\lambda-2\eta}{2}} e^{\frac{1+\lambda-2\eta}{2}\mu t} \\
&\quad \times \exp\left(-\frac{x_{\rm m}^{2(\eta-1)}}{1-e^{-2(\eta-1)\mu t}}\left(x^{2(1-\eta)}+x_0^{2(1-\eta)}e^{-2(\eta-1)\mu t}\right)\right) \\
&\quad \times I_{\frac{1+\lambda-2\eta}{2(\eta-1)}}\left(\frac{x_{\rm m}^{2(\eta-1)}x^{(1-\eta)}x_0^{(1-\eta)}}{\sinh\left((\eta-1)\mu t\right)}\right)
\end{aligned}
\tag{6.18}
$$

If μ has the same sign as $\eta-1$ and $t\to\infty$ then the time-dependent PDF reaches the steady-state

$$
P_0(x) = \frac{2|\eta-1|x_{\rm m}^{\lambda-1}}{\Gamma\left(\frac{\lambda-1}{2(\eta-1)}\right)} x^{-\lambda}\exp\left(-\left(\frac{x_{\rm m}}{x}\right)^{2(\eta-1)}\right), \tag{6.19}
$$

where $x_{\rm m}$ is defined via the equation

$$
\mu = \sigma^2(\eta-1)x_{\rm m}^{2(\eta-1)}. \tag{6.20}
$$

The time-dependent average of a power of x reads

$$
\begin{aligned}
\langle x^a\rangle_{x_0} =& \frac{\Gamma\left(\frac{\lambda-1-a}{2(\eta-1)}\right)}{\Gamma\left(\frac{\lambda-1}{2(\eta-1)}\right)} \frac{x_{\rm m}^a}{\left(1-e^{-2(\eta-1)\mu t}\right)^{\frac{a}{2(\eta-1)}}} \\
&\times {}_1F_1\left(\frac{a}{2(\eta-1)};\frac{\lambda-1}{2(\eta-1)};-\frac{x_{\rm m}^{2(\eta-1)}x_0^{2(1-\eta)}}{e^{2(\eta-1)\mu t}-1}\right)
\end{aligned}
\tag{6.21}
$$

This average is finite under the same conditions as Eq. (6.13). In particular, the average of x is equal to

$$
\langle x\rangle_{x_0} = \frac{\Gamma\left(\frac{\lambda-2}{2(\eta-1)}\right)}{\Gamma\left(\frac{\lambda-1}{2(\eta-1)}\right)} \frac{x_{\rm m}}{\left(1-e^{-2(\eta-1)\mu t}\right)^{\frac{1}{2(\eta-1)}}} {}_1F_1\left(\frac{1}{2(\eta-1)};\frac{\lambda-1}{2(\eta-1)};-\frac{x_{\rm m}^{2(\eta-1)}x_0^{2(1-\eta)}}{e^{2(\eta-1)\mu t}-1}\right) \tag{6.22}
$$

and is finite when $\lambda>2$ and $\eta>1$ or $\lambda<1$ and $\eta<1$. The average of the

square of x is equal to

$$\langle x^2 \rangle_{x_0} = \frac{\Gamma\left(\frac{\lambda-3}{2(\eta-1)}\right)}{\Gamma\left(\frac{\lambda-1}{2(\eta-1)}\right)} \frac{x_{\mathrm{m}}^2}{(1-e^{-2(\eta-1)\mu t})^{\frac{1}{\eta-1}}} \, {}_1F_1\left(\frac{1}{(\eta-1)}; \frac{\lambda-1}{2(\eta-1)}; -\frac{x_{\mathrm{m}}^{2(\eta-1)} x_0^{2(1-\eta)}}{e^{2(\eta-1)\mu t}-1}\right) \tag{6.23}$$

and is finite when $\lambda > 3$ and $\eta > 1$ or $\lambda < 1$ and $\eta < 1$.

The steady-state PDF (6.19) leads to the steady-state averages of x and x^2

$$\langle x \rangle_{\mathrm{st}} = \frac{\Gamma\left(\frac{\lambda-2}{2(\eta-1)}\right)}{\Gamma\left(\frac{\lambda-1}{2(\eta-1)}\right)} x_{\mathrm{m}} \,, \tag{6.24}$$

$$\langle x^2 \rangle_{\mathrm{st}} = \frac{\Gamma\left(\frac{\lambda-3}{2(\eta-1)}\right)}{\Gamma\left(\frac{\lambda-1}{2(\eta-1)}\right)} x_{\mathrm{m}}^2 \,. \tag{6.25}$$

The growth of the second moment $\langle x^2 \rangle_{x_0}$ can be separated into three parts. For small times

$$t \ll \frac{x_0^{2(1-\eta)}}{2(\eta-1)^2\sigma^2}$$

the diffusion is approximately normal, $\langle x^2 \rangle_{x_0}$ depends linearly on time t. For the intermediate times

$$\frac{x_0^{2(1-\eta)}}{2(\eta-1)^2\sigma^2} \ll t \ll \frac{1}{2(\eta-1)\mu} = \frac{x_{\mathrm{m}}^{2(1-\eta)}}{2(\eta-1)^2\sigma^2}$$

$\langle x^2 \rangle_{x_0}$ remains power-law function on time $\langle x^2 \rangle_{x_0} \sim t^{1/(1-\eta)}$ For large times we cannot observe anomalous diffusion, because the cut-off position x_{m} starts to influence the diffusion and $\langle x^2 \rangle_{x_0}$ relax to the steady-state value (6.25).

6.4 Anomalous diffusion and 1/f noise

Anomalous diffusion occur only for specific parameters values if $\lambda < 3$ and $\eta < 1$ (or $\lambda < 1$ and $\eta < 1$). As we can see in Fig. 12 (c) and (f), in other cases anomalous diffusion does not occur due to the localization of particles. However restrictions $\lambda > 3$ and $\eta > 1$ are compatible with condition $0 < \beta < 2$ (see Eq. 1.6) required to generate signal with $1/f$ spectrum. Thus, HDP can only generate either signals exhibiting $1/f$ noise or anomalous diffusion. In this section we study more general case of HDP presented in Chapter 4 to find out

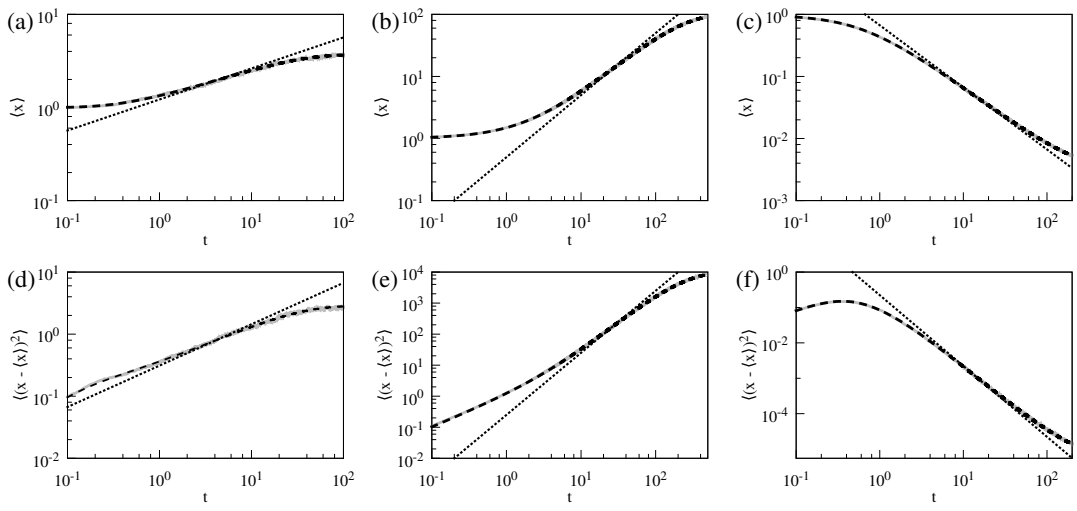

Figure 12: Dependence of the mean (a,b,c) and variance (d,e,f) on time for various values of the parameters η and λ when the position of the diffusing particle changes according to Eq. (6.17). Solid gray lines show numerical result, dashed black lines are calculated using (6.23), dotted lines show the power-law dependence on time $\sim t^{1/[2(1-\eta)]}$ for (a,b,c) and $\sim t^{1/(1-\eta)}$ for (d,e,f). The parameters are $\sigma = 1$ and $\eta = -\frac{1}{2}$, $\lambda = -1$, $x_{\mathrm{m}} = 5$ for (a,d); $\eta = \frac{1}{2}$, $\lambda = 0$, $x_{\mathrm{m}} = 100$ for (b,c); $\eta = \frac{3}{2}$, $\lambda = 5$ $x_{\mathrm{m}} = 0.01$ for (c,f). The initial position is $x_0 = 1$.

or anomalous diffusion can occur together with $1/f$ noise

We numerically investigate the dependence of the variance $\sigma^2(t)$ on time t. Anomalous scaling can appear for similar SDEs that do not exhibit $1/f$ noise if the steady state PDF has a power law tail [9]. Numerical solution of SDEs (4.7) show that for small enough times the dependence of the variance on time can be described by a power law t^{μ}. According to the most common definition of anomalous diffusion [2], anomalous diffusion is a diffusion process with nonlinear time dependency in the growth of the variance.

$$\sigma^2(t) = \langle [x(t) - \langle x(t) \rangle]^2 \rangle \sim t^{\mu} \,. \tag{6.26}$$

Unfortunately the second moment of the Lévy process is divergent $\langle x^2_{\mathrm{Levy}} \rangle = \infty$ for all times and even the mean is divergent for some cases. It has been proposed [2] to use fractional moments to analyze anomalous diffusion caused by Lévy flights, Therefore a fractional moments $\langle |x|^{\delta} \rangle$ was introduced to describe diffusion. These fractional moments are finite for all times if condition $0 < \delta < \alpha$ is satisfied. However, first and second moments are divergent only for an unbounded Lévy flight. The SDE driven by Lévy process can generate signals with finite moments if an external potential is introduced or some appropriate

boundary conditions are assumed.

A general analytical expression for steady state PDF in the case of fractional Fokker-Planck equation is not known. Therefore it is hard to find such an additional drift term that limits the size of the jumps, but does not change the power law dependence of the steady state PDF in some bounded region $x \in [x_{\min}, x_{\max}]$. Thus instead of an external potential we choose to use reflective boundary conditions at $x_{\min}$ and $x_{\max}$.

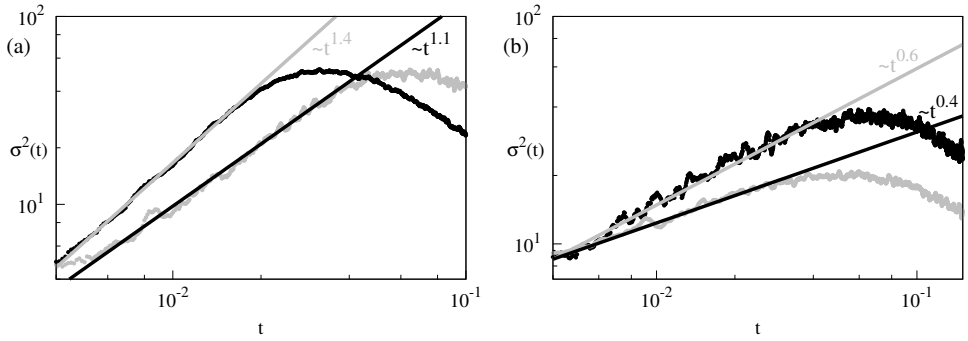

Figure 13: Dependence of the variance $\sigma^2(t)$ of the signal generated by Eq. (4.7) on time t. Gray and black strait lines show the power law dependence of the variance on time, $\sigma^2 \sim t^{\mu}$. (a) Super-diffusive behaviour when the stability index of Lévy noise $\alpha = 1.5$. Black curve corresponds to $\eta = 2.1$, gray curve to $\eta = 1.9$. The numerically determined values of the index μ are $\mu = 1.4$ and $\mu = 1.1$, respectively. (b) Sub-diffusive behaviour when the stability index of Lévy noise $\alpha = 1.2$. Black curve corresponds to $\eta = 2.1$, gray curve to $\eta = 1.9$. The numerically determined values of the index μ are $\mu = 0.6$ and $\mu = 0.4$, respectively. Other parameters of the equation are $\lambda = 3$, $x_{\min} = 1$, $x_{\max} = 10^4$, $\sigma = 1$.

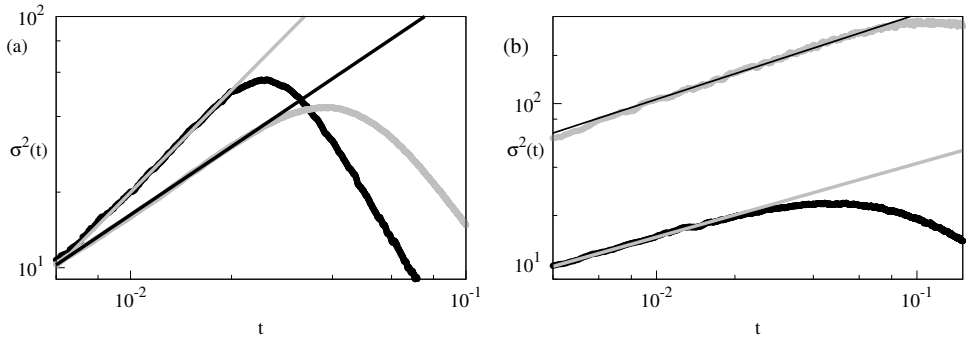

Figure 14: Dependence of the variance $\sigma^2(t)$ of the signal generated by Eq. (4.11) on time t. The stability index of Lévy noise $\alpha = 1$. Gray and black strait lines show the power law dependence of the variance on time, $\sigma^2 \sim t^{\mu}$. (a) Black curve corresponds to $\eta = 2.8$, gray curve to $\eta = 2.9$. The numerically determined values of the index μ are $\mu = 1.35$ and $\mu = 0.9$, respectively. (b) Black curve corresponds to $\eta = 2.4$, gray curve to $\eta = 2.1$. The numerically determined values of the index μ are $\mu = 0.5$. Other parameters of the equation are the same as in Fig. 13.

We have calculated the variance taking the signal of 10^5 realizations generated by SDEs (4.7) and (4.11). For computing the variance we use an incremental algorithm [188]. The dependence of the variance σ^2 on time t for various choices of parameters is shown in Fig. 13 and Fig. 14. As we can see the the power-law growth of variance is observable only for short times (approximately for 10^{-2}–10^{-1}). Due to reflective boundary conditions the variance stops growing and relax to its steady value. This problem could be solved by increasing size of simulated system. However, increased difference between reflective boundary conditions at $x_{\min}$ and $x_{\max}$ lead to much longer simulation times. So far this is beyond our numerical capabilities. We determine the exponent μ describing the growth of the variance with time by fitting the initial part of time dependence to a straight line in a double logarithmic plot. We see that the power law exponent μ describing the growth of the variance with time depends on the stability index of Lévy noise α and on the noise multiplicativity exponent η. The exponent μ increases with increasing of the noise multiplicativity exponent η. For large values of η supper-diffusion occurs ($\mu > 1$), for smaller values of η the sub-diffusion takes place. The value of η corresponding to the normal diffusion and thus making the boundary between the two regimes depends on the stability index α.

This dependence of the exponent μ on the on the noise multiplicativity exponent η we show in more detail in Fig. 14. As can be seen in Fig. 14a, the super-diffusion can be obtained for $2.8 \leq \eta < 3$. For $2.5 \leq \eta < 2.8$ we have the sub-diffusion with the exponent μ proportional to η. For $\eta < 2.5$ the exponent μ is almost independent from η and varies around $\mu = 0.5$, as can be seen in Fig. 14b.

6.5 Summary

We found that the power-law exponent in the dependence of the mean square displacement on time does not depend on the external force; this force changes only the anomalous diffusion coefficient (see Fig. 11 (d) and (e)). Anomalous diffusion occur only for specific parameters values if $\lambda < 3$ and $\eta < 1$ (or $\lambda < 1$ and $\eta < 1$). As we can see in Fig. 11 (c) and (f), in other cases anomalous diffusion does not occur due to the localization of particles. We obtained analytic expressions for the transition probability and moments in two cases:

when external force is proportional to noise induced drift and when additional external force (besides the noise induced drift) has a linear dependence on the position. Introduction of such a force leads to the restriction of the time interval when the anomalous diffusion occurs. (see Fig. 12 (d) and (e)).

In Chapter 4 we have proposed nonlinear stochastic differential equations driven by Lévy noise that generate signals exhibiting power law statistical properties: power law steady state PDF and power law spectrum in a wide range of frequencies. In addition, such nonlinear SDEs can lead to Lévy flights with anomalous diffusion, both sub-diffusion and supper-diffusion. However, we were unable to find an analytical relation between the parameters of the SDE η and α and the exponent of the anomalous diffusion μ, introduced by Eq. (6.26). Therefore we have used numerical solution of the SDE to estimate this exponent. The numerical results show that due to presence of the multiplicative noise in SDEs both sub-diffusion and supper-diffusion might occur together with $1/f^{\beta}$ noise if specific conditions are satisfied. However, power-law growth of variance is observable only for short times (approximately for 10^{-2}–10^{-1}). Due to reflective boundary conditions the variance stops growing and relax to its steady value. Therefore, more detailed numerical study is needed.

7 Conclusions

1. We have shown that nonlinear SDEs (1.1) generating power-law distributed processes with $1/f^{\beta}$ spectrum can result from diffusive particle motion in inhomogeneous medium. The proposed SDE (2.11) results from Langevin equations (2.1)- (2.2) for one-dimensional motion of a Brownian particle.

2. A pair of nonlinearly coupled nonlinear SDEs (2.26) and (2.27) can generate the signal x_t having the power-law PSD $S(f) \sim f^{-\beta}$ in arbitrarily wide range of frequencies. The exponent β is given by equation (2.28). One can interpret the first equation (2.26) as describing the fluctuations of the signal, with the fluctuating rate of change, described by the second equation (2.27)

3. Introduction of colored noise instead of white noise in HDP leads to the additional restriction of the diffusion and exponential cut-off of the distribution of particle positions. Narrower power law part in the distribution of the particle positions results in the narrower range of frequencies where the spectrum has power law behavior.

4. We obtained a class of nonlinear SDEs with Levy noise giving the power-law behavior of the PSD in any desirably wide range of frequencies and power-law steady state distribution of the signal intensity.

   We generalized nonlinear SDEs (1.1) driven by the Gaussian noise and generating signals with $1/f^{\beta}$ PSD by replacing the Gaussian noise with a more general Lévy α stable noise. This modification lead to PSD exponent dependence on noise stability index β

5. The time-fractional Fokker-Planck equation with power-law coefficients yields the resulting PSD with a power-law form $S(f) \sim f^{-\beta}$ in a wide range of frequencies, with the power-law exponent β given by Eq. (5.56). Thus, according to Eq. (5.56), the PSD with the power-law exponent equal to or larger than 1 in a wide range of intermediate frequencies.

6. We studied a influence of external force on HDP. We found that the power-law exponent in the dependence of the mean square displacement on time does not depend on the external force, this force changes only the

anomalous diffusion coefficient. In addition, the external force having the power-law exponent different from $2\eta - 1$ limits the time interval where the anomalous diffusion occurs.

Bibliography

1. T. H. Solomon, E. R. Weeks, H. L. Swinney, Observation of anomalous diffusion and Lévy flights in a two-dimensional rotating flow, Phys. Rev. Lett. **71**, 3975 (1993).

2. R. Metzler, J. Klafter, The random walk's guide to anomalous diffusion: A fractional dynamics approach, Phys. Rep. **339**, 1 (2000).

3. U. Briskot, I. A. Dmitriev, A. D. Mirlin, Relaxation of optically excited carriers in graphene: Anomalous diffusion and Lévy flights, Phys. Rev. B **89**, 075414 (2014).

4. H. C. Fogedby, Lévy flights in random environments, Phys. Rev. Lett. **73**, 2517 (1994).

5. G. Augello, D. Valenti, B. Spagnolo, Non-Gaussian noise effects in the dynamics of a short overdamped josephson junction, Eur. Phys. J. B **78**, 225 (2010).

6. D. Valenti, C. Guarcello, B. Spagnolo, Switching times in long-overlap josephson junctions subject to thermal fluctuations and non-Gaussian noise sources, Phys Rev. E **89**, 214510 (2014).

7. R. Guantes, J. L. Vega, S. Miret-Artés, Chaos and anomalous diffusion of adatoms on solid surfaces, Phys. Rev. B **64**, 245415 (2001).

8. W. D. Luedtke, U. Landman, Slip diffusion and Lévy flights of an adsorbed gold nanocluster, Phys. Rev. Lett. **82**, 3835 (1999).

9. T. Srokowski, Fractional Fokker-Planck equation for Lévy flights in nonhomogeneous environments, Phys. Rev. E **79**, 040104(R) (2009).

10. A. La Cognata, D. Valenti, A. A. Dubkov, B. Spagnolo, Dynamics of two competing species in the presence of Lévy noise sources, Phys. Rev. E **82**, 011121 (2010).

11. A. L. Cognata, D. Valenti, B. Spagnolo, A. Dubkov, Two competing species in super-diffusive dynamical regimes, Eur. Phys, J. B. **77**, 273 (2010).

12. D. Schertzer, M. Larchev, J. Duan, V. V. Yanovsky, S. Lovejoy, Fractional Fokker-Planck equation for nonlinear stochastic differential equations driven by non-Gaussian Lévy stable noises, J. Math. Phys **42**, 200 (2001).

13. T. Srokowski, Multiplicative Lévy processes: Itô versus stratonovich interpretation, Phys. Rev. E **80**, 051113 (2009).

14. D. Brockmann, T. Geisel, Particle dispersion on rapidly folding random heteropolymers, Phys. Rev. Lett. **91**, 048303 (2003).

15. D. Brockmann, I. Sokolov, Lévy flights in external force fields: From models to equations, Chem. Phys. **284**, 409 (2002).

16. D. Brockmann, T. Geisel, Lévy flights in inhomogeneous media, Phys. Rev. Lett. **90**, 170601 (2003).

17. P. D. Ditlevsen, Observation of α-stable noise induced millennial climate changes from an ice-core record, Geophys. Res. Lett. **26**, 1441 (1999).

18. Y. Marandet, H. Capes, L. Godbert-Mouret, R. Guirlet, M. Koubiti, R. Stamm, A spectroscopic investigation of turbulence in magnetized plasmas, Commun. Nonlinear. Sci. Commun. **8**, 469 (2003).

19. N. Mercadier, W. Guerin, M. Chevrollier, R. Kaiser, Lévy flights of photons in hot atomic vapours, Nat. Phys. **5**, 602 (2009).

20. A. Weron, K. Burnecki, S. Mercik, K. Weron, Complete description of all self-similar models driven by Lévy stable noise, Phys. Rev. E **71**, 016113 (2005).

21. H. Scher, G. Margolin, R. Metzler, J. Klafter, B. Berkowitz, The dynamical foundation of fractal stream chemistry: The origin of extremely long retention times, Geophys. Res. Lett. **29**, 5–1–5–4 (2002).

22. I. Golding, E. C. Cox, Physical nature of bacterial cytoplasm, Phys. Rev. Lett. **96**, 098102 (2006).

23. M. Weiss, M. Elsner, F. Kartberg, T. Nilsson, Anomalous subdiffusion is a measure for cytoplasmic crowding in living cells, Biophys. J. **87**, 3518 (2004).

24. G. M. Zaslavsky, Fractional kinetic equation for hamiltonian chaos, Physica D **76**, 110 (1994).

25. T. Srokowski, A. Kaminska, Diffusion equations for a markovian jumping process, Phys. Rev. E **74**, 021103 (2006).

26. S. M. A. Tabei, S. Burov, H. Y. Kim, A. Kuznetsov, T. Huynh, J. Jureller, L. H. Philipson, A. R. Dinner, N. F. Schere, Intracellular transport of insulin granules is a subordinated random walk, Proc. Natl Acad. Sci. USA **110**, 4911 (2013).

27. A. V. Weigel, B. Simon, M. M. Tamkun, D. Krapf, Ergodic and nonergodic processes coexist in the plasma membrane as observed by single-molecule tracking, Proc. Natl Acad. Sci. USA **108**, 6438 (2011).

28. J.-H. Jeon, V. Tejedor, S. Burov, E. Barkai, C. Selhuber-Unkel, K. Berg-Sørensen, L. Oddershede, R. Metzler, *In Vivo* anomalous diffusion and weak ergodicity breaking of lipid granules, Phys. Rev. Lett. **106**, 048103 (2011).

29. I. Y. Wong, M. L. Gardel, D. R. Reichman, E. R. Weeks, M. T. Valentine, A. R. Bausch, D. A. Weitz, Anomalous diffusion probes microstructure dynamics of entangled f-actin networks, Phys. Rev. Lett. **92**, 178101 (2004).

30. H. Scher, E. W. Montroll, Anomalous transit-time dispersion in amorphous solids, Phys. Rev. B **12**, 2455 (1975).

31. M. Schubert, E. Preis, J. C. Blakesley, P. Pingel, U. Scherf, D. Neher, Mobility relaxation and electron trapping in a donor/acceptor copolymer, Phys. Rev. B **87**, 024203 (2013).

32. J.-H. Jeon, H. Martinez-Seara Monne, M. Javanainen, R. Metzler, Anomalous diffusion of phospholipids and cholesterols in a lipid bilayer and its origins, Phys. Rev. Lett. **109**, 188103 (2012).

33. G. R. Kneller, K. Baczynski, M. Pasienkewicz-Gierula, Communication: Consistent picture of lateral subdiffusion in lipid bilayers: Molecular dynamics simulation and exact results, J. Chem. Phys **135**, 141105 (2011).

34. E. Kepten, I. Bronshtein, Y. Garini, Improved estimation of anomalous diffusion exponents in single-particle tracking experiments, Phys. Rev. E **87**, 052713 (2013).

35. J. Szymanski, M. Weiss, Elucidating the origin of anomalous diffusion in crowded fluids, Phys. Rev. Lett. **103**, 038102 (2009).

36. J.-H. Jeon, N. Leijnse, L. B. Oddershede, R. Metzler, Anomalous diffusion and power-law relaxation of the time averaged mean squared displacement in worm-like micellar solutions, New J. Phys. **15**, 045011 (2013).

37. T. Kühn, T. O. Ihalainen, J. Hyväluoma, N. Dross, S. F. Willman, J. Langowski, M. Vihinen-Ranta, J. Timonen, Protein diffusion in mammalian cell cytoplasm, PLoS ONE **6**, e22962 (2011).

38. A. G. Cherstvy, A. V. Chechkin, R. Metzler, Anomalous diffusion and ergodicity breaking in heterogeneous diffusion processes, New J. Phys. **15**, 083039 (2013).

39. A. G. Cherstvy, R. Metzler, Population splitting, trapping, and non-ergodicity in heterogeneous diffusion processes, Phys. Chem. Chem. Phys **15**, 20220–20235 (2013).

40. A. G. Cherstvy, R. Metzler, Nonergodicity, fluctuations, and criticality in heterogeneous diffusion processes, Phys. Rev. E **90**, 012134 (2014).

41. Y. T. Maeda, T. Tlusty, A. Libchaber, Effects of long DNA folding and small RNA stem–loop in thermophoresis, Proc. Natl. Acad. Sci. **109**, 17972 (2012).

42. C. B. Mast, S. Schink, U. Gerland, D. Braun, Escalation of polymerization in a thermal gradient, Proc. Natl. Acad. Sci. **110**, 8030 (2013).

43. R. Haggerty, S. M. Gorelick, Multiple-rate mass transfer for modeling diffusion and surface reactions in media with pore-scale heterogeneity, Water Resources Res. **31**, 2383 (1995).

44. M. Dentz, D. Bolster, Distribution- versus correlation-induced anomalous transport in quenched random velocity fields, Phys. Rev. Lett. **105**, 244301 (2010).

45. L. F. Richardson, Atmospheric diffusion shown on a distance-neighbour graph, Proc. R. Soc. Lond. A **110**, 709 (1926).

46. B. O'Shaughnessy, I. Procaccia, Analytical solutions for diffusion on fractal objects, Phys. Rev. Lett. **54**, 455 (1985).

47. C. Loverdo, O. Bénichou, R. Voituriez, A. Biebricher, I. Bonnet, P. Desbiolles, Quantifying hopping and jumping in facilitated diffusion of DNA-binding proteins, Phys. Rev. Lett. **102**, 188101 (2009).

48. B. P. English, V. Hauryliuk, A. Sanamrad, S. Tankov, N. H. Dekker, J. Elf, Single-molecule investigations of the stringent response machinery in living bacterial cells, Proc. Natl Acad. Sci. USA **108**, E365 (2011).

49. T. Srokowski, Anomalous diffusion in nonhomogeneous media: Time-subordinated Langevin equation approach, Phys. Rev. E **89**, 030102(R) (2014).

50. M. Dentz, P. Gouze, A. Russian, J. Dweik, F. Delay, Time-domain random walk modeling of heterogeneous diffusion and sorption in porous media, Adv. Water Res. **49**, 13 (2012).

51. X. Zhou, Cooperative atomic scattering of light from a laser with a colored noise spectrum, Phys. Rev. A **80**, 023818 (2009).

52. S. Kim, S. H. Park, C. S. Ryu, Colored-noise-induced multistability in nonequilibrium phase transitions, Phys. Rev. E **58**, 7994 (1998).

53. R. Lande, Risks of population extinction from demographic and environmental stochasticity and random catastrophes, Am. Nat. **142**, 911 (1993).

54. A. Kamenev, B. Meerson, B. Shklovskii, How colored environmental noise affects population extinction, Phys. Rev. Lett. **101**, 268103 (2008).

55. Y. Wang, Y. Lai, , Z. Zheng, Onset of colored-noise-induced synchronization in chaotic systems, Phys. Rev. E **79**, 056210 (2009).

56. L. Gammaitoni, Hänggi, F. Marchesoni, Stochastic resonance, Rev. Mod. Phys. **70**, 223 (1998).

57. D. Nozaki, D. J. Mar, P. Grigg, J. J. Collins, Effects of colored noise on stochastic resonance in sensory neurons, Phys. Rev. Lett. **82**, 2402 (1999).

58. L. M. Ward, P. E. Greenwood, $1/f$ noise, Scholarpedia **2**(12), 1537 (2007).

59. M. B. Weissman, $1/f$ noise and other slow, nonexponential kinetics in condensed matter, Rev. Mod. Phys. **60**, 537 (1988).

60. A. L. Barabasi, R. Albert, Emergence of scaling in random networks, Science **286**, 509 (1999).

61. T. Gisiger, Scale invariance in biology: Coincidence or footprint of a universal mechanism?, Biol. Rev. **76**, 161 (2001).

62. E.-J. Wagenmakers, S. Farrell, R. Ratcliff, Estimation and interpretation of $1/f^{\alpha}$ noise in human cognition, Psychonomic Bull. Rev. **11**, 579 (2004).

63. G. Szabó, G. Fáth, Evolutionary games on graphs, Phys. Rep. **446**, 97 (2007).

64. C. Castellano, S. Fortunato, V. Loreto, Statistical physics of social dynamics, Rev. Mod. Phys. **81**, 591 (2009).

65. A. A. Balandin, Low-frequency $1/f$ noise in graphene devices, Nature Nanotechnology **8**, 549 (2013).

66. S. Kogan, *Electronic Noise and Fluctuations in Solids* (Cambridge University Press, Cambridge, 2008).

67. M. Li, W. Zhao, On $1/f$ noise, Math. Problems Eng. **2012**, 673648 (2012).

68. V. Orlyanchik, M. B. Weissman, M. A. Torija, M. Sharma, C. Leighton, Strongly inhomogeneous conduction in cobaltite films: Non-Gaussian resistance noise, Phys. Rev. B **78**, 094430 (2008).

69. S. V. Melkonyan, Non-Gaussian conductivity fluctuations in semiconductors, Physica B **405**, 379 (2010).

70. E. Marinari, G. Parisi, D. Ruelle, P. Windey, Random walk in a random environment and $1/f$ noise, Phys. Rev. Lett. **50**, 1223 (1983).

71. B. Kaulakys, T. Meškauskas, Modeling $1/f$ noise, Phys. Rev. E **58**, 7013 (1998).

72. B. Kaulakys, Autoregressive model of $1/f$ noise, Phys. Lett. A **257**, 37 (1999).

73. B. Kaulakys, V. Gontis, M. Alaburda, Point process model of 1/f noise vs a sum of Lorentzians, Phys. Rev. E **71**, 051105 (2005).

74. B. Kaulakys, J. Ruseckas, Stochastic nonlinear differential equation generating $1/f$ noise, Phys. Rev. E **70**, 020101(R) (2004).

75. B. Kaulakys, J. Ruseckas, V. Gontis, M. Alaburda, Nonlinear stochastic models of $1/f$ noiseand power-law distributions, Physica A **365**, 217 (2006).

76. J. Ruseckas, B. Kaulakys, V. Gontis, Herding model and $1/f$ noise, EPL **96**, 60007 (2011).

77. V. Gontis, J. Ruseckas, A. Kononovicius, A long-range memory stochastic model of the return in financial markets, Physica A **389**, 100–106 (2010).

78. J. Mathiesen, L. Angheluta, P. T. H. Ahlgren, M. H. Jensen, Excitable human dynamics driven by extrinsic events in massive communities, PNAS **110**, 17259 (2013).

79. A. Kononovicius, V. Gontis, Agent based reasoning for the non-linear stochastic models of long-range memory, Physica A **391**, 1309 (2012).

80. M. Jeanblanc, M. Yor, M. Chesney, *Mathematical Methods for Financial Markets* (Springer, Berlin, 2009).

81. M. Turelli, Random environments and stochastic calculus, Theor. Pop. Biol. **12**, 140–178 (1977).

82. J. Smythe, F. Moss, P. V. E. McClintock, Observation of a noise-induced phase transition with an analog simulator, Phys. Rev. Lett. **51**, 1062 (1983).

83. C. W. Gardiner, *Handbook of Stochastic Methods for Physics, Chemistry and the Natural Sciences* (Springer-Verlag, Berlin, 2004).

84. G. Pesce, A. McDaniel, S. Hottovy, J. Wehr, G. Volpe, Stratonovich-to-Itô transition in noisy systems with multiplicative feedback, Nat. Commun. **4**, 2733 (2013).

85. J. Ruseckas, B. Kaulakys, Scaling properties of signals as origin of $1/f$ noise, J. Stat. Mech. P06005 (2014).

86. J. Ruseckas, B. Kaulakys, $1/f$ noise from nonlinear stochastic differential equations, Phys. Rev. E **81**, 031105 (2010).

87. W. H. Press, S. A. Teukolsky, W. T. Vetterling, *Numerical Recipies* (Cambridge University Press, 2007), 3 edition.

88. P. E. Kloeden, E. Platen, *Numerical Solution of Stochastic Differential Equations* (Springer, Berlin, 1999).

89. V. Mackevicius, *Stochastic Analysis* (Vilnius University Press, 2005).

90. B. Kaulakys, J. Ruseckas, Stochastic nonlinear differential equation generating $1/f$ noise, Physical Review E **70**, 020101 (2004).

91. B. Kaulakys, J. Ruseckas, V. Gontis, M. Alaburda, Nonlinear stochastic models of $1/f$ noise and power-law distributions, Physica A **365**, 217–221 (2006).

92. B. Kaulakys, M. Alaburda, Modeling scaled processes and $1/f^{\beta}$ noise using non-linear stochastic differential equations, Journal of Statistical Mechanics P02051 (2009).

93. B. Kaulakys, M. Alaburda, Modeling scaled processes and $1/f^{\beta}$noise using nonlinear stochastic differential equations, J. Stat. Mech. **2009**, P02051 (2009).

94. J. Bernamont, Fluctuations in the resistance of thin films, Proc. Phys. Soc. London **49**, 138 (1937).

95. A. L. McWhorter, in R. H. Kingston (ed.), *Semiconductor Surface Physics* (University of Pennsylvania Press, Philadelphia, 1957), 207–228.

96. K. S. Ralls, W. J. Skocpol, L. D. Jackel, R. E. Howard, L. A. Fetter, R. W. Epworth, D. M. Tennant, Discrete resistance switching in submicrometer silicon inversion layers: Individual interface traps and low-frequency ($1/f$?) noise, Phys. Rev. Lett. **52**, 228 (1984).

97. C. T. Rogers, R. A. Buhrman, Composition of $1/f$ noise in metal-insulator-metal tunnel junctions, Phys. Rev. Lett. **53**, 1272 (1984).

98. F. N. Hooge, T. G. M. Kleinpenning, L. K. J. Vadamme, Experimental studies on $1/f$ noise, Rep. Prog. Phys. **44**, 479 (1981).

99. P. Dutta, P. M. Horn, Low-frequency fluctuations in solids: $1/f$ noise, Rev. Mod. Phys. **53**, 497 (1981).

100. C. M. Van Vliet, A survey of results and future prospects on quantum $1/f$ noise and $1/f$ noise in general, Solid-State Electron. **34**, 1 (1991).

101. H. Wong, Low-frequency noise study in electron devices: Review and update, Microelectron. Reliab. **43**, 585 (2003).

102. S. Erland, P. E. Greenwood, L. M. Ward, "$1/f^{\alpha}$ noise" is equivalent to an eigenstructure power relation, EPL **95**, 60006 (2011).

103. A. A. Ali, Self-organized criticality in a sandpile model with threshold dissipation, Phys. Rev. E **52**, R4595 (1995).

104. S. Maslov, C. Tang, Y. C. Zhang, $1/f$ noise in bak-tang-wiesenfeld models on narrow stripes, Phys. Rev. Lett. **83**, 2449 (1999).

105. S. B. Lowen, M. C. Teich, *Fractal-Based Point Processes* (Wiley-Interscience, 2005).

106. R. V. Chamberlin, D. M. Nasir, "$1/f$ noise from the laws of thermodynamics for finite-size fluctuations, Phys. Rev. E **90**, 012142 (2014).

107. H. Risken, *The Fokker-Planck equation, Methods of Solution and Applications* (Springer-Verlag, 1989).

108. J. M. Sancho, M. San Miguel, D. Dürr, Adiabatic elimination for systems of brownian particles with nonconstant damping coefficients, J. Stat. Phys. 291 (1982).

109. B. Kaulakys, R. Kazakevicius, J. Ruseckas, Modeling Gaussian and non-Gaussian $1/f$ noise by the linear stochastic differential equations, in *Noise and Fluctuations (ICNF), 2013 22nd International Conference on* (2013), 1–4, doi: 10.1109/ICNF.2013.6578944.

110. H. G. Schuster, *Deterministic Chaos* (VCH, Weinheim, 1988).

111. T. Kuhn, L. Reggiani, L. Varani, Coupled-Langevin-equation analysis of hot-carrier transport in semiconductors, Phys. Rev B. **45**, 1903 (1992).

112. P. G. Lind, A. Mora, J. A. C. Gallas, M. Haase, Reducing stochasticity in the north atlantic oscillation index with coupled Langevin equations, Phys. Rev. E **72**, 056706 (2005).

113. P. Jizba, H. Kleinert, Superpositions of probability distributions, Phys. Rev. E **78**, 031122 (2008).

114. P. Milan, M. Wächter, J. Peinke, Stochastic modeling and performance monitoring of wind farm power production, J. Renew. Sustain. Energy **6**, 03311 (2014).

115. P. E. Kloeden, E. Platen, *Numerical Solution of Stochastic Differential Equations* (Springer-Verlag, Berlin, 1992).

116. J.-P. Eckmann, E. Moses, D. Sergi, Entropy of dialogues creates coherent structures in e-mail traffic, Proc. Natl. Acad. Sci. USA **101**, 14333 (2004).

117. J. G. Oliveira, A.-L. Barabási, Human dynamics: Darwin and Einstein correspondence patterns, Nature **437**, 1251 (2005).

118. Z. Dezsö, E. Almaas, A. Lukács, B. Rácz, I. Szakadát, A.-L. Barabási, Dynamics of information access on the web, Phys. Rev. E **73**, 066132 (2006).

119. A. Vázquez, J. G. Oliveira, Z. Dezsö, K.-I. Goh, I. Kondor, A.-L. Barabási, Modeling bursts and heavy tails in human dynamics, Phys. Rev. E **73**, 036127 (2006).

120. T. Kemuriyama, H. Ohta, Y. Sato, S. Maruyama, M. Tandai-Hiruma, K. Kato, Y. Nishida, A power-law distribution of inter-spike intervals in renal sympathetic nerve activity in salt-sensitive hypertension-induced chronic heart failure, BioSystems **101**, 144 (2010).

121. Á. Corral, Long-term clustering, scaling, and universality in the temporal occurrence of earthquakes, Phys. Rev. Lett. **92**, 108501 (2004).

122. C. Godano, A new expression for the earthquake interevent time distribution, Geophys. J. Int. **202**, 219 (2015).

123. M. Karsai, K. Kaski, A.-L. Barabási, J. Kertész, Universal features of correlated bursty behaviour, Sci. Rep. **2**, 397 (2012).

124. D. Kulasiri, *Stochastic Dynamics. Modeling Solute Transport in Porous Media* (North-Holland, 2002).

125. T. Franosch, M. Grimm, M. Belushkin, F. M. Mor, G. Foffi, L. Forró, S. Jeney, Resonances arising from hydrodynamic memory in brownian motion, Nature **478**, 85 (2011).

126. L. Landau, E. Lifshits, *Fluid Mechanics, Course of Theoretical Physics Vol 6* (Butterworth-Heinemann, 1987).

127. S. Hottovy, G. Volpe, J. Wehr, Thermophoresis of brownian particles driven by coloured noise, EPL **99**, 60002 (2012).

128. R. Piazza, A. Parola, Thermophoresis in colloidal suspensions, J. Phys.: Condens. Matter **20**, 153102 (2008).

129. R. Piazza, Thermophoresis: Moving particles with thermal gradients, Soft Matter **4**, 1740 (2008).

130. A. W. Ghosh, S. V. Khare, Rotation in an asymmetric multidimensional periodic potential due to colored noise, Phys. Rev. Lett. **84**, 5243 (2000).

131. E. Wong, M. Zakai, On the convergence of ordinary integrals to stochastic integrals, Ann. Math. Stat. **36**, 1560 (1965).

132. J. L. Doob, The elementary Gaussian processes, Ann. Math. Stat. **15**, 229 (1944).

133. P. Hänggi, P. Jung, Colored noise in dynamical systems, Adv. Chem. Phys. **89**, 239 (1995).

134. P. Jung, P. Hänggi, Dynamical systems: A unified colored-noise approximation, Phys. Rev. A **35**, 4464 (1987).

135. R. Graham, A. Schenzle, Stabilization by multiplicative noise, Phys. Rev. A **26**, 1676 (1982).

136. H. Sigurgeirsson, A. M. Stuart, A model for preferential concentration, Phys. Fluids **14**, 4352 (2002).

137. R. Kupferman, G. A. Pavliotis, A. M. Stuart, Ito versus Stratonovich white-noise limits for systems with inertia and colored multiplicative noise, Phys. Rev. E **70**, 036120 (2004).

138. H. Takayasu, Stable distribution and Lévy process in fractal turbulence, Prog. Theor. Phys. **72**, 471 (1984).

139. I. A. Min, I. Mezic, A. Leonard, Lévy stable distributions for velocity and velocity difference in systems of vortex elements, Phys. Fluids **8**, 1169 (1996).

140. S. Marksteiner, K. Ellinger, P. Zoller, Anomalous diffusion and Lévy walks in optical lattices, Phys. Rev. A **53**, 3409 (1996).

141. S. Jespersen, R. Metzler, H. C. Fogedby, Lévy flights in external force fields: Langevin and fractional Fokker-Planck equations and their solutions, Phys. Rev. E **59**, 2736 (1999).

142. A. Chechkin, V. Gonchar, J. Klafter, R. M. L. Tanatarov, Stationary states of non-linear oscillators driven by Lévy noise, Chem. Phys. **284**, 233 (2002).

143. S. I. Denisov, W. Horsthemke, P. Hänggi, Steady-state Lévy flights in a confined domain, Phys. Rev. E **77**, 061112 (2008).

144. A. Dubkov, Transient dynamics of verhulst model with fluctuating saturation parameter, Acta Phys. Pol. B **43**, 935 (2012).

145. M. A. Lomholt, T. Ambjörnsson, R. Metzler, Optimal target search on a fast-folding polymer chain with volume exchange, Phys. Rev. Lett. **95**, 260603 (2005).

146. H. C. Fogedby, Langevin equations for continuous time Lévy flights, Phys. Rev. E **50**, 1657 (1994).

147. H. C. Fogedby, Lévy flights in quenched random force fields, Phys. Rev. E **58**, 1690 (1998).

148. A. Janicki, A. Weron, *Simulation and Chaotic Behaviour of* α *- Stable Stochastic Processes* (Marcel Dekker, New York, 1994).

149. P. D. Ditlevsen, Anomalous jumping in a double-well potential, Phys. Rev. E **60**, 172 (1999).

150. S. G. Samko, A. A. Kilbas, O. I. Marichev, *Fractional Integrals and Derivatives: Theory and Applications* (Gordon and Breach, New York, 1993).

151. J. Ruseckas, B. Kaulakys, Intermittency in relation with $1/f$ noise and stochastic differential equations, Chaos **23**, 023102 (2013).

152. M. Magdziarz, A. Weron, Can one see α -stable variables and processes?, Stat. Sci. **9**, 109 (1994).

153. M. Magdziarz, A. Weron, Competition between subdiffusion and Lévy flights: A monte carlo approach, Phys Rev. E **75**, 056702 (2007).

154. Y. J. Liu, Discretization of a class of reflected diffusion processes, Mathematics and Computers in Simulation **38**, 103 (1995).

155. R. Pettersson, Approximations for stochastic differential equations with reflecting convex boundaries, Stochastic Processes and their Applications **59**, 295 (1995).

156. J. I. Deza, R. R. Deza, H. S. Wio, Wide-spectrum energy harvesting out of colored Lévy-like fluctuations, by monostable piezoelectric transducers, EPL **100**, 38001 (2012).

157. V. Méndez, D.Campos, W. Horsthemke, Efficiency of harvesting energy from colored noise by linear oscillators, Phys Rev. E **88**, 022124 (2013).

158. R. Metzler, E. Barkai, J. Klafter, Deriving fractional Fokker-Planck equations from a generalised master equation, Europhys. Lett. **46**, 431 (1999).

159. E. Barkai, R. Metzler, J. Klafter, From continuous time random walks to the fractional Fokker-Planck equation, Phys. Rev. E **61**, 132 (2000).

160. A. K. Jonscher, A. Jurlewicz, K. Weron, Stochastic schemes of dielectric relaxation in correlated-cluster systems, Contemp. Phys. **44**, 329 (2003).

161. J. Sabelko, J. Ervin, M. Gruebele, Observation of strange kinetics in protein folding, Proc. Natl. Acad. Sci. USA **96**, 6031 (1999).

162. R. Metzler, J. Klafter, J. Jortner, Hierarchies and logarithmic oscillations in the temporal relaxation patterns of proteins and other complex systems, Proc. Natl. Acad. Sci. USA **96**, 11085 (1999).

163. J. Sung, E. Barkai, R. J. Silbey, S. Lee, Fractional dynamics approach to diffusion-assisted reactions in disordered media, J. Chem. Phys. **116**, 2338 (2002).

164. K. Seki, M. Wojcik, M. Tachiya, Fractional reaction-diffusion equation, J. Chem. Phys. **119**, 2165 (2003).

165. R. Metzler, J. Klafter, The restaurant at the end of the random walk: Recent developments in the description of anomalous transport by fractional dynamics, J. Phys. A: Math. Gen. **37**, R161 (2004).

166. S. B. Yuste, L. Acedo, Some exact results for the trapping of subdiffusive particles in one dimension, Physica A **336**, 334 (2004).

167. C. W. Chow, K. L. Liu, Fokker–Planck equation and subdiffusive fractional Fokker–Planck equation of bistable systems with sinks, Physica A **341**, 87 (2004).

168. A. A. Stanislavsky, Fractional dynamics from the ordinary Langevin equation, Phys. Rev. E **67**, 021111 (2003).

169. P. Hänggi, P. Talkner, M. Borkovec, Reaction-rate theory: Fifty years after Kramers, Rev. Mod. Phys. **62**, 251 (1990).

170. S. C. Kou, X. S. Xie, Generalized Langevin equation with fractional Gaussian noise: Subdiffusion within a single protein molecule, Phys. Rev. Lett. **93**, 180603 (2004).

171. J. D. Bao, Y. Z. Zhuo, F. A. Oliveira, P. Hänggi, Intermediate dynamics between Newton and Langevin, Phys. Rev. E **74**, 061111 (2006).

172. W. Min, G. Luo, B. J. Cherayil, S. C. Kou, X. S. Xie, Observation of a power-law memory kernel for fluctuations within a single protein molecule, Phys. Rev. Lett. **94**, 198302 (2005).

173. M. Y. Yim, K. L. Liu, Linear response and stochastic resonance of subdiffusive bistable fractional Fokker–Planck systems, Physica A **369**, 329 (2006).

174. A. Piryatinska, A. I. Saichev, W. A. Woyczynski, Physica A **349**, 375 (2005).

175. M. Magdziarz, K. Weron, Anomalous diffusion schemes underlying the Cole–Cole relaxation: The role of the inverse-time α - stable subordinator, Physica A **367**, 1 (2006).

176. A. A. Stanislavsky, Memory effects and macroscopic manifestation of randomness, Phys. Rev. E **61**, 4752 (2000).

177. R. Metzler, E. Barkai, J. Klafter, Anomalous diffusion and relaxation close to thermal equilibrium: A fractional Fokker-Planck equation approach, Phys. Rev. Lett. **82**, 3563 (1999).

178. R. Metzler, W. G. Glöckle, T. F. Nonnenmacher, Fractional model equation for anomalous diffusion, Physica A **211**, 13 (1994).

179. A. A. Vedenov, Theory of a weakly turbulent plasma, Rev. Plasma Phys. **3**, 229 (1967).

180. W. Deng, Numerical algorithm for the time fractional Fokker–Planck equation, J. Comput. Phys. **227**, 1510 (2007).

181. J. Gajda, M. Magdziarz, Fractional Fokker-Planck equation with tempered α - stable waiting times: Langevin picture and computer simulation, Phys. Rev. E **82**, 011117 (2010).

182. M. Magdziarz, Stochastic representation of subdiffusion processes with time-dependent drift, Stoch. Proc. Appl. **119**, 3238 (2009).

183. M. Magdziarz, Langevin picture of subdiffusion with infinitely divisible waiting times, J. Stat. Phys. **135**, 763 (2009).

184. R. Weron, On the Chambers-Mallows-Stuck method for simulating skewed stable random variables, Stat. Probab. Lett. **28**, 165 (1996).

185. I. Goychuk, E. Heinsalu, M. Patriarca, G. Schmid, P. Hänggi, Current and universal scaling in anomalous transport, Phys. Rev. E **73**, 020101(R) (2006).

186. J. L. A. Dubbeldam, A. Milchev, V. G. Rostiashvili, T. A. Vilgis, Driven polymer translocation through a nanopore: A manifestation of anomalous diffusion, EPL **79**, 18002 (2007).

187. T. Kühn, T. O. Ihalainen, J. Hyväluoma, N. Dross, S. F. Willman, L. Langowski, M. Vihinen-Ranta, J. Timonen, Protein diffusion in mammalian cell cytoplasm, PLoS One **6**, e22962 (2011).

188. D. E. Knuth, *The Art of Computer Programming*, volume 2: Seminumerical Algorithms (Addison-Wesley, Boston, 1998), 3rd edition.

Acknowledgements

Foremost I would like to express my gratitude to my scientific supervisor dr. Julius Ruseckas. I am utmostly thankful for his supervision, overwhelming support and valuable lessons in science and life.

I would like to thank to my scientific supervisor of master and bachelor thesis professor Bronislovas Kaulakys for insightful discussions and helpful advices. Many thanks goes to fellow students, researchers and other staff of Vilnius University for creative and friendly atmosphere.

I acknowledge the financial support by the Research Council of Lithuania and Vilnius University Doctoral Studies Mobility Fund.

Last but not the least, I would like to thank my family and friends for their patience, kind support.